

Report

BBMT0600183

date: February 7, 2007

December 12 – 15, 2006

client:

Fondacija Arheoloski Park
“Bosanska Piramida Sunca”
Fra Andela Zvizdovica br. 1/B11
71000 Sarajevo
Bosnia and Herzegovina

projekt:

radar measurements to find inhomogenities in the ground

task from:

Summer 2006

content of task:

inhomogenities and structures under the ceiling

editor:

Dr.-Ing. A. Hasenstab
Ing. Dragan Juricevic
M.Eng. Sven Homburg
Dipl.-Ing. Annett Schönitz
Dipl.-Ing. Harry Deinhard

phone number:

+49 (0) 911 655-5561

faxnumber:

+49 (0) 911 655-5536

e-mail:

andreas.hasenstab@lga.de

INDEX

	Seite
CONCLUSION.....	4
1 MOTIVE AND TASK	5
2 MEASURINGSYSTEM	5
2.1 RADAR	5
2.2 LIMITATION OF THE METHOD	6
2.3 WAY OF MEASURING	6
2.4 COORDINATING SYSTEM OF THE MEASURING AREA	8
2.5 MEASURING BASIS	8
3 MEASURINGFIELD GRASSLAND AT TOP OF KAPIJA	9
3.1 LOCAL CONDITIONS	9
3.2 COORDINATING SYSTEM OF THE MEASURING AREA	10
3.3 MEASURING BASIS	10
3.4 RESULTS OF THE MEASUREMENTS.....	11
3.5 EVALUATION OF RESULTS	13
3.6 RADARGRAMS OF MEASUREMENTS.....	14
4 MEASUREMENTS AT THE KAPIJA.....	23
4.1 LOCAL CONDITIONS	23
4.2 COORDINATING SYSTEM OF THE MEASURING AREA	25
4.3 RESULTS OF THE MEASUREMENTS.....	27
4.4 EVALUATION OF RESULTS	28
4.5 RADARGRAMS OF MEASUREMENTS.....	30
5 STONE PLATES ABOVE GRASSLAND OF KAPIJA.....	38
5.1 LOCAL CONDITIONS	38
5.2 COORDINATING SYSTEM OF THE MEASURING AREA	39
5.3 RESULTS OF THE MEASUREMENTS.....	40
5.4 EVALUATION OF RESULTS	41
5.5 RADARGRAMS OF MEASUREMENTS.....	42
6 STONEPLATES SONDE 4A.....	45
6.1 LOCAL CONDITIONS	45
6.2 COORDINATING SYSTEM OF THE MEASURING AREA	47
6.3 RESULTS OF THE MEASUREMENTS.....	48
6.4 EVALUATION OF RESULTS	51
6.5 RADARGRAMS OF MEASUREMENTS.....	52
7 MEASUREMENTS AT SONDE 12	63
7.1 LOCAL CONDITIONS	63
7.2 RESULTS OF THE MEASUREMENTS.....	64
7.3 EVALUATION OF RESULTS	69
8 MEASUREMENTS AT PLATEAU A AND B	71
8.1 LOCAL CONDITIONS	71
8.2 RESULTS OF THE MEASUREMENTS.....	71
8.3 CONCLUSSION OF RESULTS.....	74

9	MEASUREMENTS AT PLATEAU AND PYRAMIDE.....	76
9.1	LOCAL CONDITIONS	76
9.2	RESULTS OF THE MEASUREMENTS.....	78
10	MEASUREMENTS AT BOTTOM OF VALLEY	87
10.1	LOCAL CONDITIONS	87
10.2	CONCLUSION OF RESULTS.....	87
11	MEASUREMENTS AT VRATNICA KAMENI HRAM AND DOLOVI VALJAK.....	90
11.1	LOCAL CONDITIONS	90
11.2	RESULTS OF THE MEASUREMENTS.....	93
11.3	EVALUATION OF RESULTS	99

CONCLUSION

Radar measurements have been carried out at the area close to Visoco at important places to find inhomogenities in the ground. These measurements were done with two different radar antennas, one 270 MHz antenna which has a capacity to go into the ground up to 5 m and an 100 MHz antenna which makes measurements up to the depth of 20 m dependent on the surrounding conditions.

During the measurements in December (12.12. – 15.12.) the weather was good, but the ground has been very wet. That means the damping of the signals were very high. Nevertheless the results of the measurements have been good and a lot of inhomogenities were found like stone plates and other strong reflectors.

Measurements were done at:

North surface of a hill near Visoco called „pyramid of the sun“

- Grassland at top of Kapija
- at the Kapija
- Stone plates above grassland of kapija
- stoneplates SONDE 4A
- at Sonde 12
- Plateau

Plateau

- Measurements at Plateau A and B

Bottom of Valley

- Measurements at bottom of valley

Vratnica Kameni Hram and Dolovi Valjak

- Measurements at Vratnica Kameni Hram and Dolovi Valjak

Together 44 areas were marked with position and depth where inhomogenities are and there excavations can be made.

The depth of the marked inhomogenities differ between 0,8 m and 5 m.

MOTIVE AND TASK

The LGA Bautechnik GmbH / TÜVRheinland was asked to make measurements with georadar at some areas in Visoko to find inhomogenities in the ground. With results of GPR measurement it is possible to explore exact excavations to be sure what kind of inhomogenities are in the ground. The areas of the measurements from 13.12. - 14.12.2006 are shown below.

1 MEASURINGSYSTEM

1.1 Radar

Ground penetrating radar is a nondestructive geophysical method that produces a continuous cross-sectional profile or record of subsurface features, without drilling, probing, or digging.

Ground penetrating radar (GPR) profiles are used for evaluating the location and depth of buried objects and to investigate the presence and continuity of natural subsurface conditions and features.

Ground penetrating radar operates by transmitting pulses of ultra high frequency radio waves (microwave electromagnetic energy) down into the ground through a transducer (also called an antenna). The transmitted energy is reflected from various buried objects or distinct contacts between different earth materials.

The antenna then receives the reflected waves and stores them in the digital control unit.

When the transmitted signal enters the ground, it contacts objects or subsurface strata with different electrical conductivities and dielectric constants. Part of the ground penetrating radar waves reflect off of the object or interface; while the rest of the waves pass through to the next interface.

The reflected signals return to the antenna, pass through the antenna, and are received by the digital control unit. The control unit registers the reflections against two-way travel time in nanoseconds and then amplifies the signals.

The output signal voltage peaks are plotted on the ground penetrating radar profile as different color bands by the digital control unit.

For each reflected wave, the radar signal changes polarity twice. These polarity changes produce three bands on the radar profile for each interface contacted by the radar wave.

Ground penetrating radar waves can reach depths up to 100 feet (30 meters) in low conductivity materials such as dry sand or granite. Moist clays, shale, and other high conductivity materials, may attenuate or absorb GPR signals, greatly decreasing the depth of penetration to 3 feet (1 meter) or less.

The depth of penetration is also determined by the GPR antenna used. Antennas with low frequencies of from 25 to 200 MHz obtain subsurface reflections from deeper depths (about 30 to 100 feet or more), but have low resolution. These low frequency antennas are used for investigating the geology of a site, such as for locating sinkholes or fractures, and to locate large, deep buried objects.

Antennas with higher frequencies of from 300 to 1,500 MHz obtain reflections from shallow depths (0 to about 30 feet), and have high resolution. These high frequency antennas are used to investigate surface soils and to locate small or large, shallow, buried objects, such as utilities, and also rebar in concrete.

1.2 Limitation of the method

Radar is an indirect method, e.g. the accuracy and quality of the measured results depend on physical properties of the tested medium.

Error of measurement caused by an inhomogeneous structure are possible. The indirect measuring system is limited by the named influences and to get exact information it is the best to isolate areas non-destructive and then look destructive like digging.

1.3 Way of measuring

The measurements were accomplished with a radar system SIR 20 (GSSI) and 270 MHz and 100 MHz a radar antenna. The radar antennas were pulled over the range which can be examined and the data were registered and archived by a measuring computer (SIR 20). The length regulation took place with a survey wheel. For the calibration of the radar facility some calibration measurements were done.



figure 1: radar equipment left: computer, middle and right: radar antenna 270 kHz



figure 2: radar antenna 100 kHz

1.4 Coordinating System of the measuring area

The measuring lines go parallel or in right angle to the hill.

1.5 measuring basis

Measured data:	time of flight and amplitude of waves
equipment:	digital geo radar equipment GSSI SIR20
sensor:	270 MHz; 100 kHz
way admission:	wheel with increment giver
registration length:	70 – 200 nsek, corresponds to 4 - 20 m range
calibration:	stone plates with known dimension

2 MEASURINGFIELD GRASSLAND AT TOP OF KAPIJA

2.1 Local conditions



figure 3: area of measurements

The measurements were carried out at different areas close to "Kapija".



figure 4: view of measurements on grassland

2.2 Coordinating System of the measuring area

The measuring lines go parallel or in right angle to the hill.

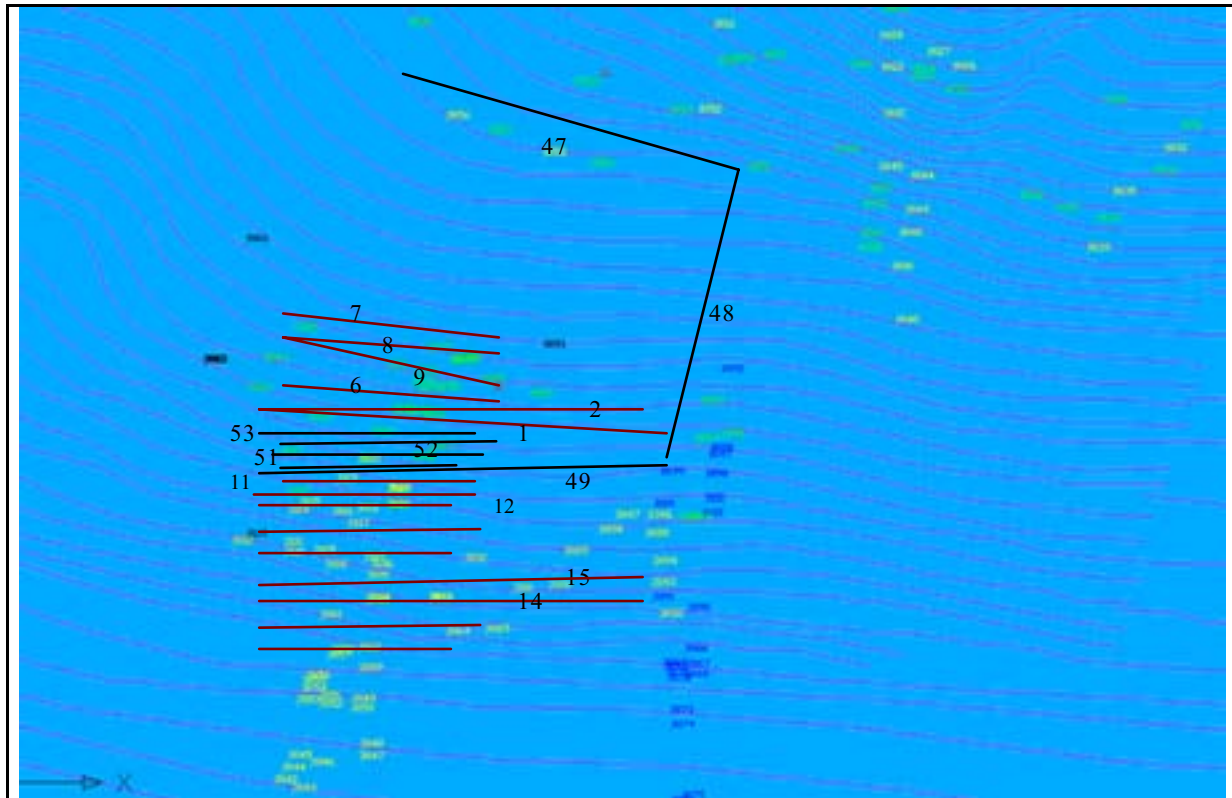


figure 5: overview of position of measuring lines

2.3 measuring basis

Measured data:	time of flight and amplitude of waves
equipment:	digital geo radar equipment GSSI SIR20
sensor:	270 MHz; 100 kHz
way admission:	wheel with increment giver
registration length:	70 – 200 nsek, corresponds to 4 - 20 m range
calibration:	stone plates with known dimension

2.4 RESULTS OF THE MEASUREMENTS

The measurements were done with an 270 MHz and an 100 MHz radar antenna. The ground was very wet which means the damping of the signals is high. Anywhere the results of the measurements were in the first 4 m very good. Following the results of measurements at the area called “Kapija” and the grassland closed to it are shown.

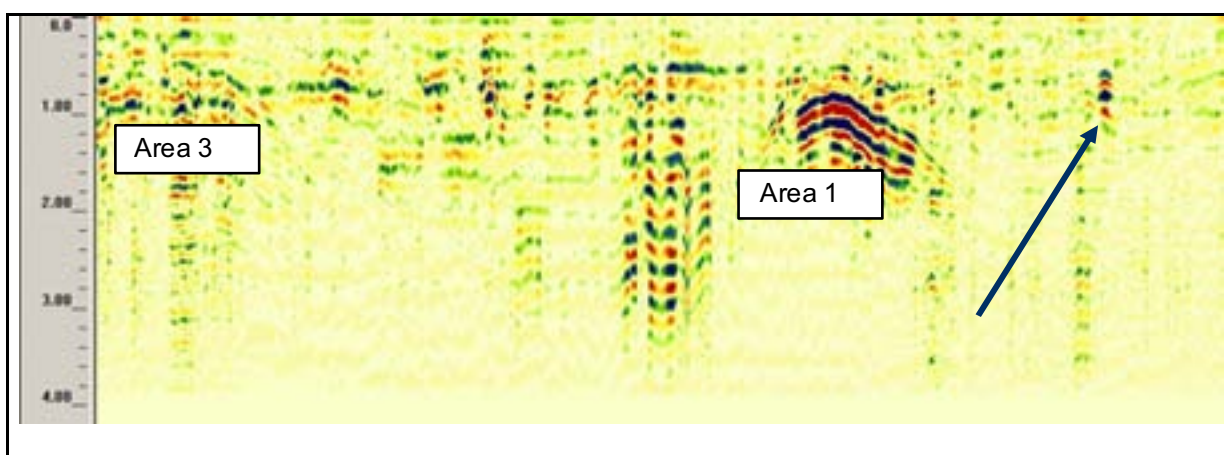


figure 6: radargram of a measuring along measuring line 49 (length: 50 m, GSSI, f = 270 MHz) with very interesting inhomogeneity in grassland

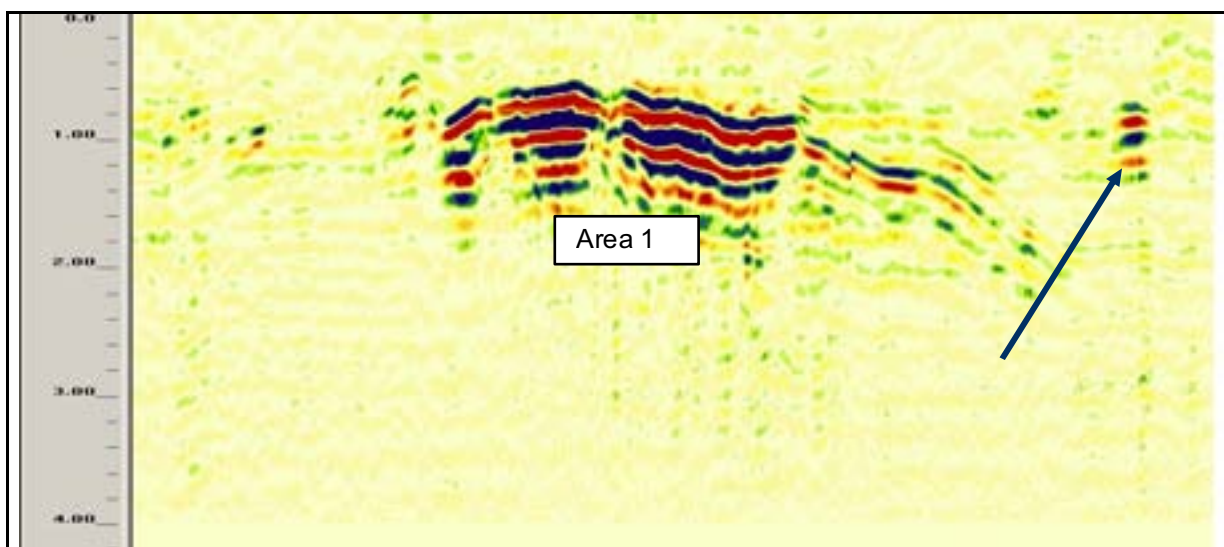


figure 7: radargram of a measuring along measuring line 51 (length: 22 m, GSSI, f = 270 MHz) with inhomogeneities

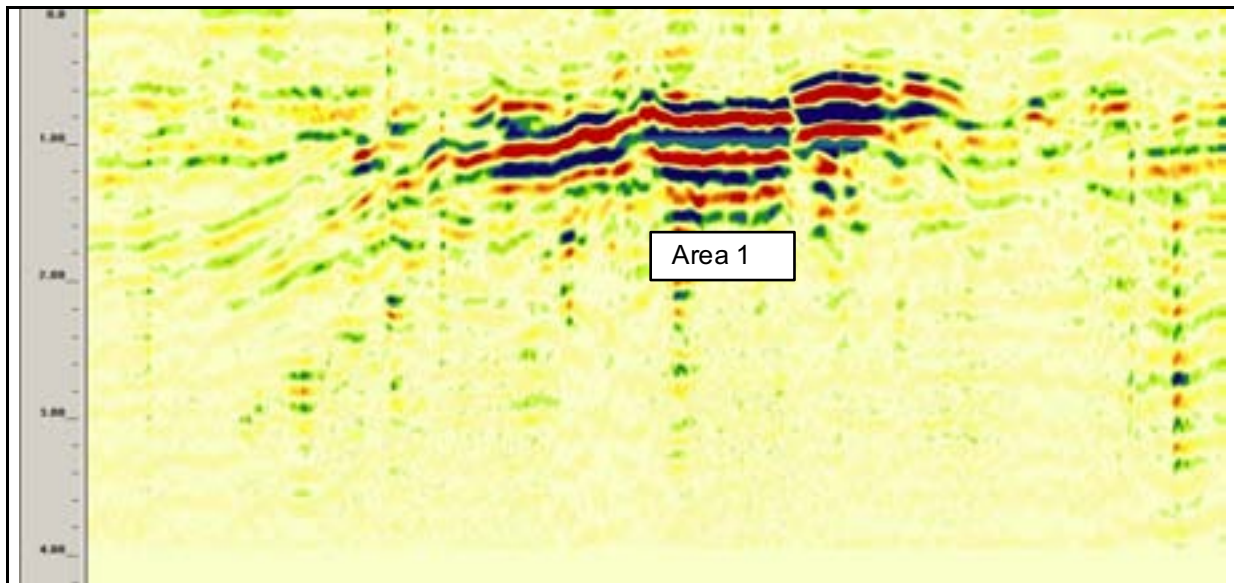


figure 8: radargram of a measuring along measuring line 52 (length: 19 m, GSSI, f = 270 MHz) with inhomogeneities

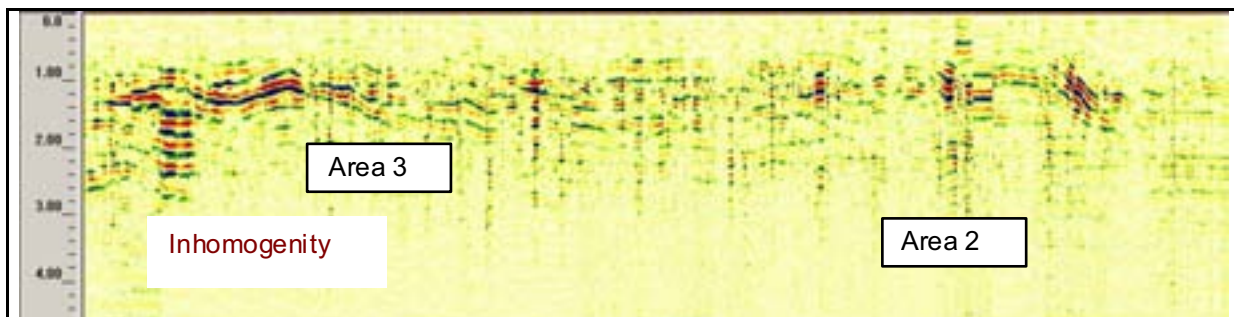
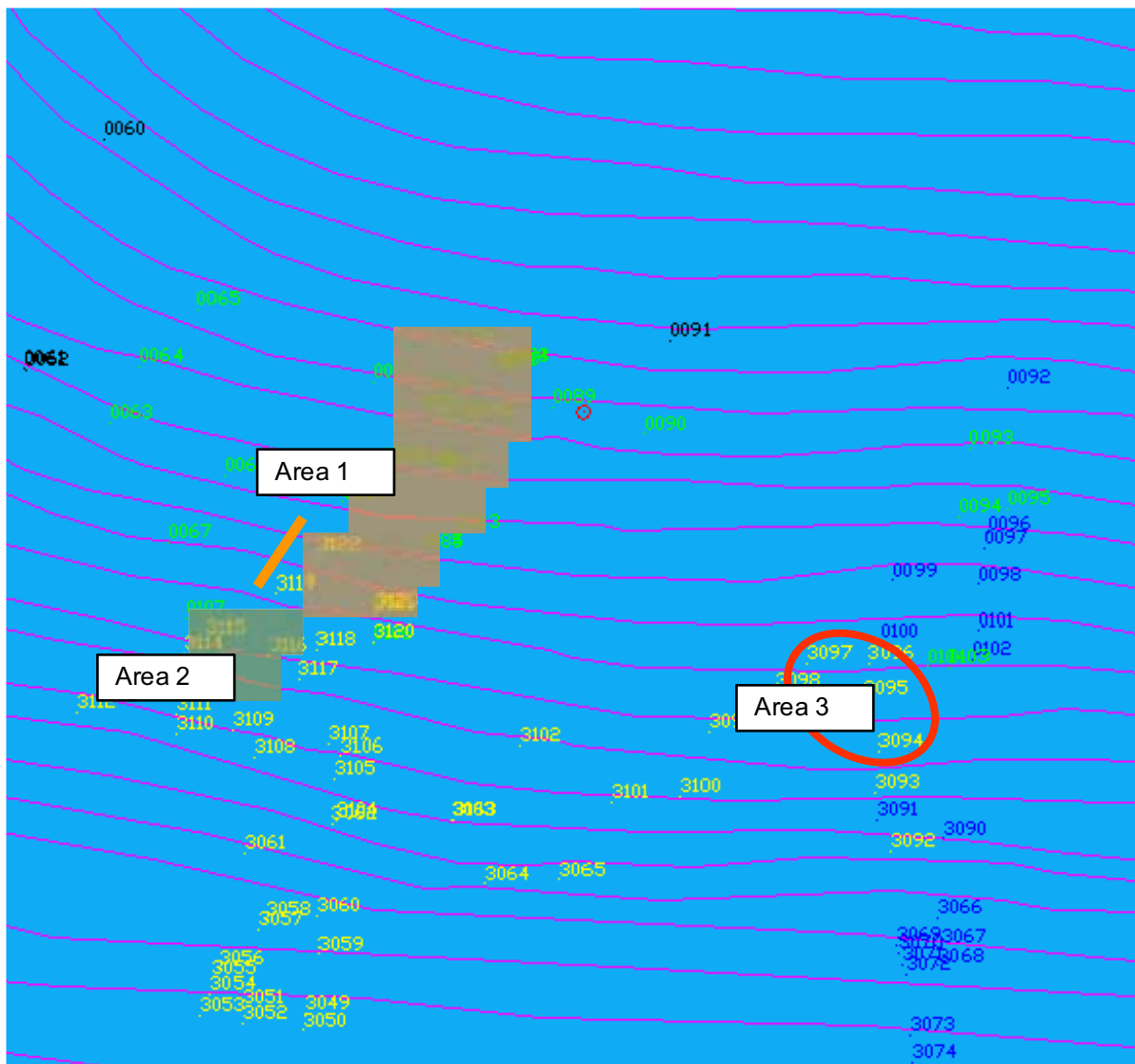


figure 9: radargram of a measuring along measuring line 15 (length: 57 m, GSSI, f = 270 MHz) with inhomogeneities

2.5 EVALUATION OF RESULTS



In the picture above the measuring lines and the areas with inhomogeneities are shown.

Area 1:	Large inhomogeneity in a varying depth of: 0,8-1,5 m
Pipe parallel to Area 1:	inhomogeneity depth of: 0,8-1,0 m
Area 2	Top of Area 1 Depth of inhomogeneity: 0,9 - 1,1 m
Area 3:	Depth of inhomogeneity: 1,0-1,3 m

2.6 RADARGRAMS OF MEASUREMENTS

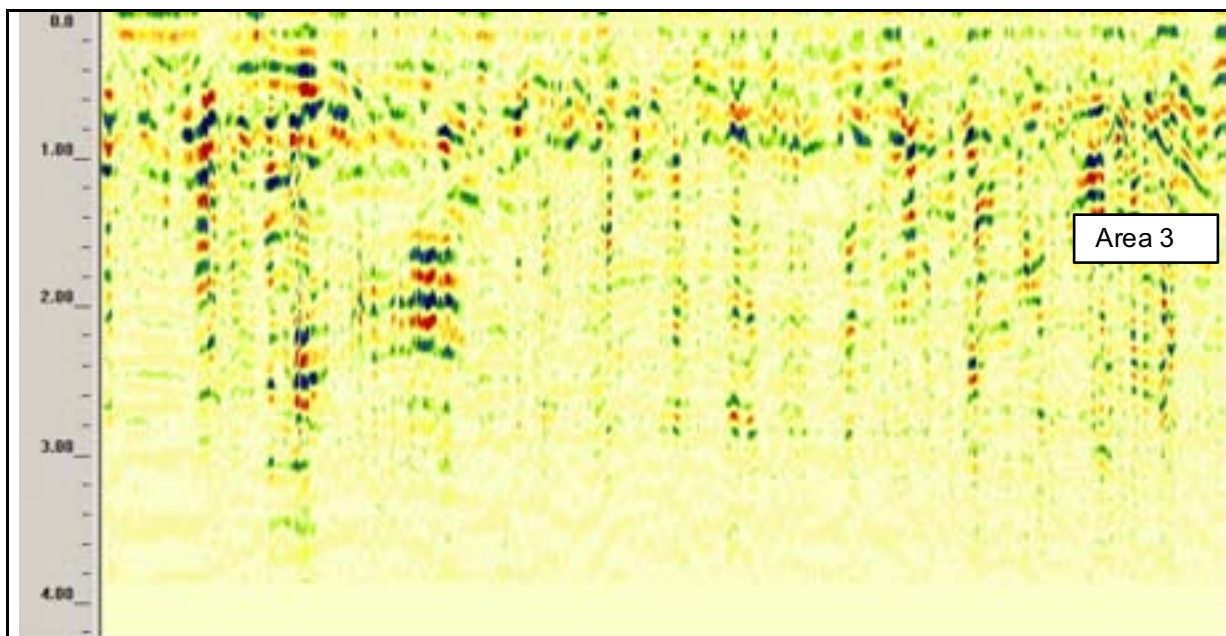


figure 10: radargram of a measuring along measuring line 48 (length: 44 m, GSSI, $f = 270$ MHz) with inhomogeneities

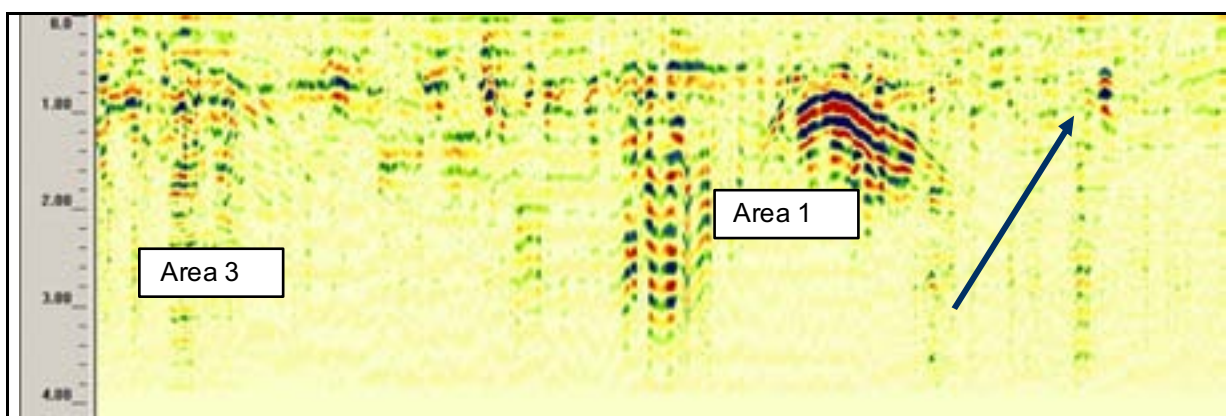


figure 11: radargram of a measuring along measuring line 49 (length: 50 m, GSSI, $f = 270$ MHz) with very interesting inhomogeneity

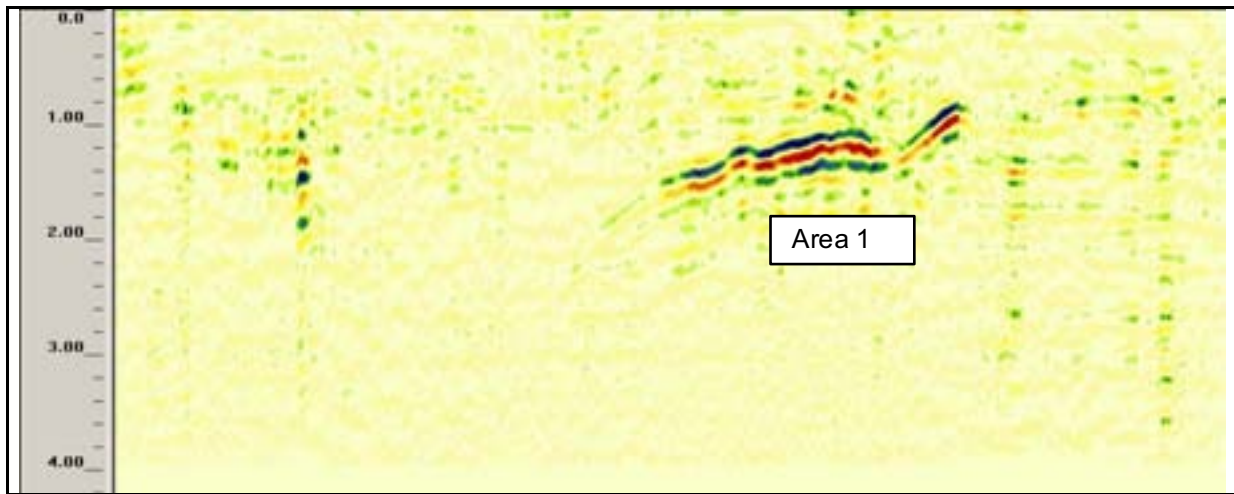


figure 12: radargram of a measuring along measuring line 50 (length: 26 m, GSSI, f = 270 MHz) with inhomogenities

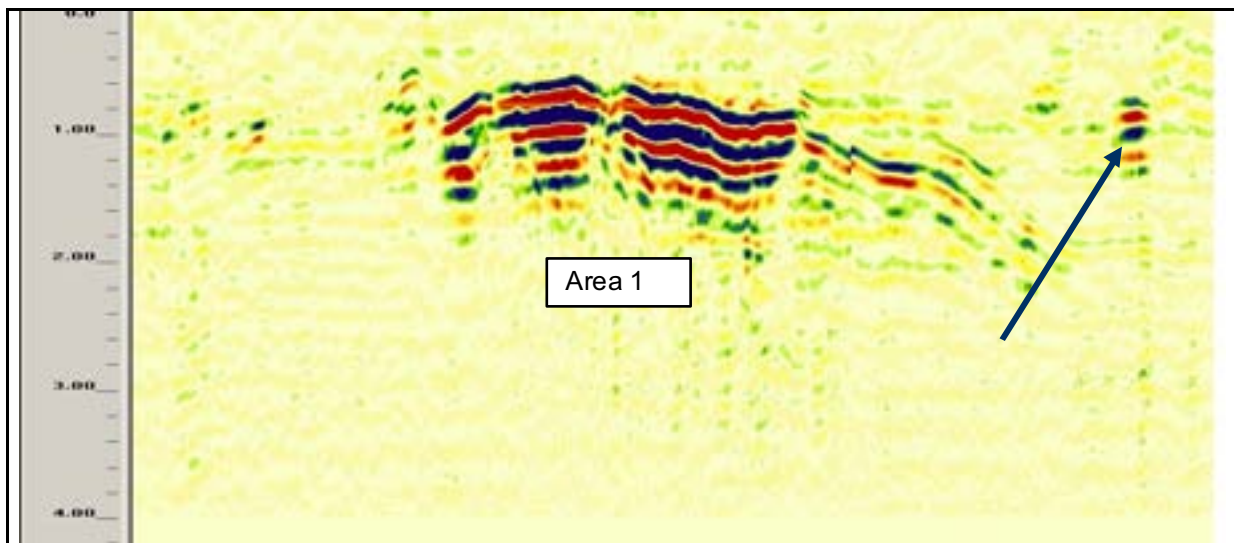


figure 13: radargram of a measuring along measuring line 51 (length: 22 m, GSSI, f = 270 MHz) with inhomogenities

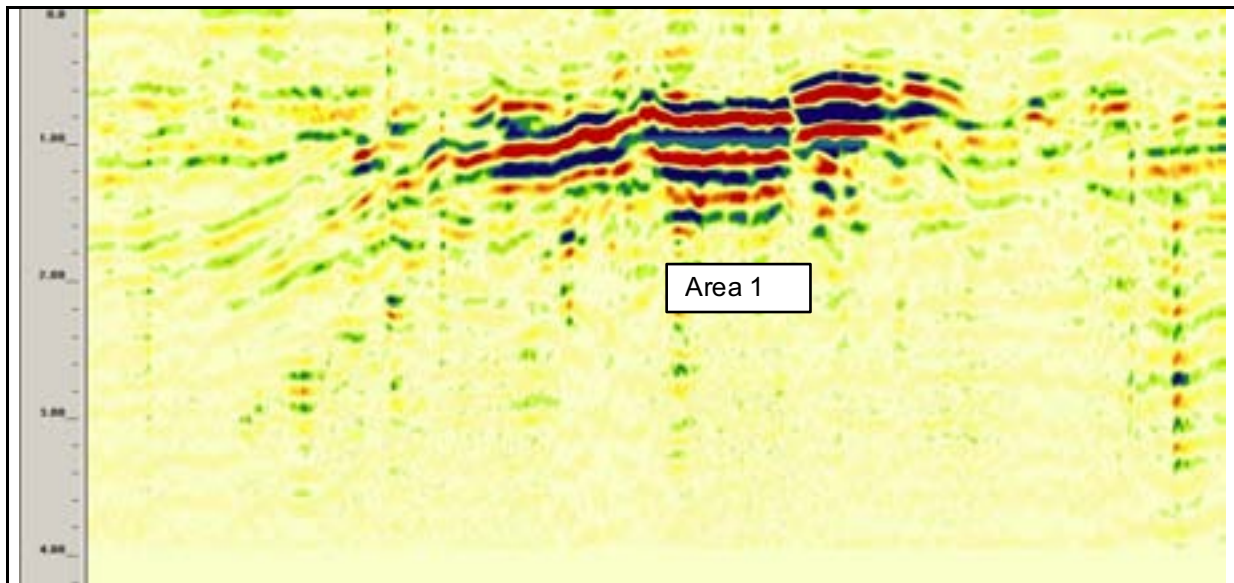


figure 14: radargram of a measuring along measuring line 52 (length: 19 m, GSSI, $f = 270$ MHz) with inhomogenities

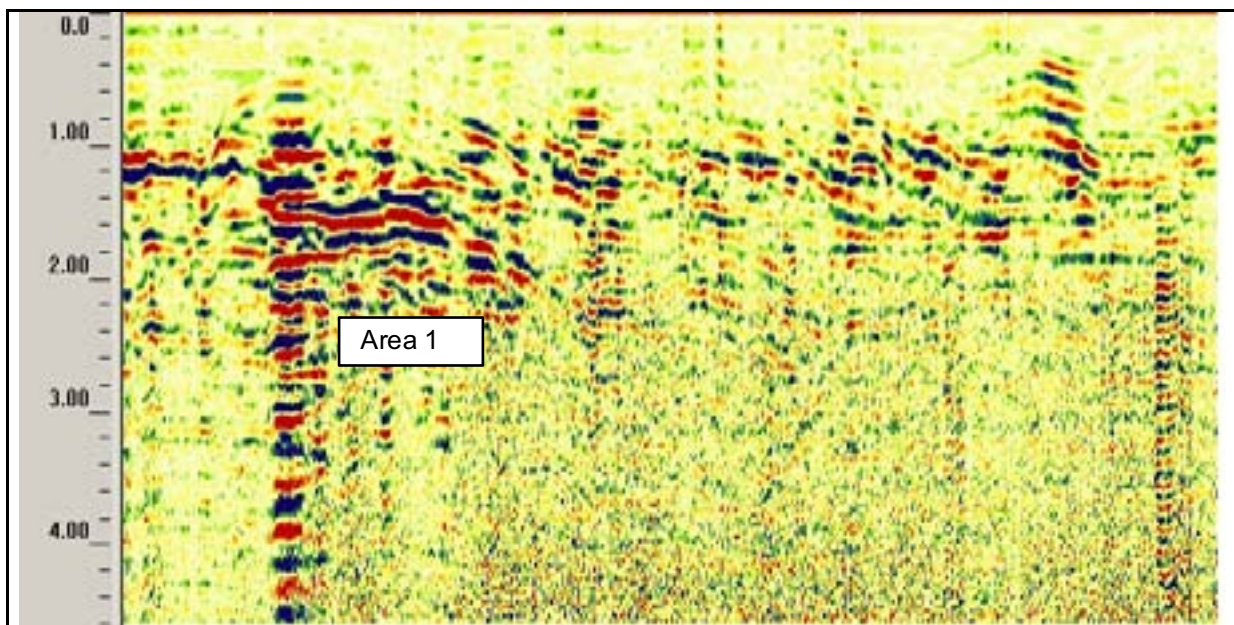


figure 15: radargram of a measuring along measuring line 6 (length: 23,45 m, GSSI, $f = 270$ MHz) with inhomogenities

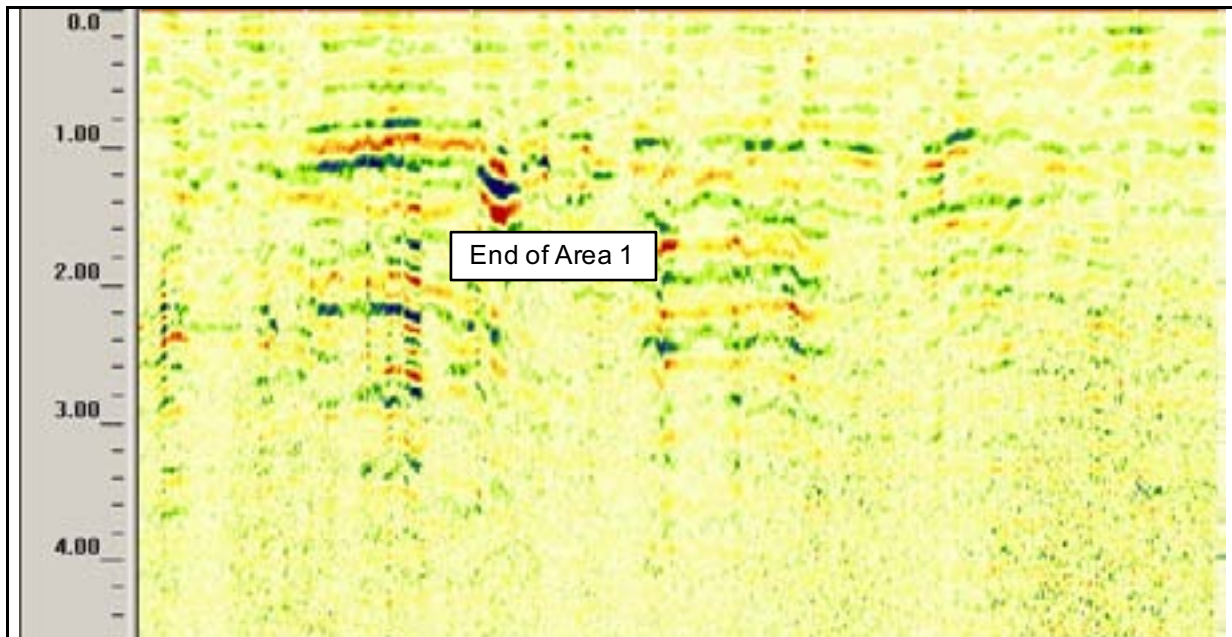


figure 16: radargram of a measuring along measuring line 7 (length: 20,5 m, GSSI, $f = 270$ MHz) with no inhomogeneities

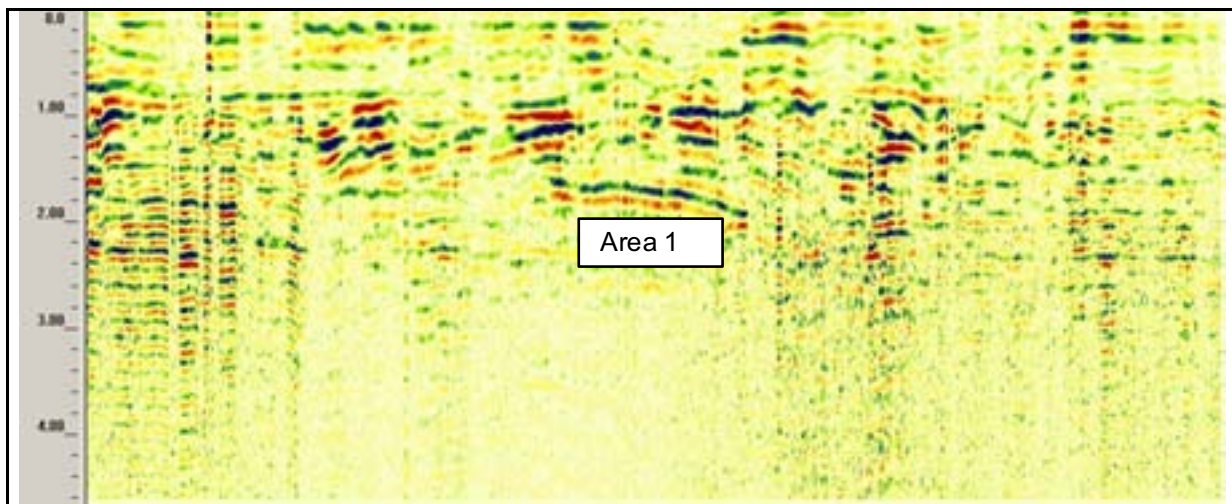


figure 17: radargram of a measuring along measuring line 8 (length: 19 m, GSSI, $f = 270$ MHz) with inhomogeneities

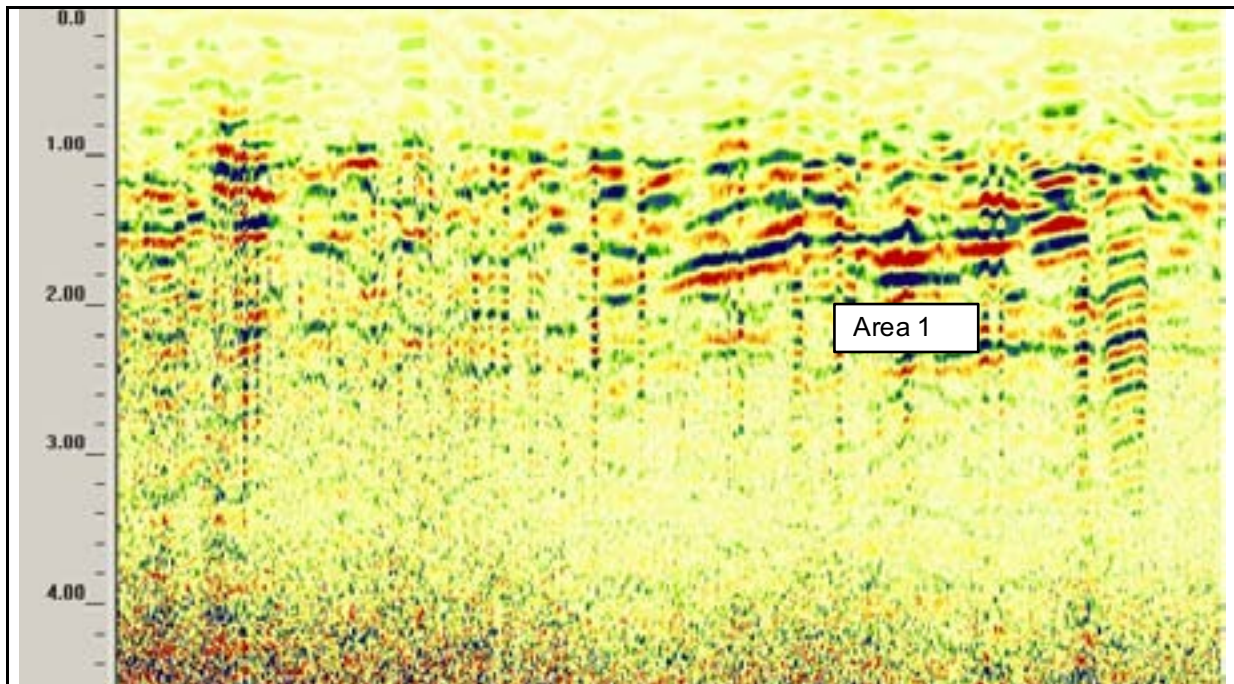


figure 18: radargram of a measuring along measuring line 9 (length: 12,6 m, GSSI, f = 270 MHz) with inhomogeneities

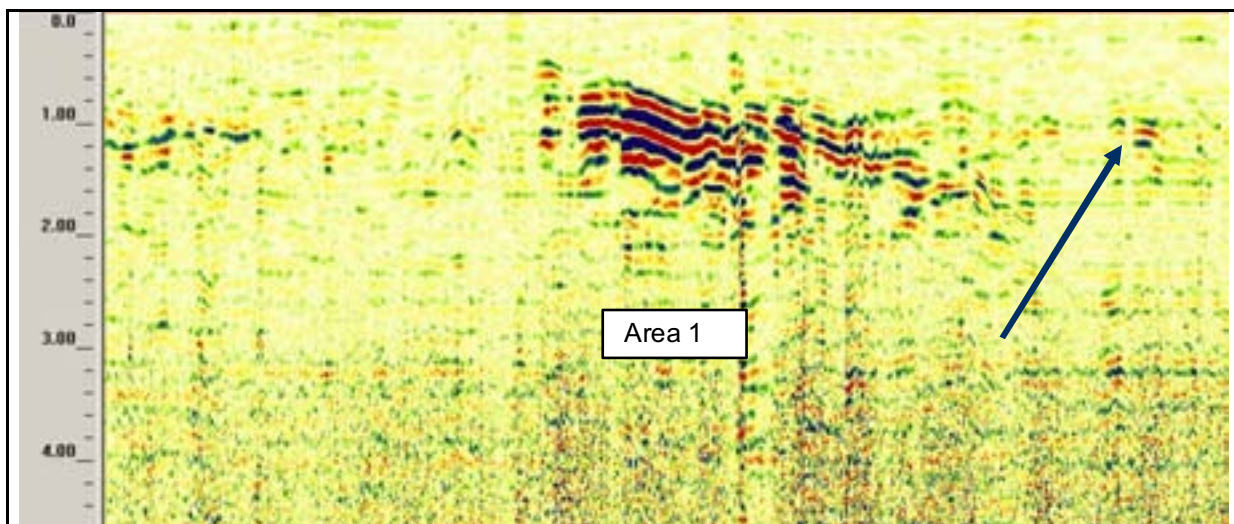


figure 19: radargram of a measuring along measuring line 10 (length: 29 m, GSSI, f = 270 MHz) with inhomogeneities

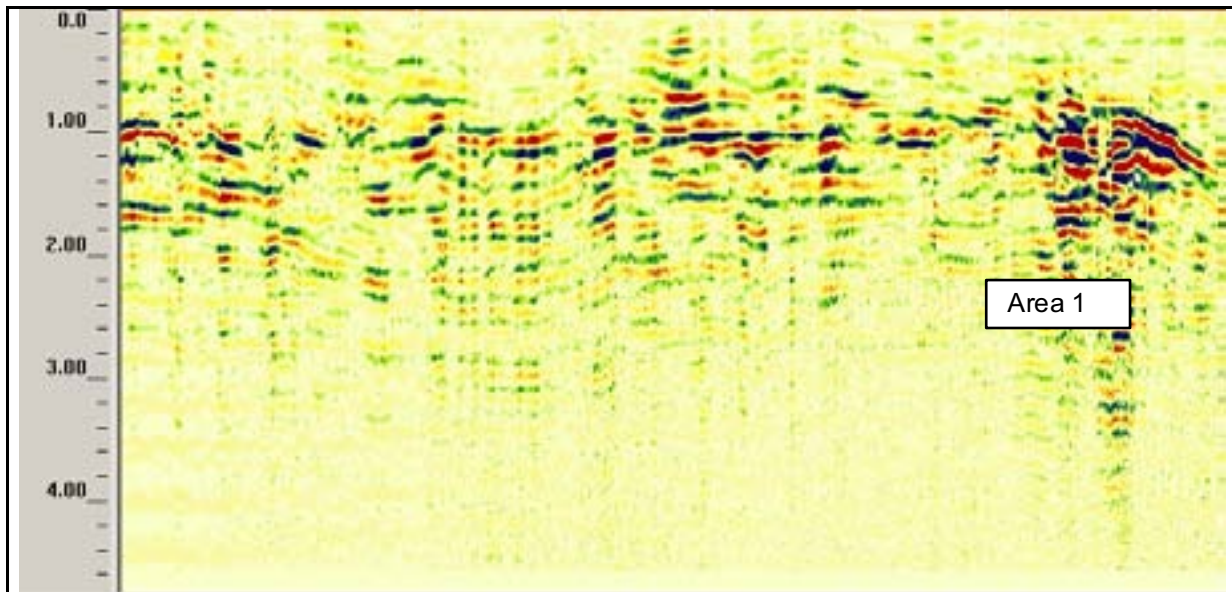


figure 20: radargram of a measuring along measuring line 11 (length: 23,7 m, GSSI, f = 270 MHz) with inhomogenities

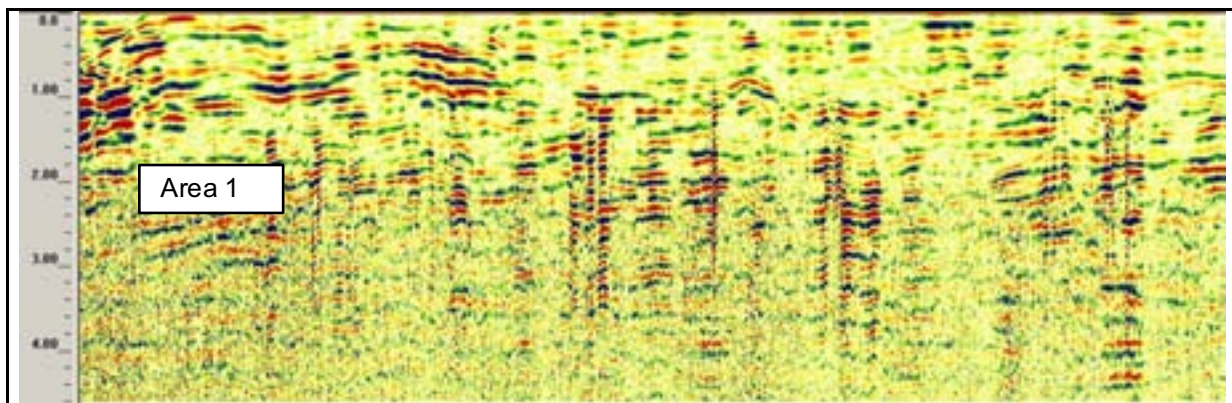


figure 21: radargram of a measuring along measuring line 12 (length: 19 m, GSSI, f = 270 MHz) with inhomogenities

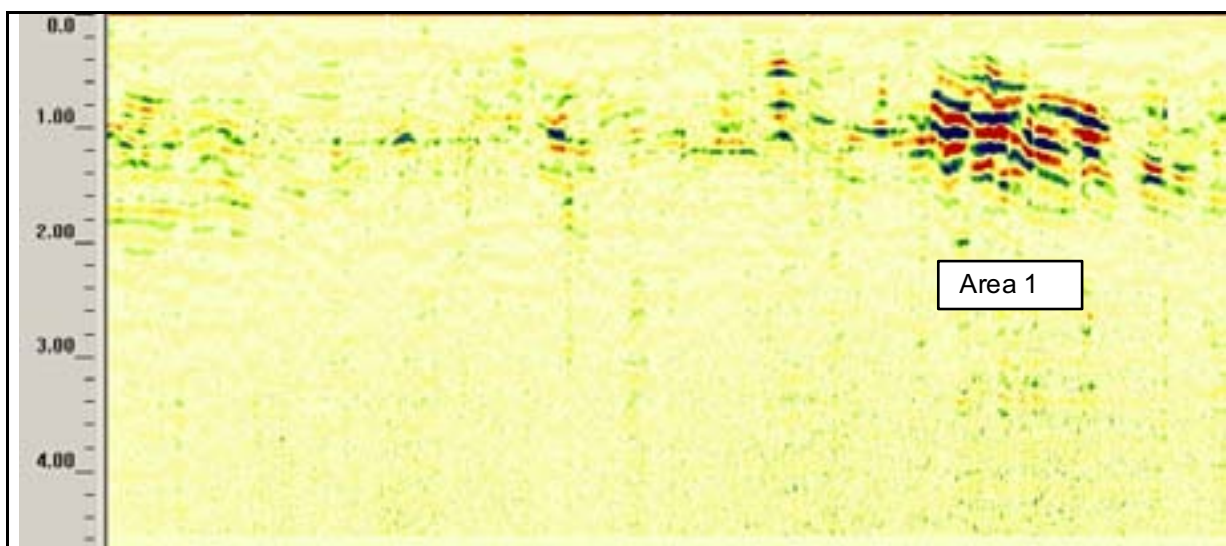


figure 22: radargram of a measuring along measuring line 13 (length: 25,3 m, GSSI, f = 270 MHz) with inhomogeneities

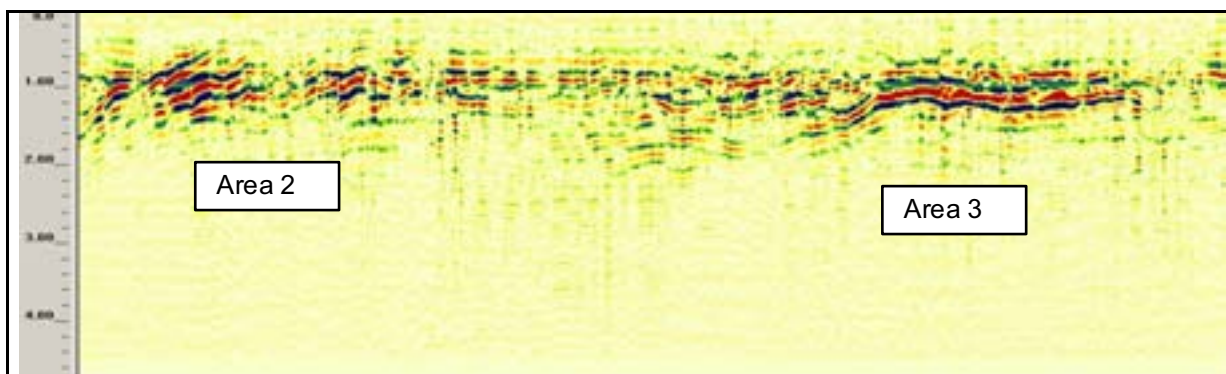


figure 23: radargram of a measuring along measuring line 14 (length: 51 m, GSSI, f = 270 MHz) with inhomogeneities

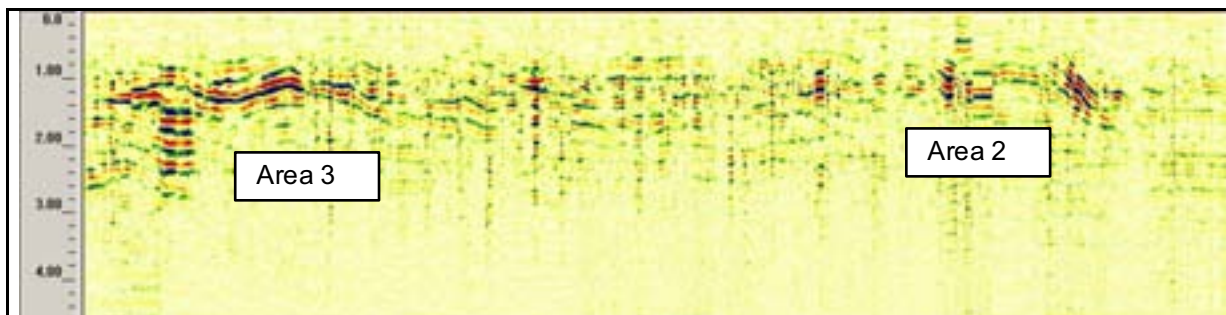


figure 24: radargram of a measuring along measuring line 15 (length: 57 m, GSSI, f = 270 MHz) with inhomogeneities

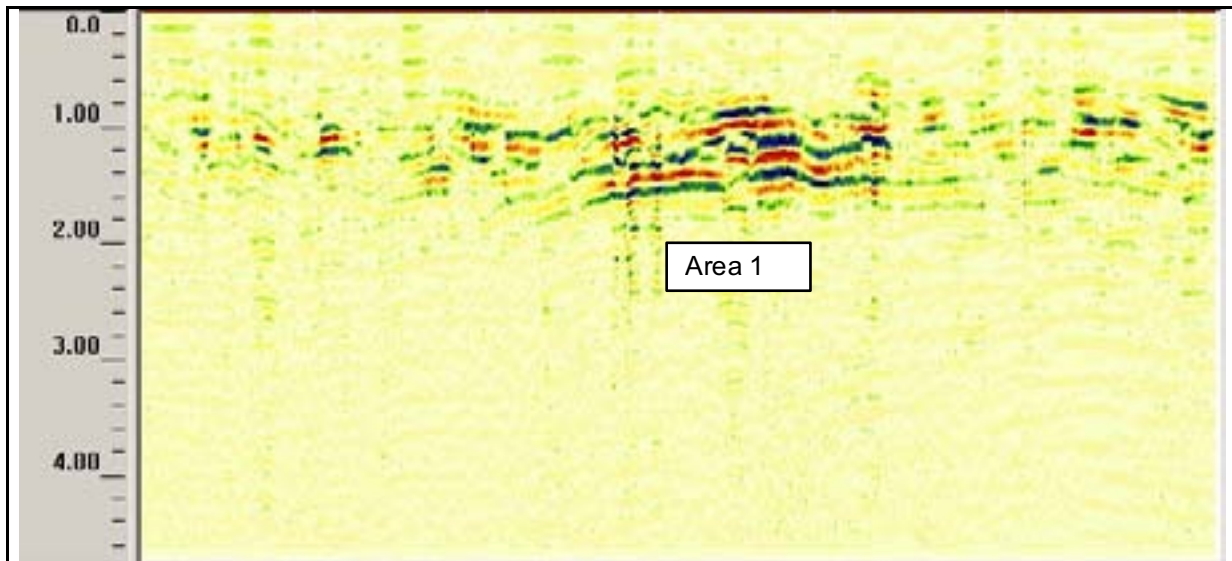


figure 25: radargram of a measuring along measuring line 16 (length: 19,6 m, GSSI, $f = 270$ MHz) with inhomogenities

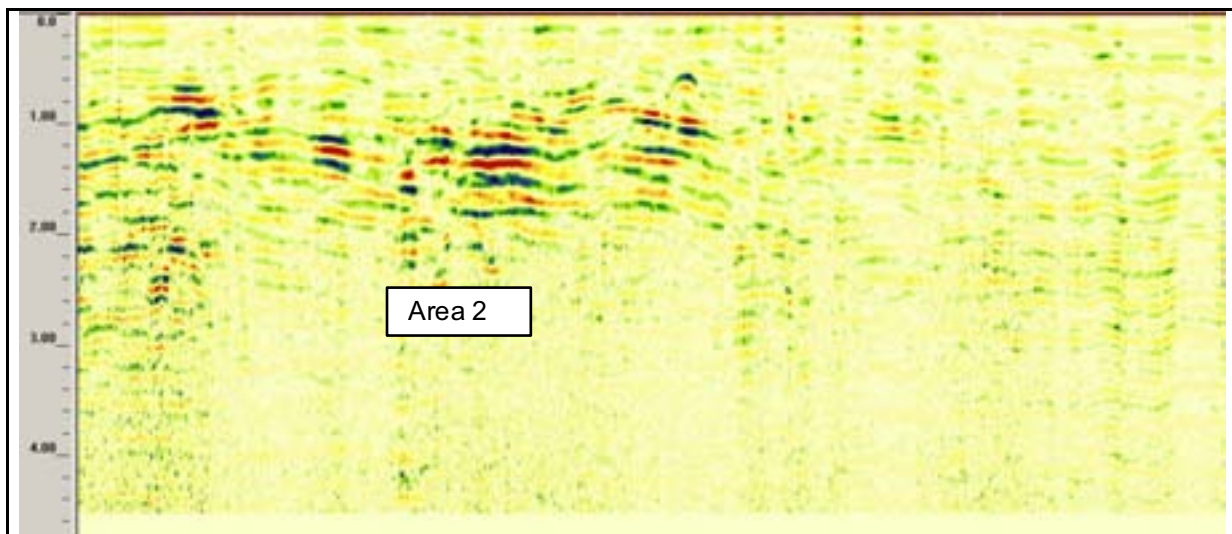


figure 26: radargram of a measuring along measuring line 17 (length: 19,4 m, GSSI, $f = 270$ MHz) with inhomogenities

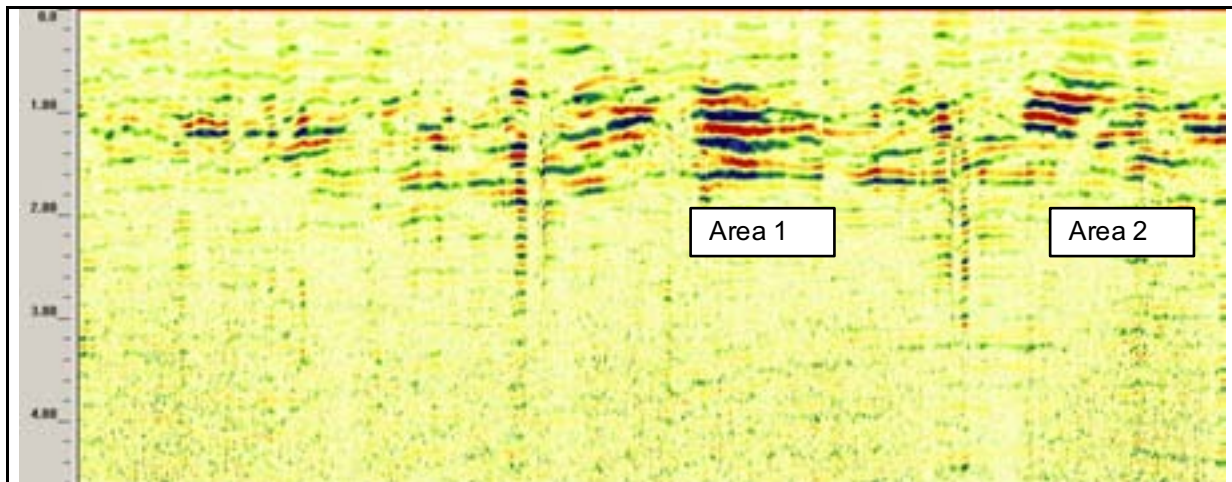
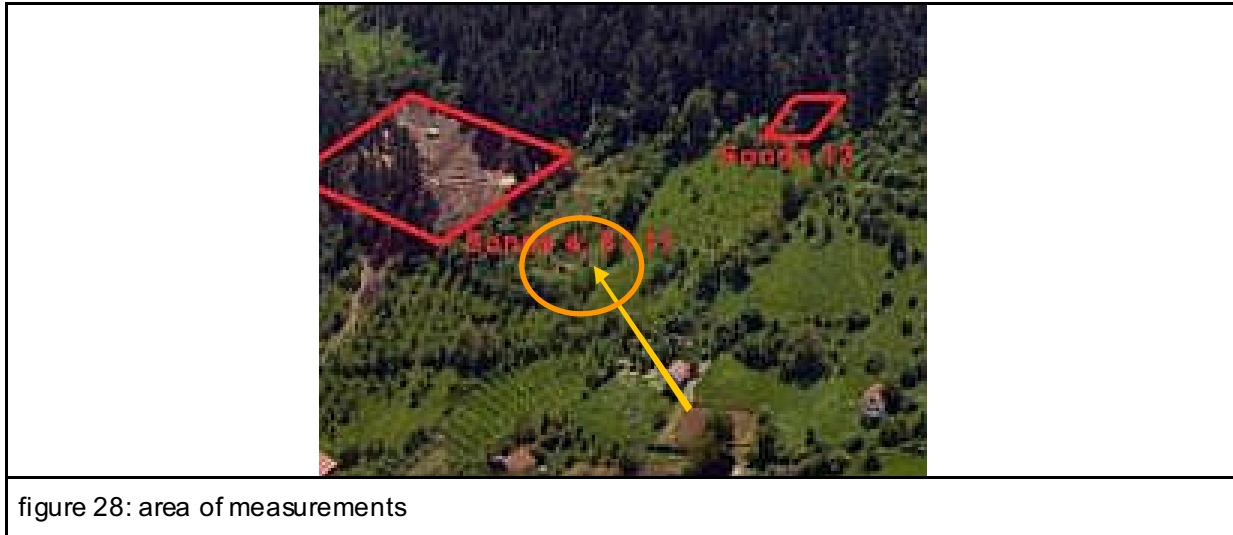


figure 27: radargram of a measuring along measuring line 18 (length: 19,4 m, GSSI, $f = 270$ MHz) with inhomogenities

3 MEASUREMENTS AT THE KAPIJA

3.1 Local conditions



The measurements were carried out at different areas close to "Kapija".

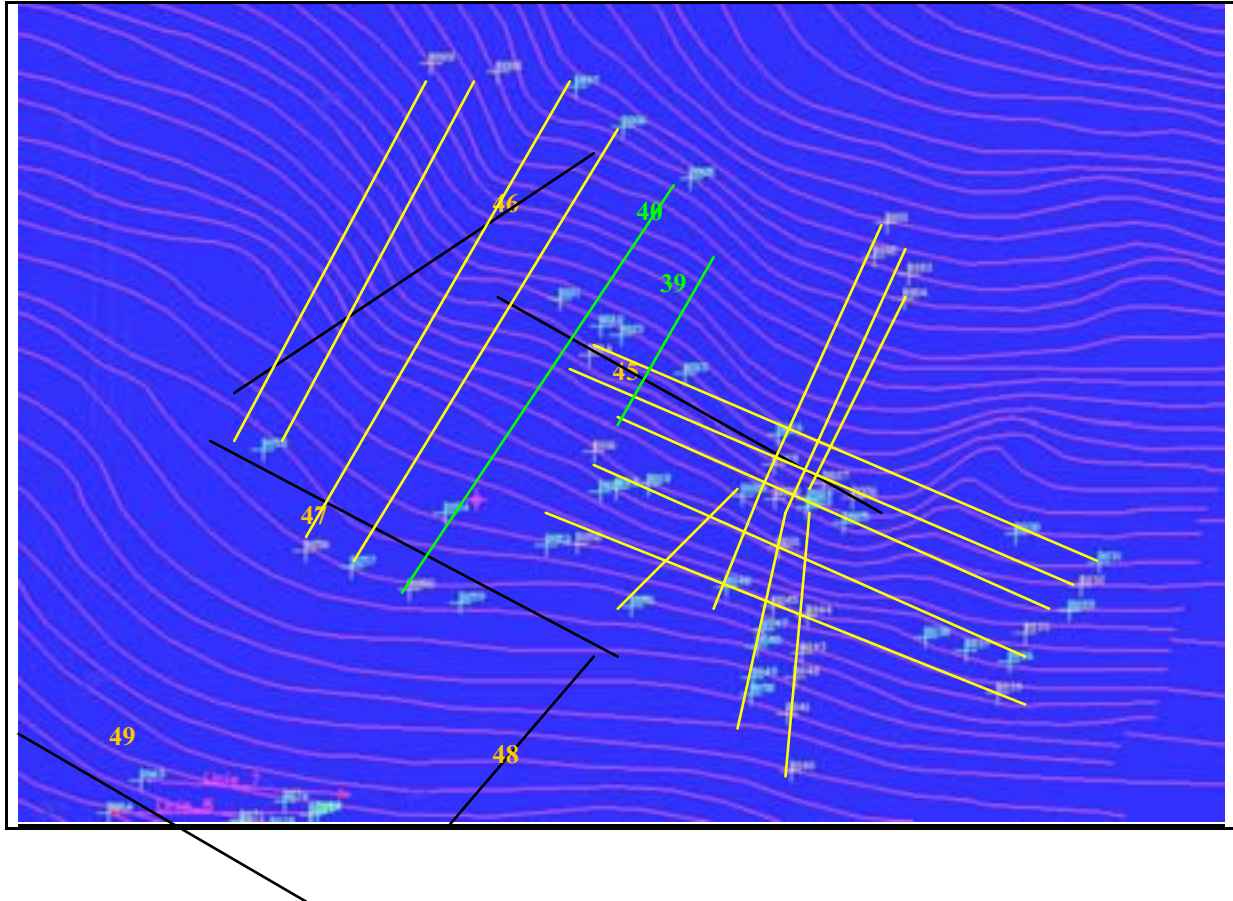




figure 30: view of measurements at area closed to kapija

3.2 Coordinating System of the measuring area

The measuring lines go parallel or in right angle to the hill.



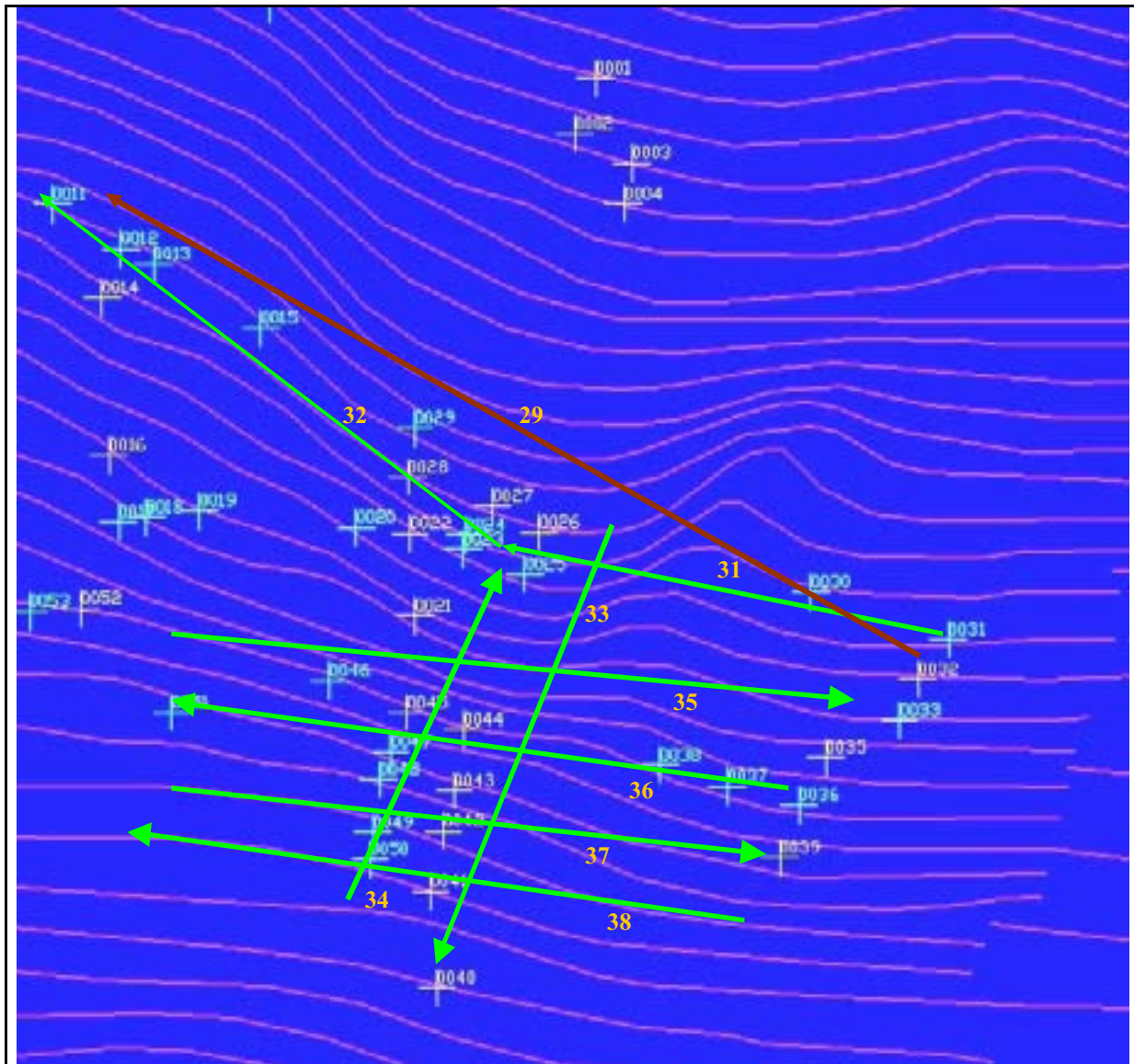


figure 31: overview of position of measuring lines

3.3 RESULTS OF THE MEASUREMENTS

The measurements were done with an 270 MHz and an 100 MHz radar antenna. The ground was very wet which means the damping of the signals is high. Anywhere the results of the measurements were in the first 4 m very good. Following the results of measurements at the areacalld “Kapija” and the grassland closed to it are shown.

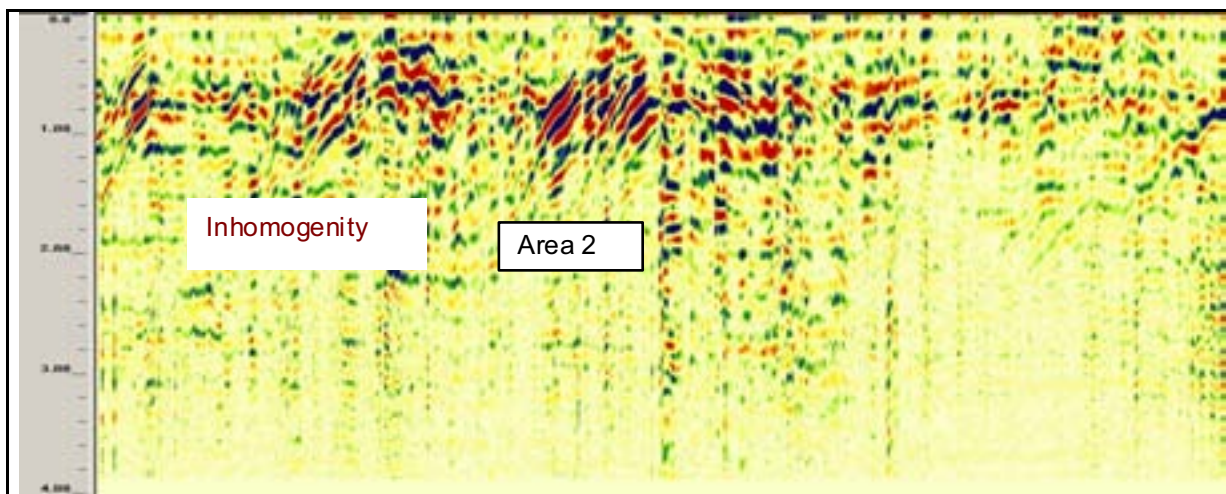


figure 32: radargram of a measuring along measuring line 32 (length: 48,3 m, GSSI, f = 270 MHz) with inhomogenities and edge of Kapija

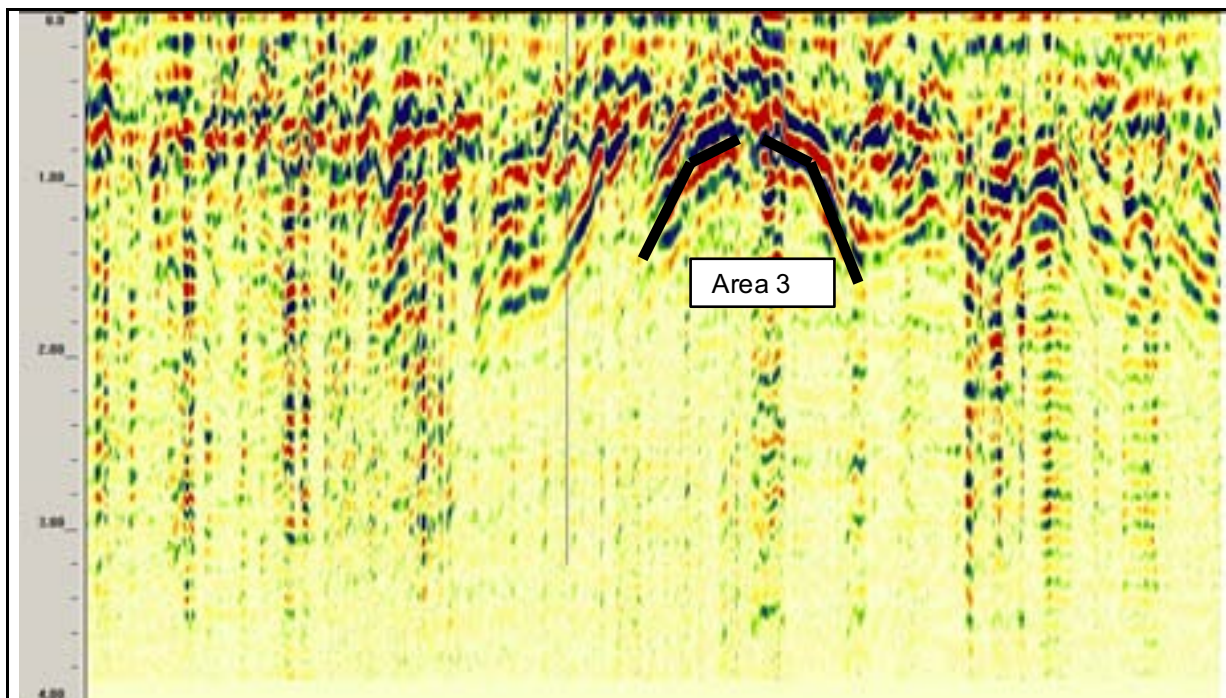


figure 33: radargram of a measuring along measuring line 37 (length: 57 m, GSSI, f = 270 MHz) with important inhomogeneity at top of “Kapija”

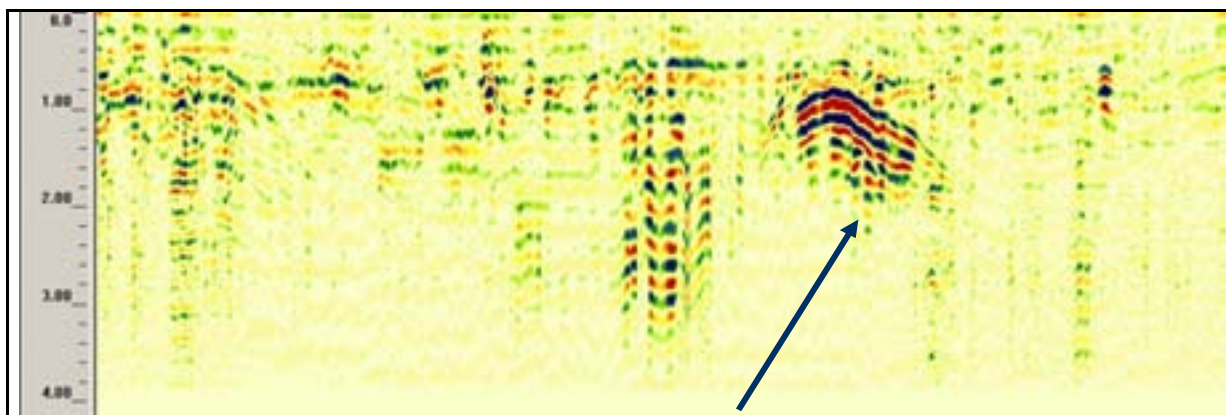
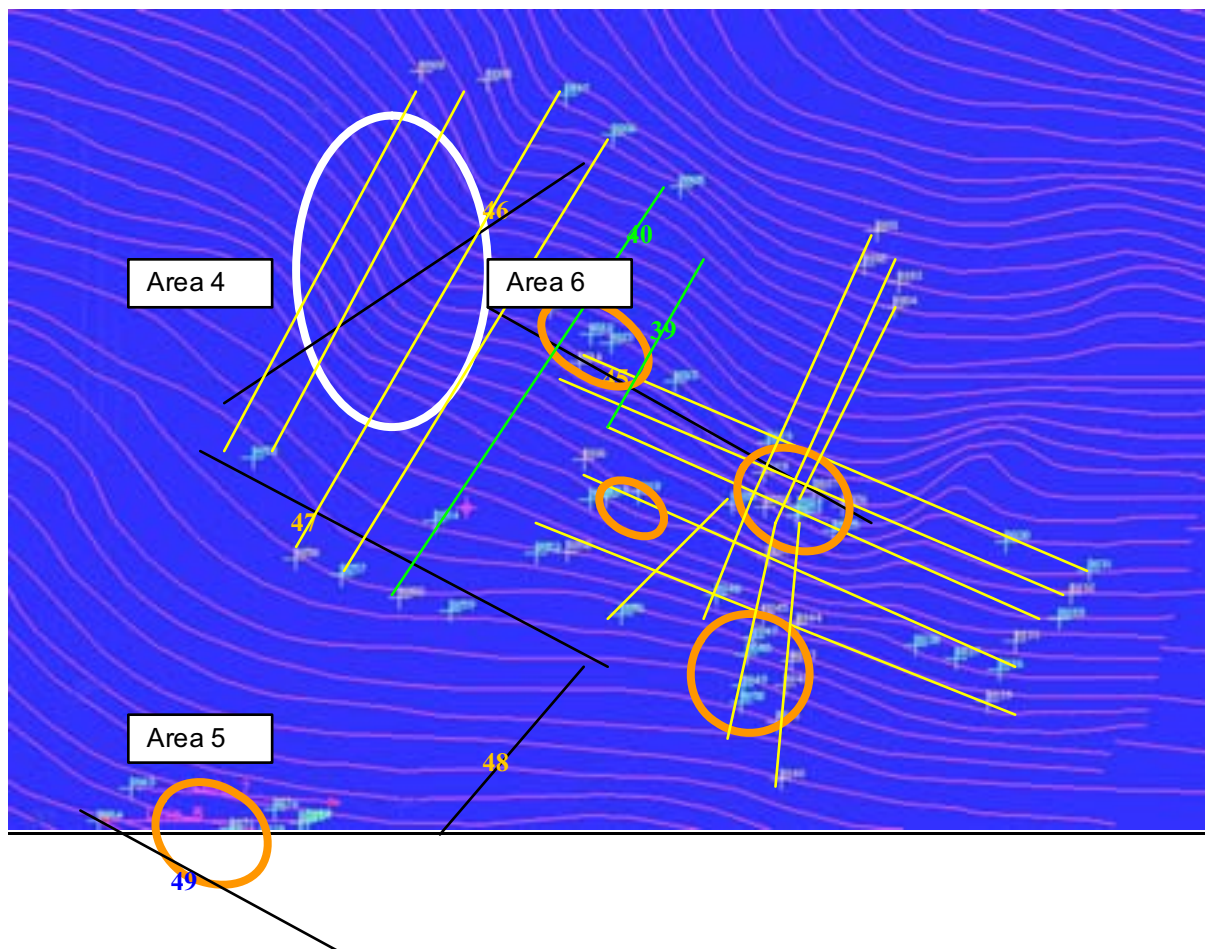
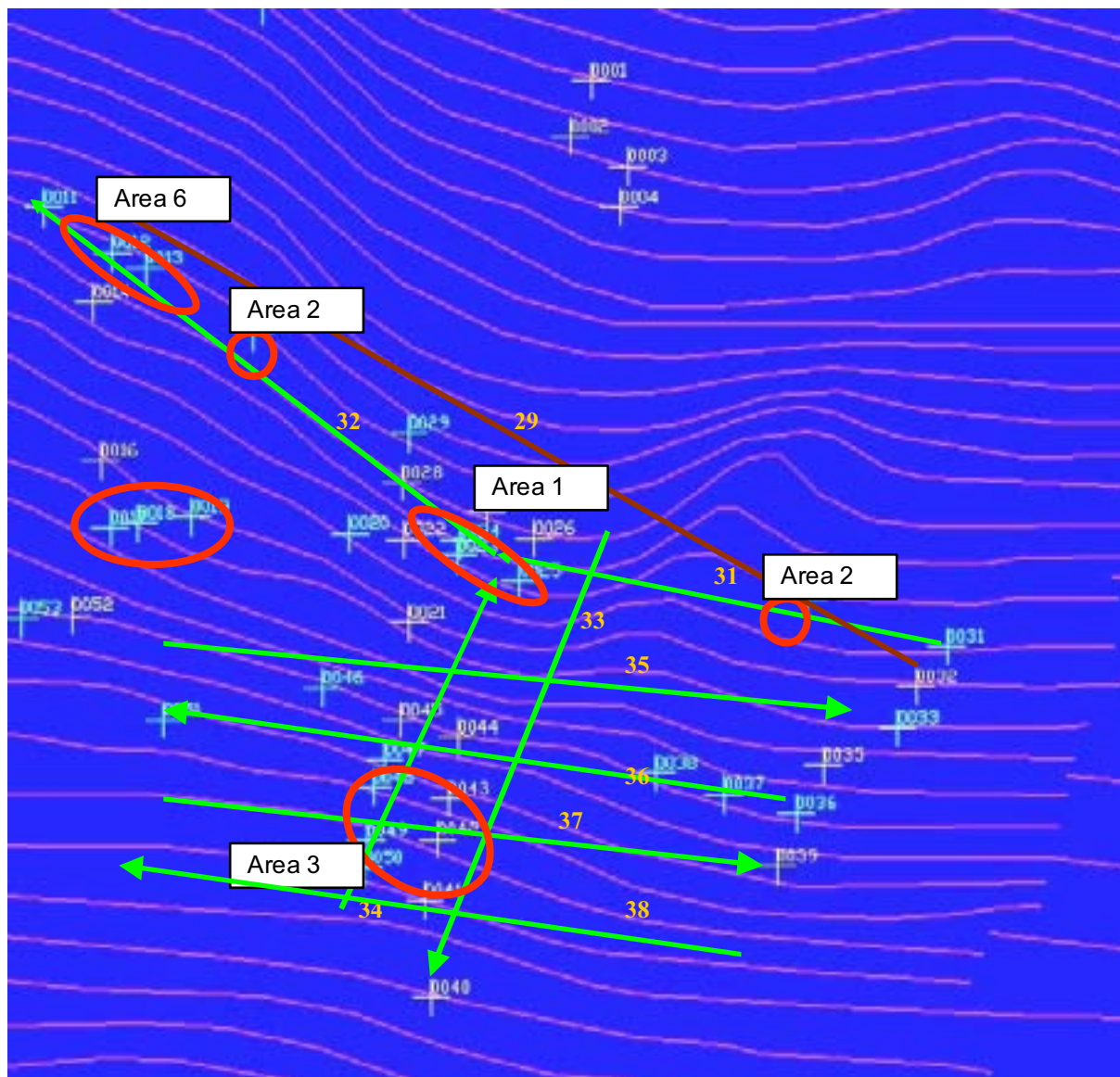


figure 34: radargram of a measuring line 49 (length: 50 m, GSSI, f = 270 MHz) with very interesting inhomogeneity in grassland

3.4 EVALUATION OF RESULTS

In the picture above the measuring lines and the areas with inhomogeneities are shown.





Area 1:	Depth of inhomogeneity: 0,8-1,0 m
Area 2	Edge of Kapija (left and right) Depth of inhomogeneity: 0,9 - 1,2 m
Area 3:	Edge of Kapija (top) Depth of inhomogeneity: 0,9-1,0 m
Area 4:	In the whole area are no inhomogenies
Area 5:	North of all the measuring area Depth of inhomogeneity: 0,9-1,0 m
Area 6:	Closed to area 2, outside of "Kapija" Depth of inhomogeneity: 1,5 – 2,1 m

3.5 RADARGRAMS OF MEASUREMENTS

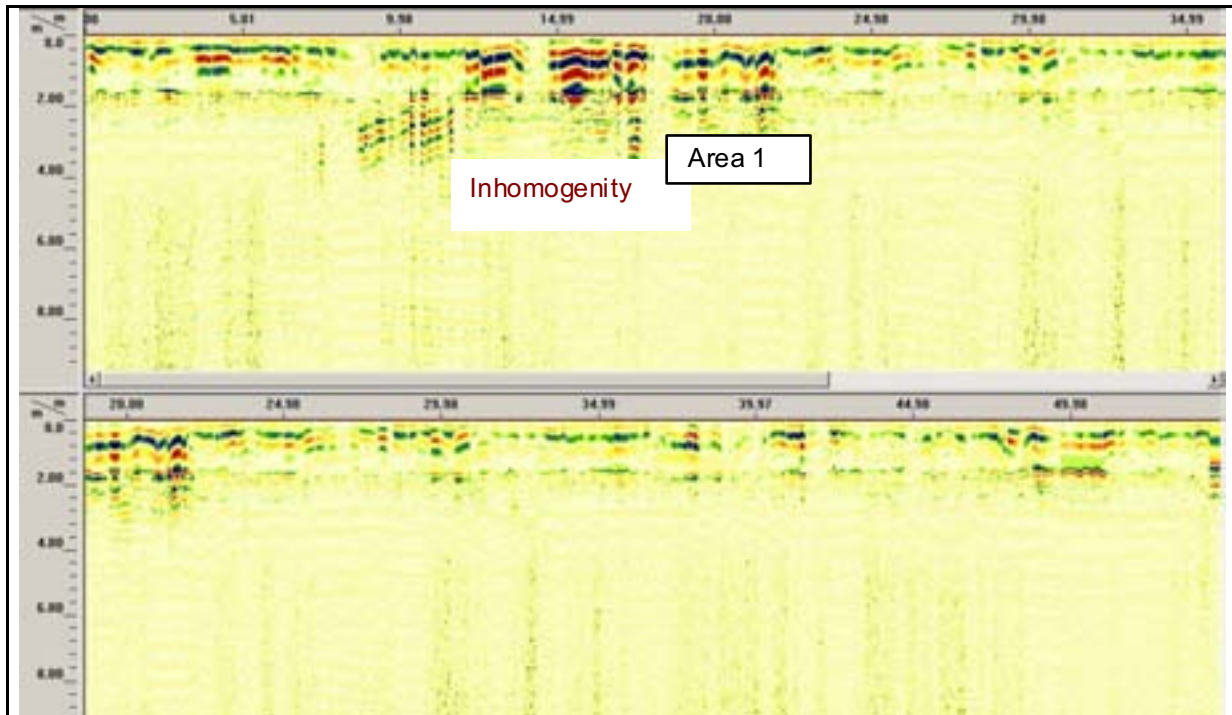


figure 35: radargram of a measuring along measuring line 29 (length: 55,0 m, GSSI, f = 100 MHz) with inhomogeneity

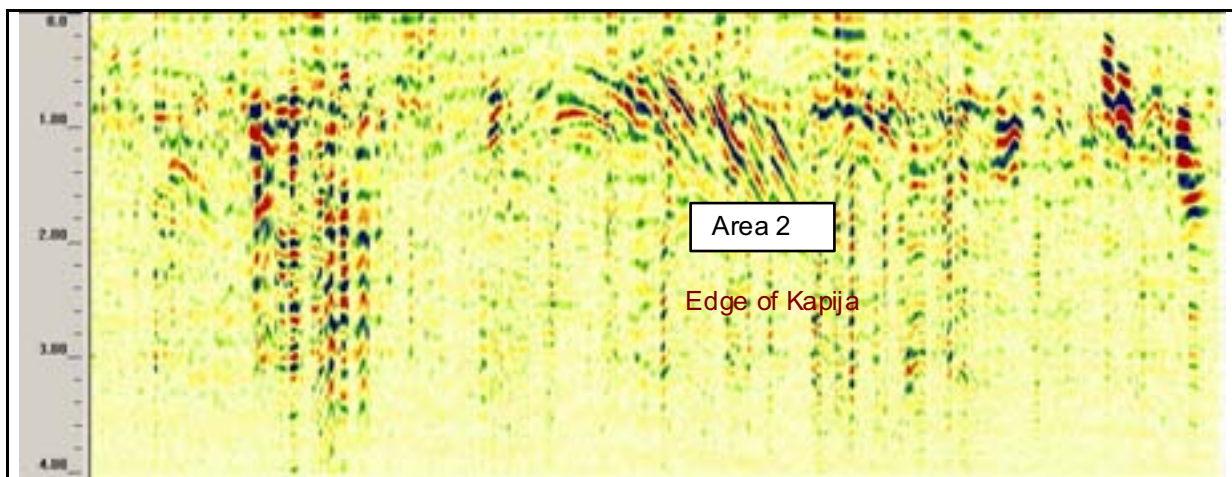


figure 36: radargram of a measuring along measuring line 31 (length: 52,1 m, GSSI, f = 270 MHz) with inhomogeneities and edge of Kapija

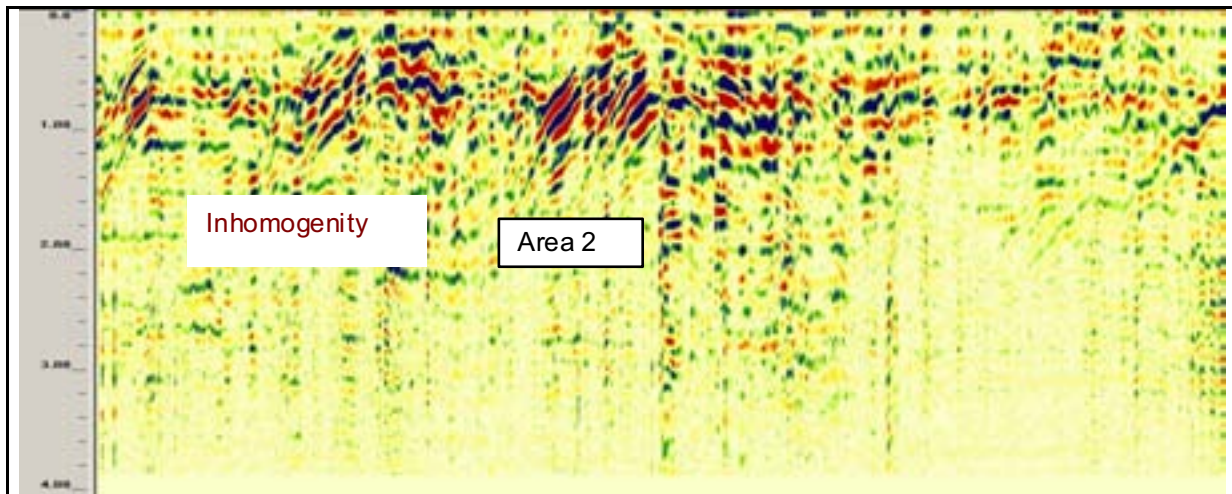


figure 37: radargram of a measuring along measuring line 32 (length: 48,3 m, GSSI, f = 270 MHz) with inhomogenities and edge of Kapija

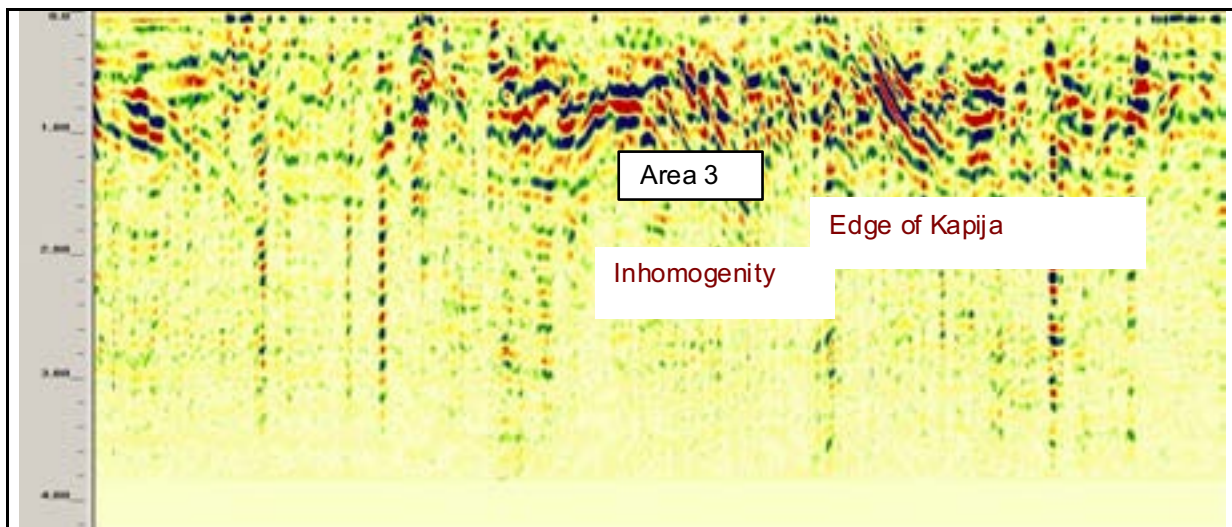


figure 38: radargram of a measuring along measuring 33 line (length: 50,4 m, GSSI, f = 270 MHz) with inhomogenities and edge of Kapija

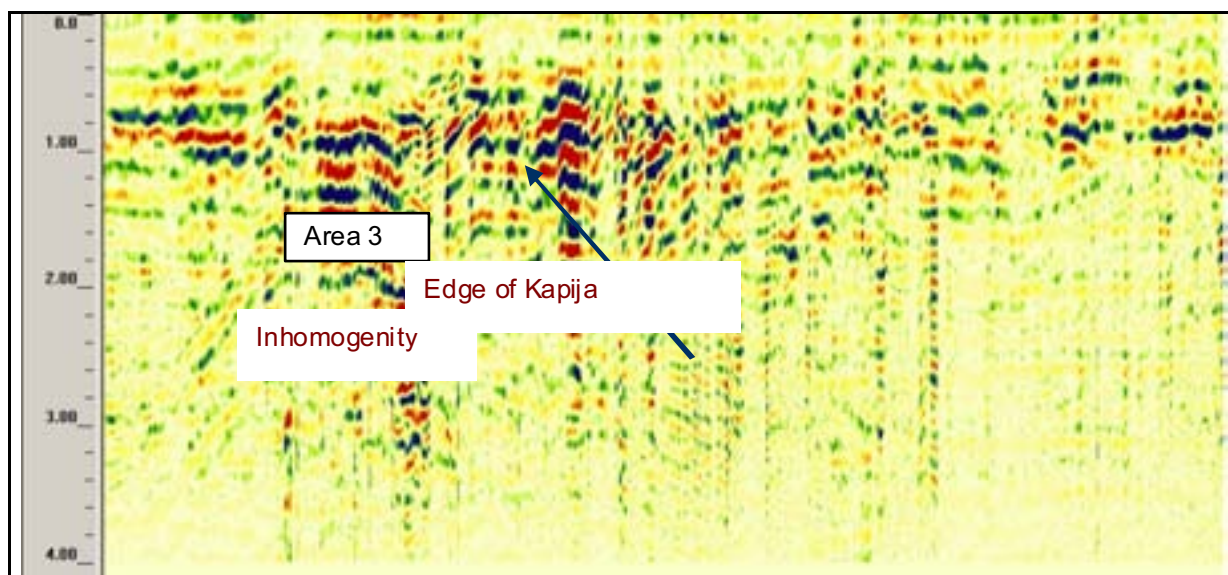


figure 39: radargram of a measuring along measuring line 34 (length: 46,1 m, GSSI, f = 270 MHz) with inhomogeneities and edge of Kapija

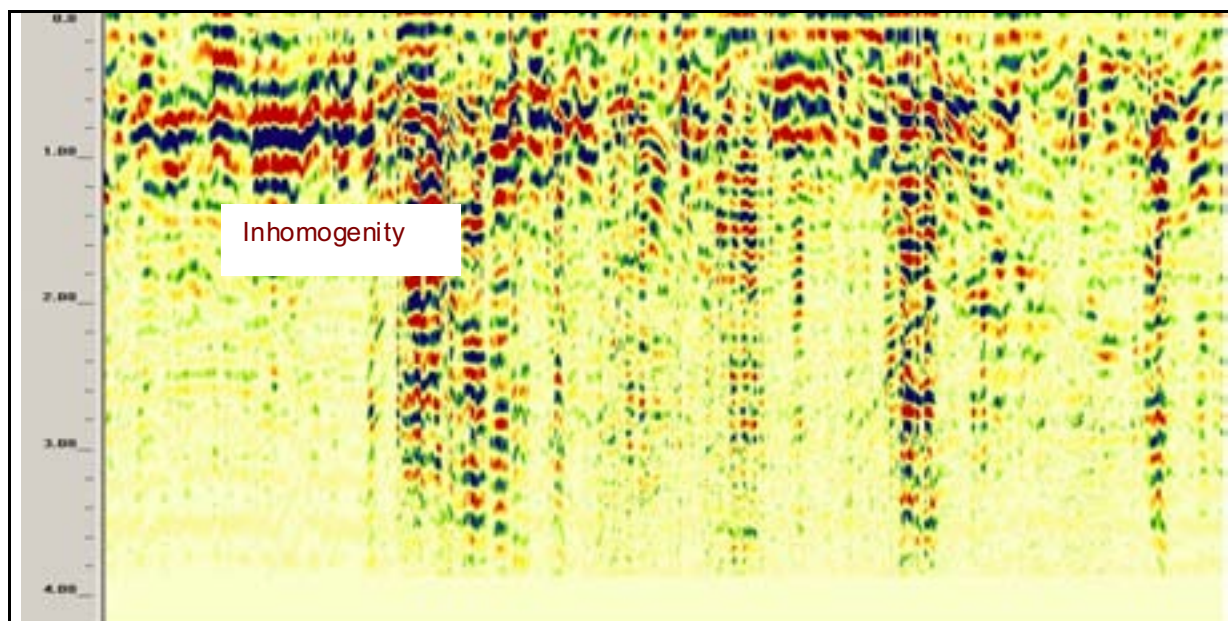


figure 40: radargram of a measuring along measuring line 35 (length: 43,9 m, GSSI, f = 270 MHz) with inhomogeneities

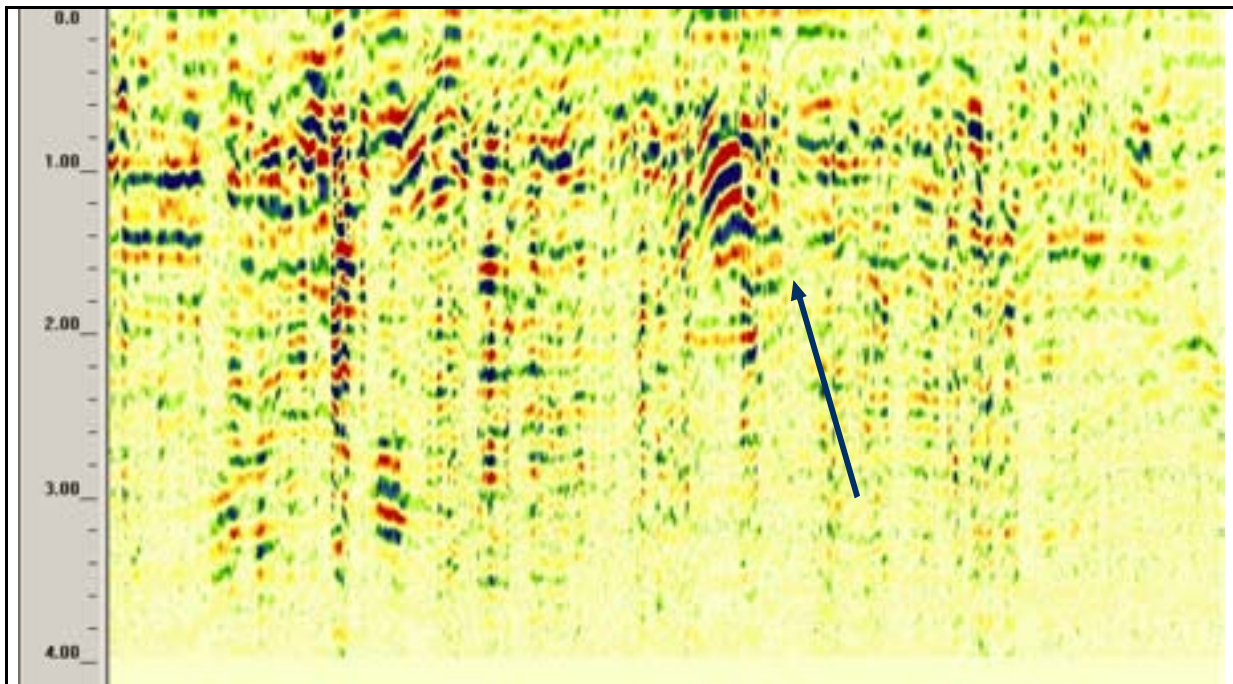


figure 41: radargram of a measuring along measuring line 36 (length: 42 m, GSSI, $f = 270$ MHz) with inhomogeneities

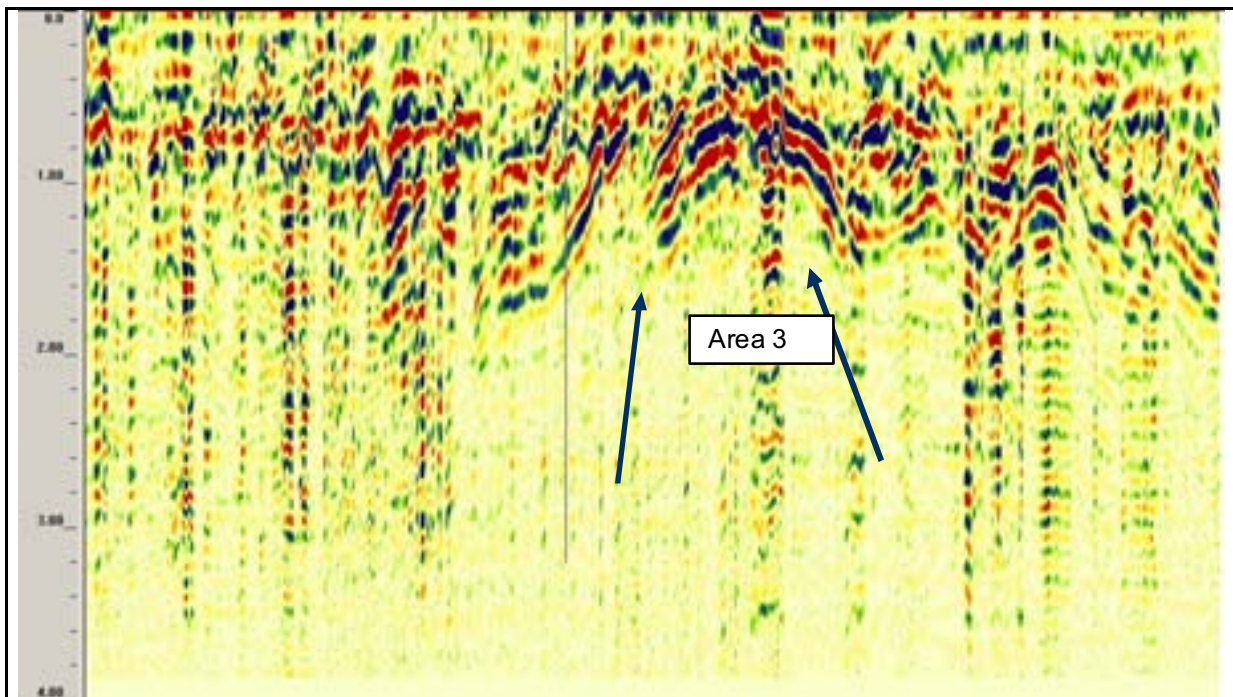


figure 42: radargram of a measuring along measuring line 37 (length: 57 m, GSSI, $f = 270$ MHz) with important inhomogeneity

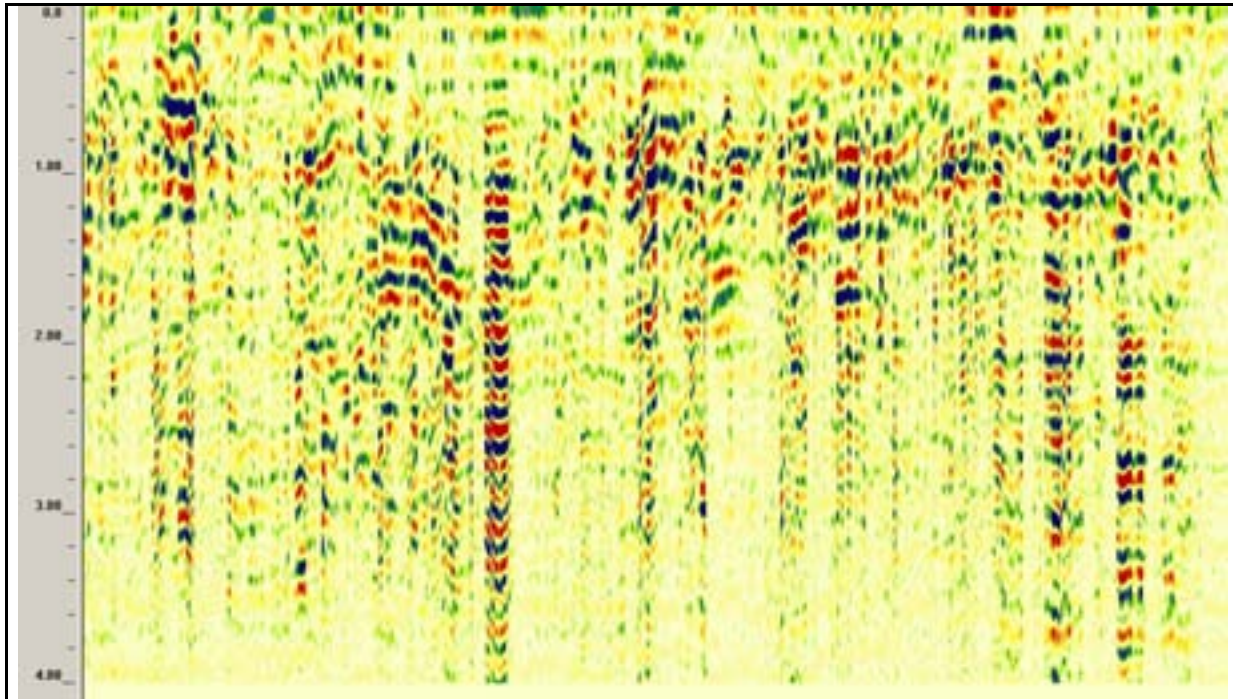


figure 43: radargram of a measuring along measuring line 38 (length: 57 m, GSSI, f = 270 MHz) with small reflectors

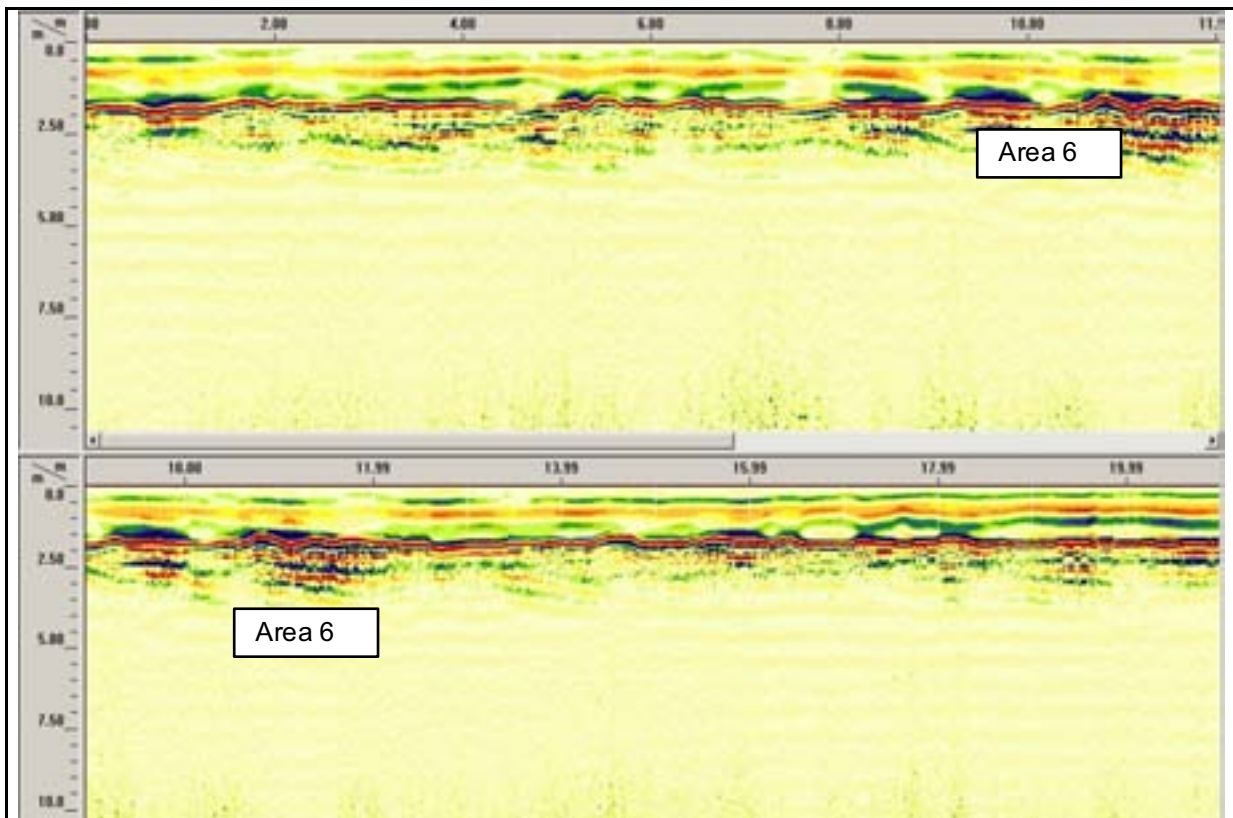


figure 44: radargram of a measuring along measuring line 39 (length: 21 m, GSSI, f = 100 MHz) with inhomogeneities

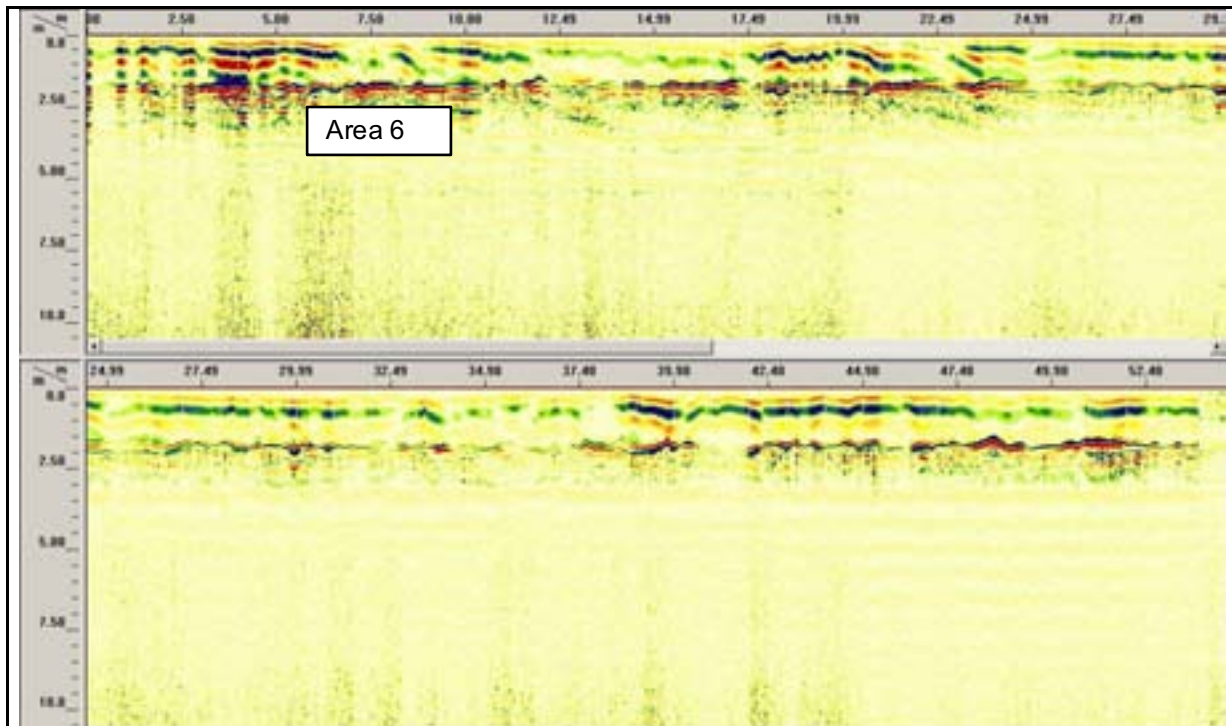


figure 45: radargram of a measuring along measuring line 40 (length: 54,5 m, GSSI, f = 100 MHz) with small inhomogenities

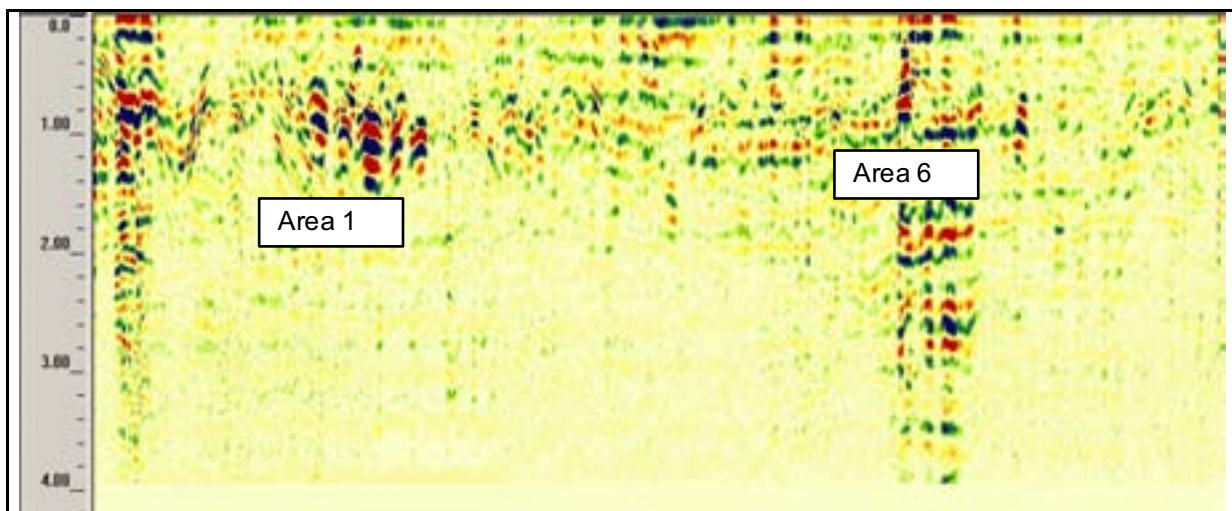


figure 46: radargram of a measuring along measuring line 45 (length: 51 m, GSSI, f = 270 MHz) with inhomogenities

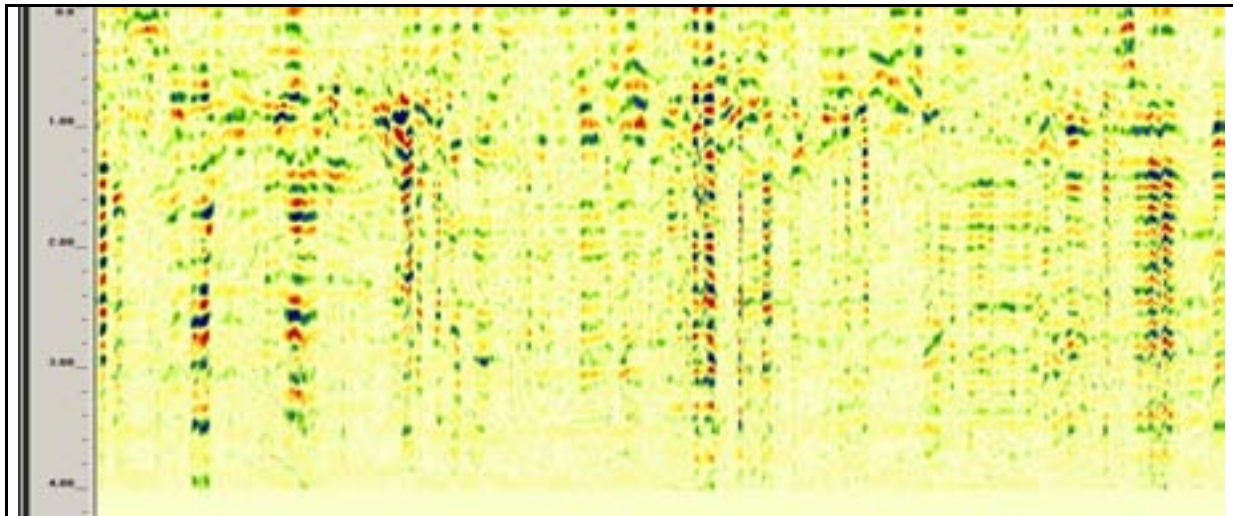


figure 47: radargram of a measuring along measuring line 46 (length: 43 m, GSSI, $f = 270$ MHz) with no inhomogenities

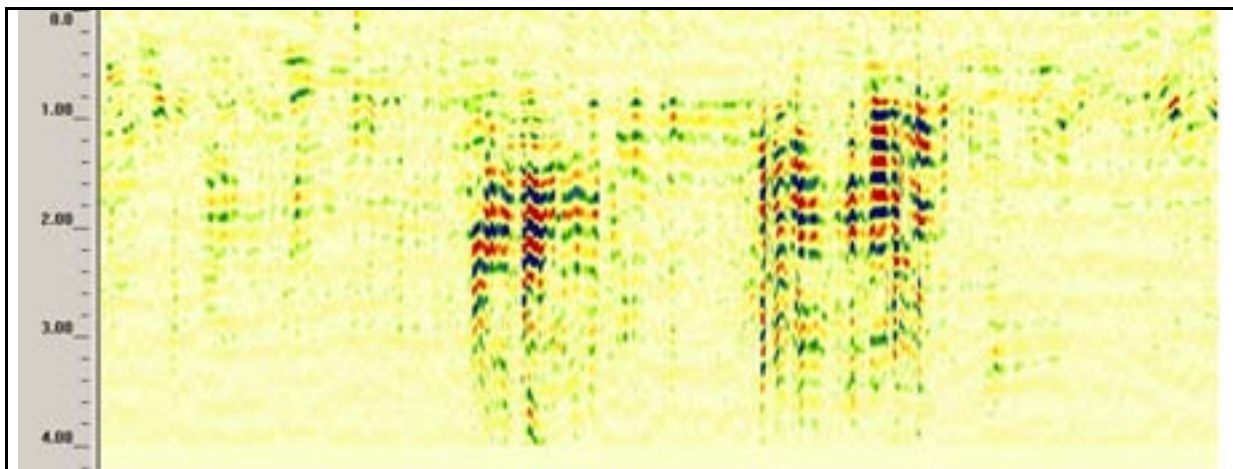


figure 48: radargram of a measuring along measuring line 47 (length: 46 m, GSSI, $f = 270$ MHz) with inhomogenities

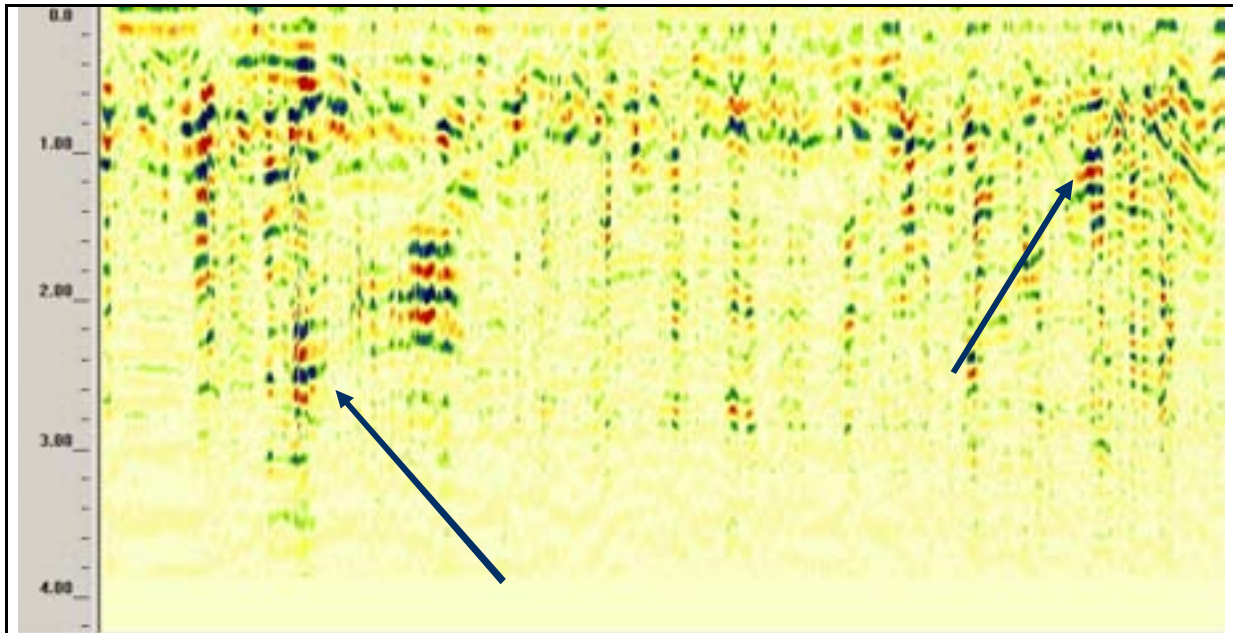


figure 49: radargram of a measuring along measuring line 48 (length: 44 m, GSSI, f = 270 MHz) with inhomogenities

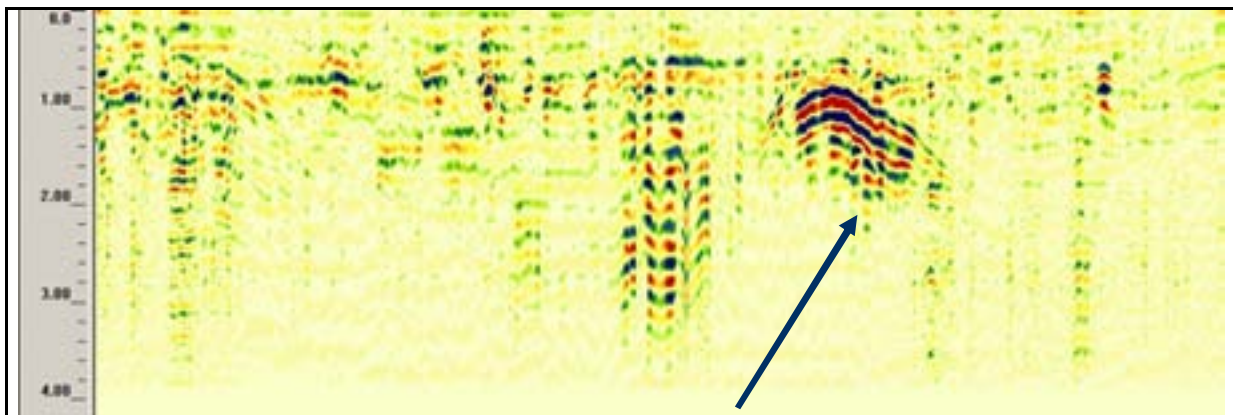


figure 50: radargram of a measuring along measuring line 49 (length: 50 m, GSSI, f = 270 MHz) with very interesting inhomogeneity

4 STONE PLATES ABOVE GRASSLAND OF KAPIJA

4.1 Local conditions



figure 51: area of measurements

The measurements were done at different areas near to the stone plates at the edge of the forest.



figure 52: view of measurements with sticks to sign the inhomogeneities

4.2 Coordinating System of the measuring area

The measuring lines go parallel or in right angle to the hill.

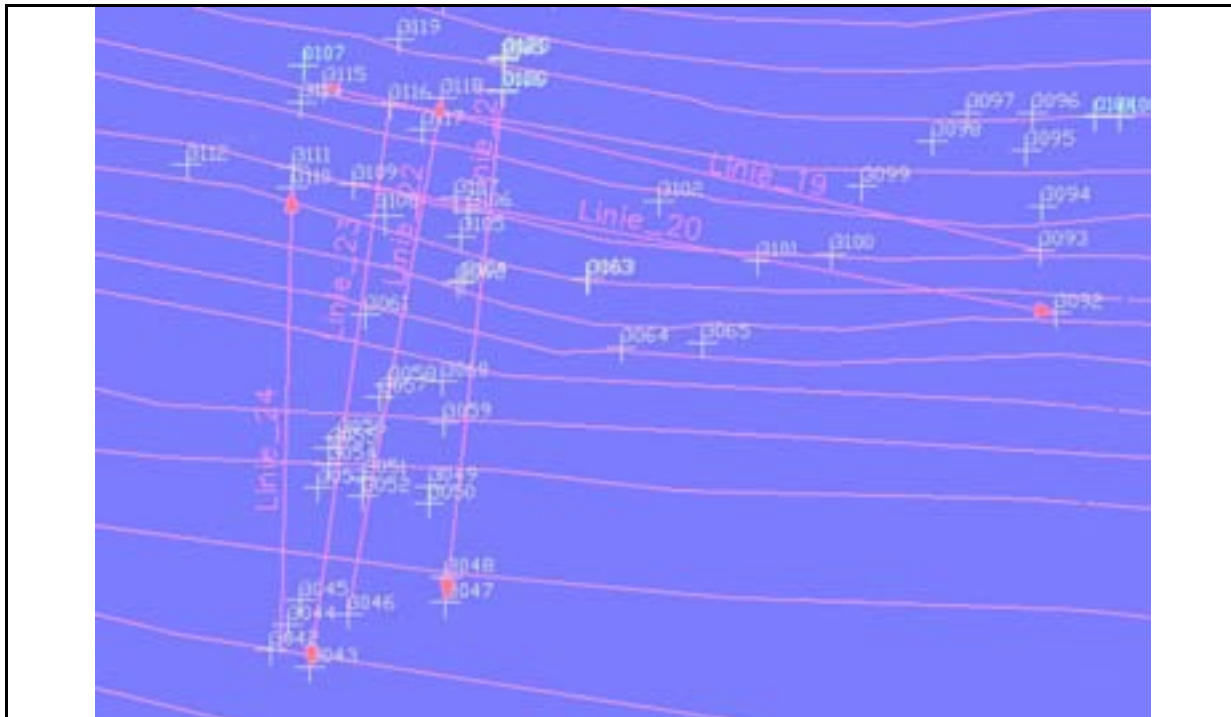


figure 53: overview of position of measuring lines 19-24

4.3 RESULTS OF THE MEASUREMENTS

The measurement shows, that it is possible to find inhomogenities with radar. Beside the expected echo of the stone plates are even some other results.

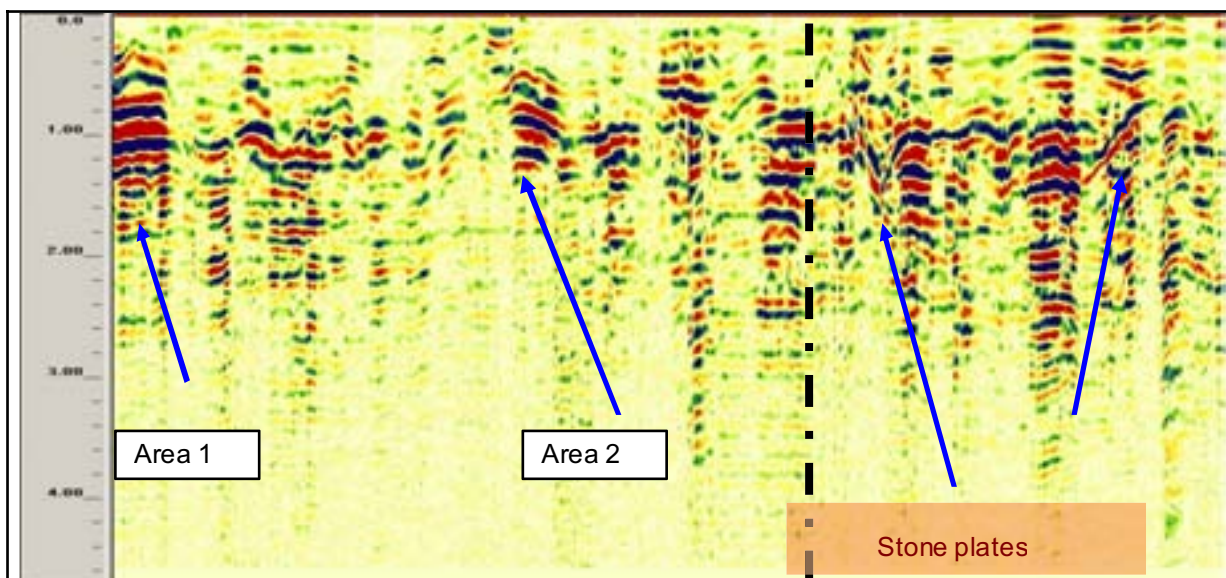


figure 54: radargram of a measuring line 24 (length: 27 m) (GSSI, f = 270 MHz), the left two arrows show inhomogenities in the ground, the right arrows show the beginning and end of the stone plates

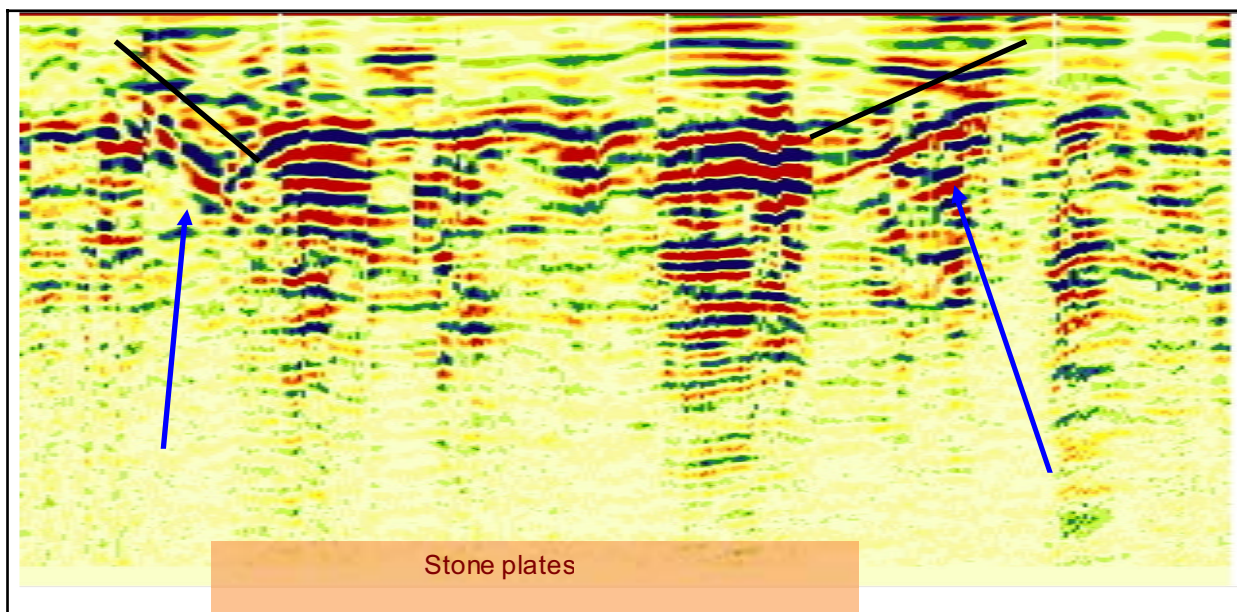
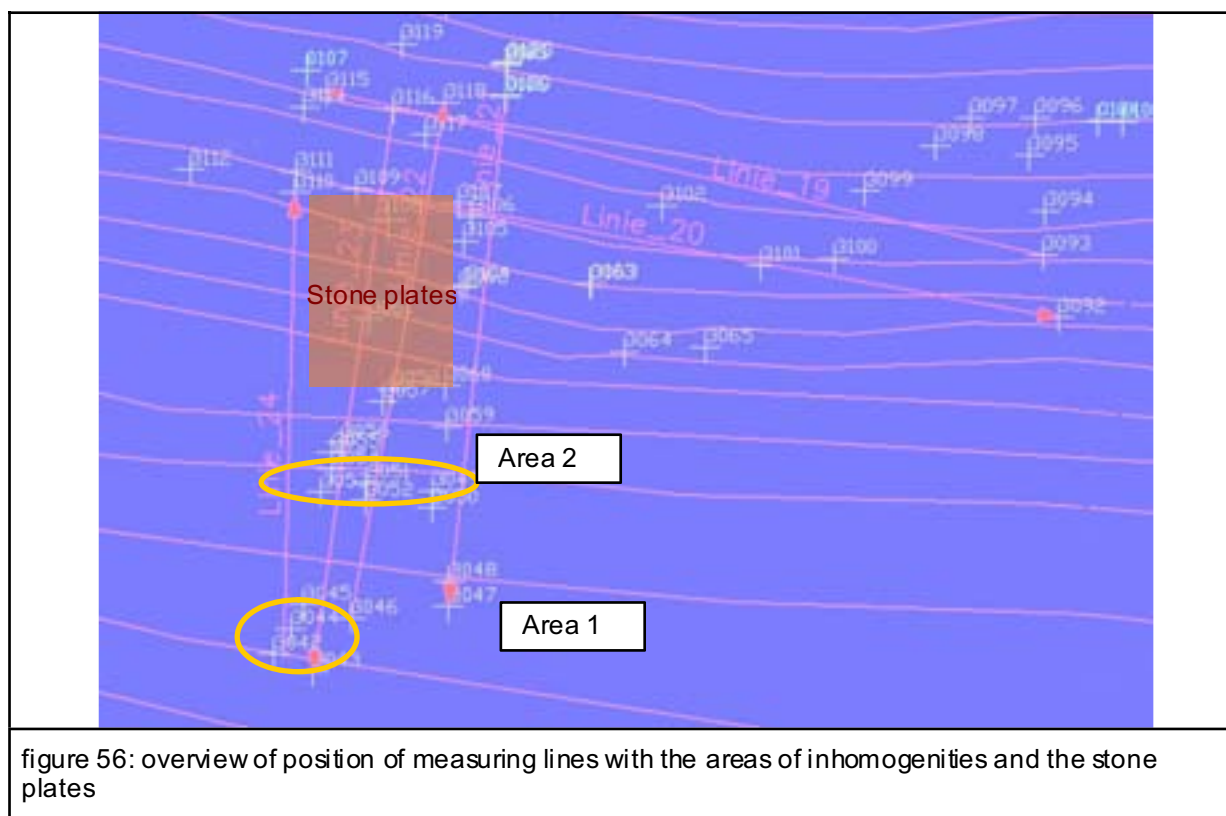


figure 55: part of radargram above to see more details: left the beginning and right the end of the stone plates, because of the moving of the antenna like a diagonal line

4.4 EVALUATION OF RESULTS



Area 1:	At the end of line 23 and beginning of line 24 (in the forest) Depth of inhomogeneity: 0,9 m
Area 2	Area hit by line 21, line 22, line 23, line 24 Depth of inhomogeneity: 1,2 m



figure 57: marked inhomogeneities in the measuring field (Area 2)

4.5 RADARGRAMS OF MEASUREMENTS

In the appendix all radargrams of the measurements are shown.

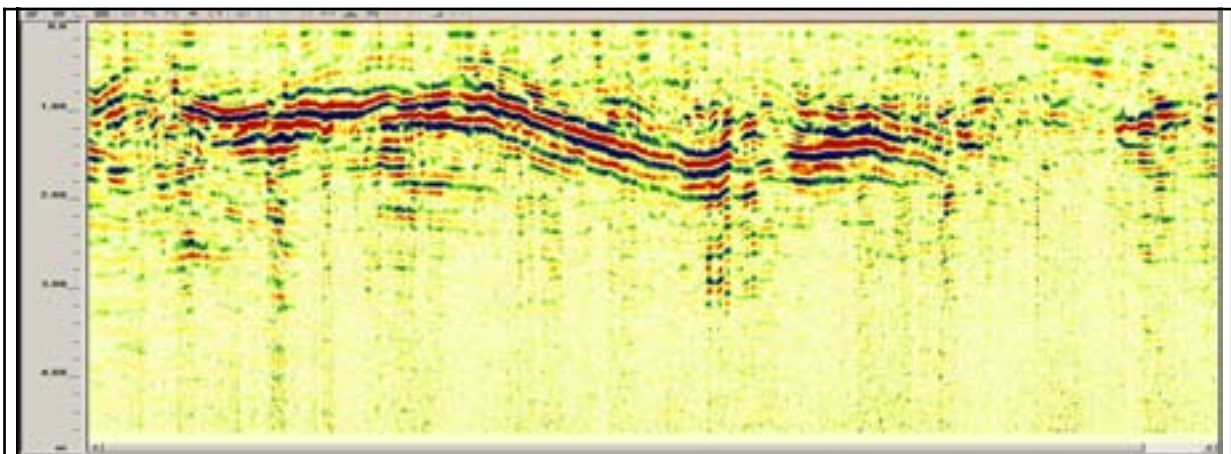


figure 58: radargram of a measuring along measuring line 19 (length: 38,5 m GSSI, $f = 270$ MHz) with echo from a depth of 1,0 - 1,5 m along the line

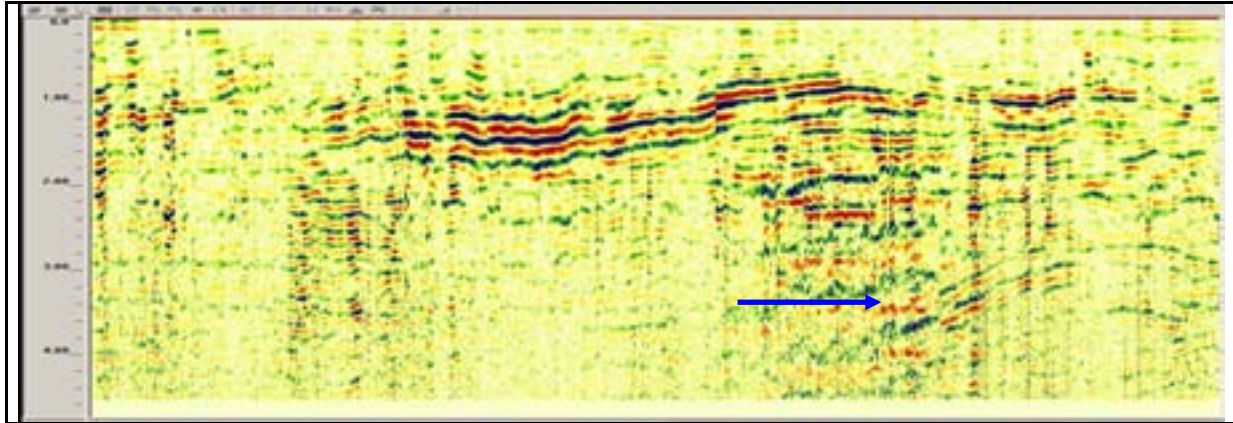


figure 59: radargram of a measuring along measuring line 20 (length: 38 m, GSSI, f = 270 MHz) with echo from a depth of 1,2 – 0,9 m along the line (and also echo from 3,5 m in the right part)

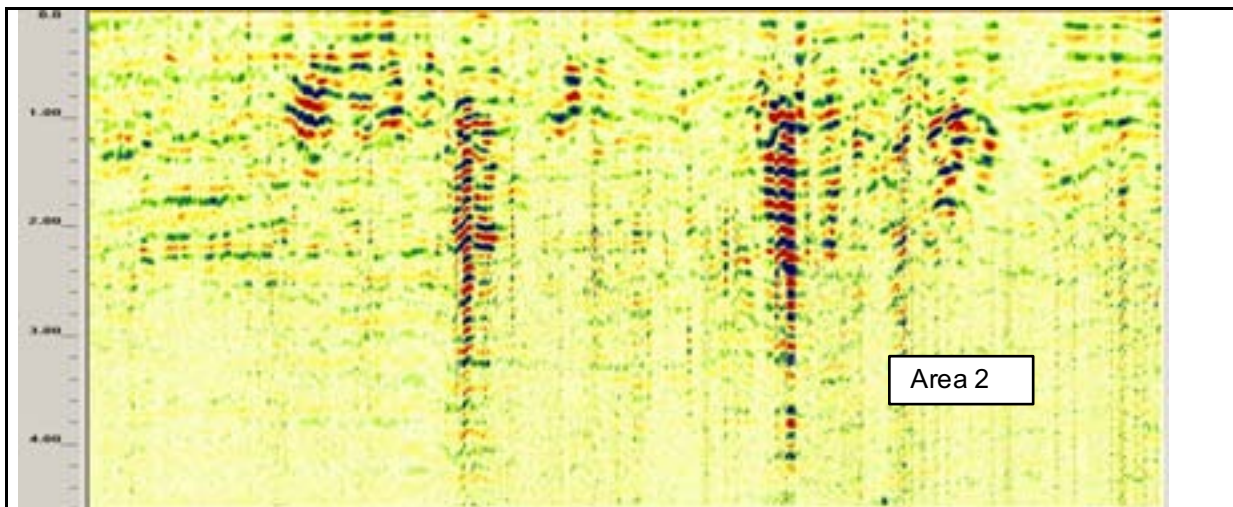


figure 60: radargram of a measuring along measuring line 21 (length: 29 m, GSSI, f = 270 MHz)

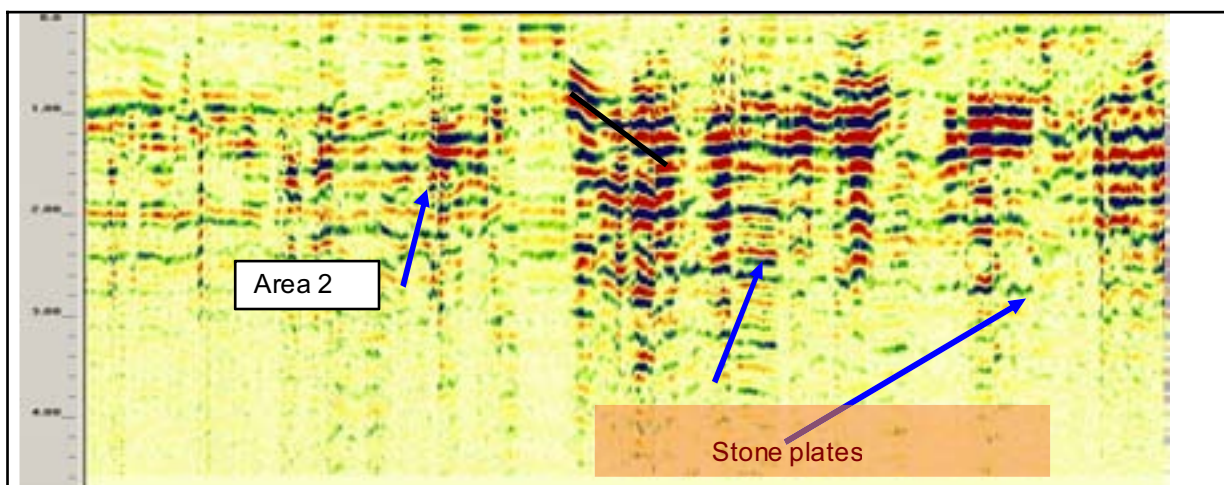


figure 61: radargram of a measuring along measuring line 22 (length: 31,5 m, GSSI, f = 270 MHz), on the right side echo of the stone plates

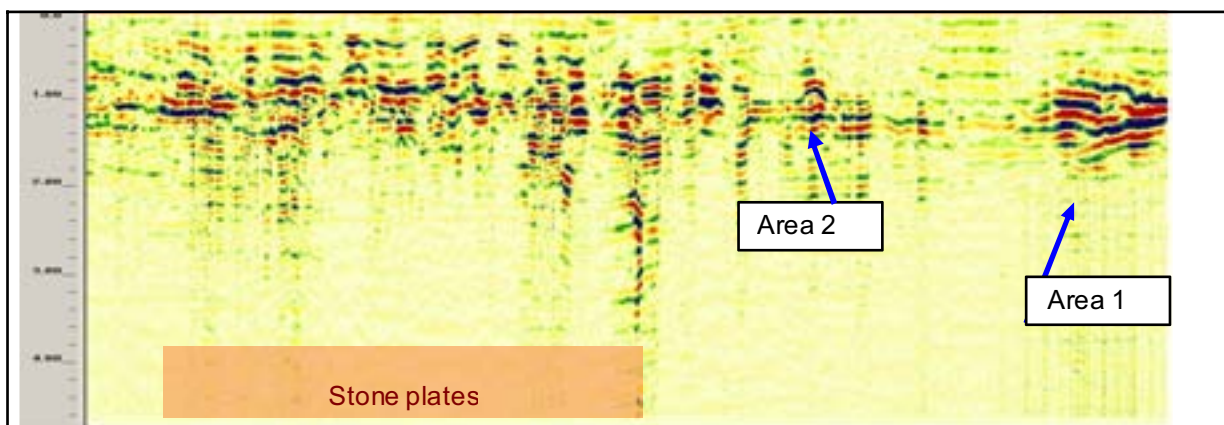


figure 62: radargram of a measuring along measuring line 23 (length: 32 m, GSSI, f = 270 MHz) stone plates on the left side, inhomogeneity on the right side

5 STONEPLATES SONDE 4A

5.1 Local conditions



figure 63: area of measurements

The measurements were carried out at different areas close to Sonde 4A.

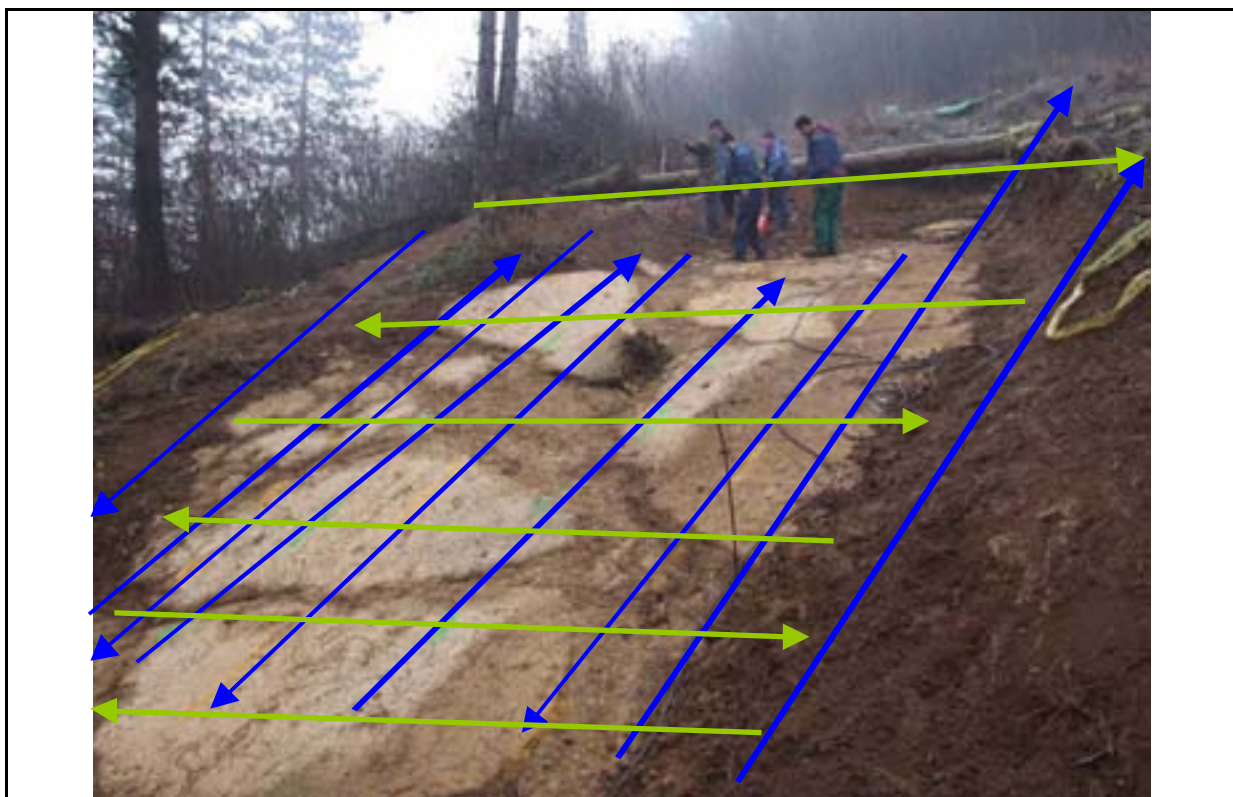


figure 64: view of measurements on stone plates



figure 65: view of measuring area



figure 66: The electricity cable doped to the measuring area. The high voltage influenced the 100 MHz radar measurement.

5.2 Coordinating System of the measuring area

The measuring lines go parallel or in right angle to the hill.

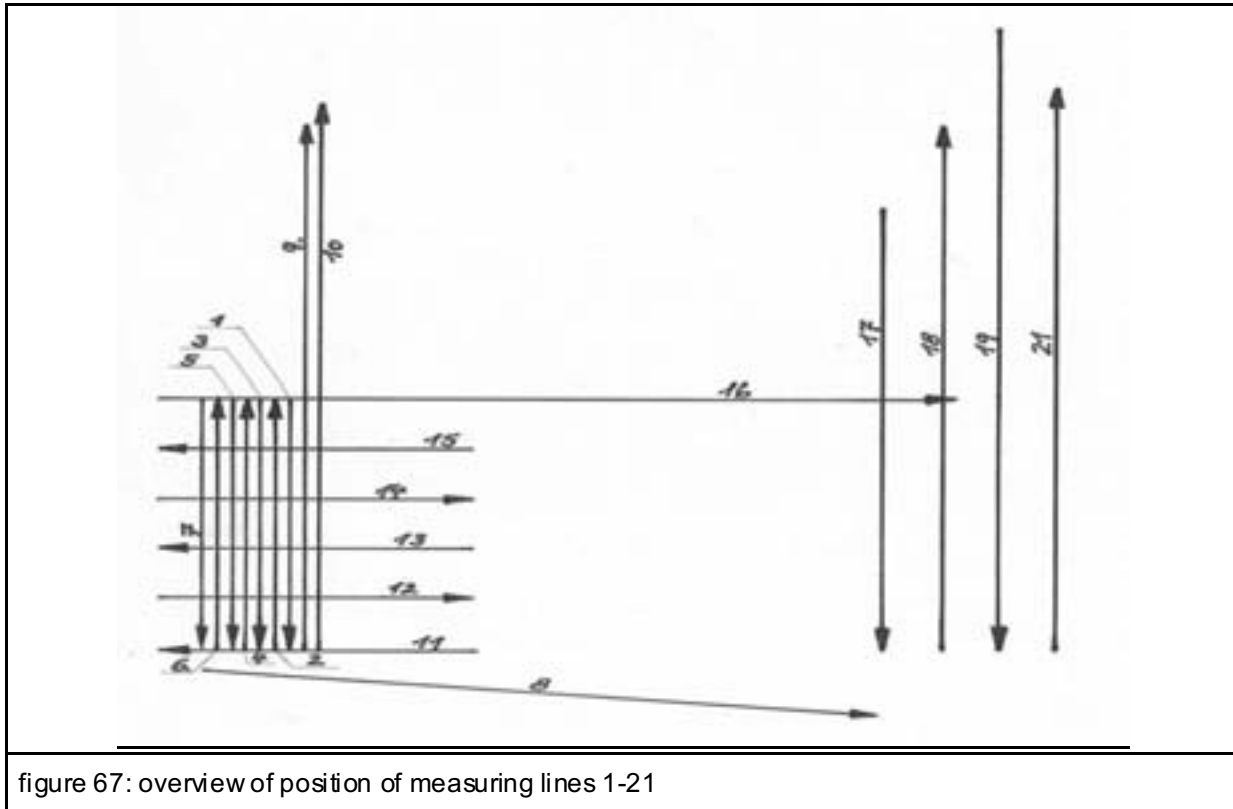


figure 67: overview of position of measuring lines 1-21

5.3 RESULTS OF THE MEASUREMENTS

The measurements were carried out with an 270 MHz and an 100 MHz radar antenna. The ground was very wet, what result to bad conditions for radar measurements. Anyw here the results with the 270 MHz antenna were very good. The results of the 100MHz antenna were not so good, the damping and the influences of area around and the signals from the electricity were to high. Following the results of measurements at the stone plates are shown. The radargram below, show that in some areas just the upper layer of stone plates is found.

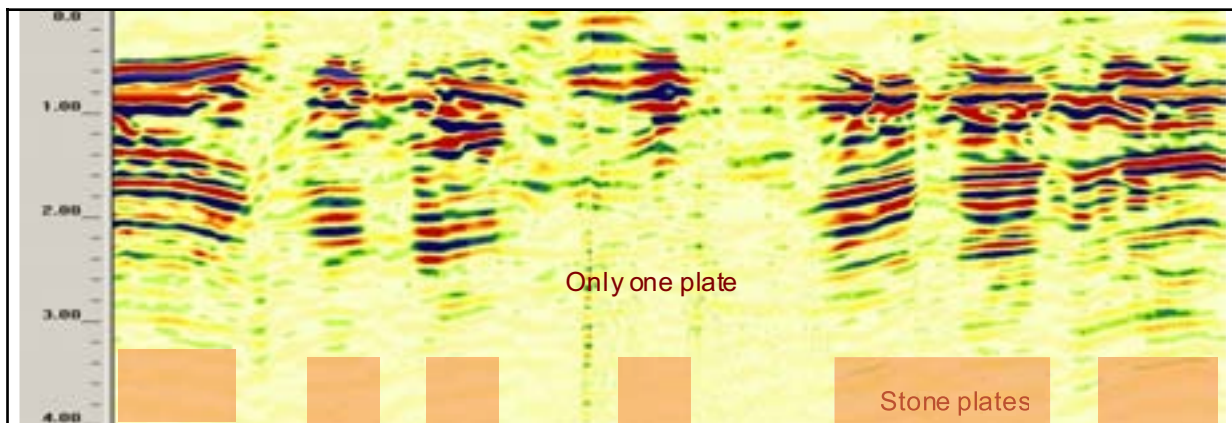


figure 68: radargram of a measuring along line 3 (length: 12,4 m, GSSI, f = 270 MHz) with two layers of stone plates, in the middle of the measurement the second plate is missing

To get a better understanding of the structure some radargrams were registered in parallel lines (here every 0,5 m) and time slides have been calculated.

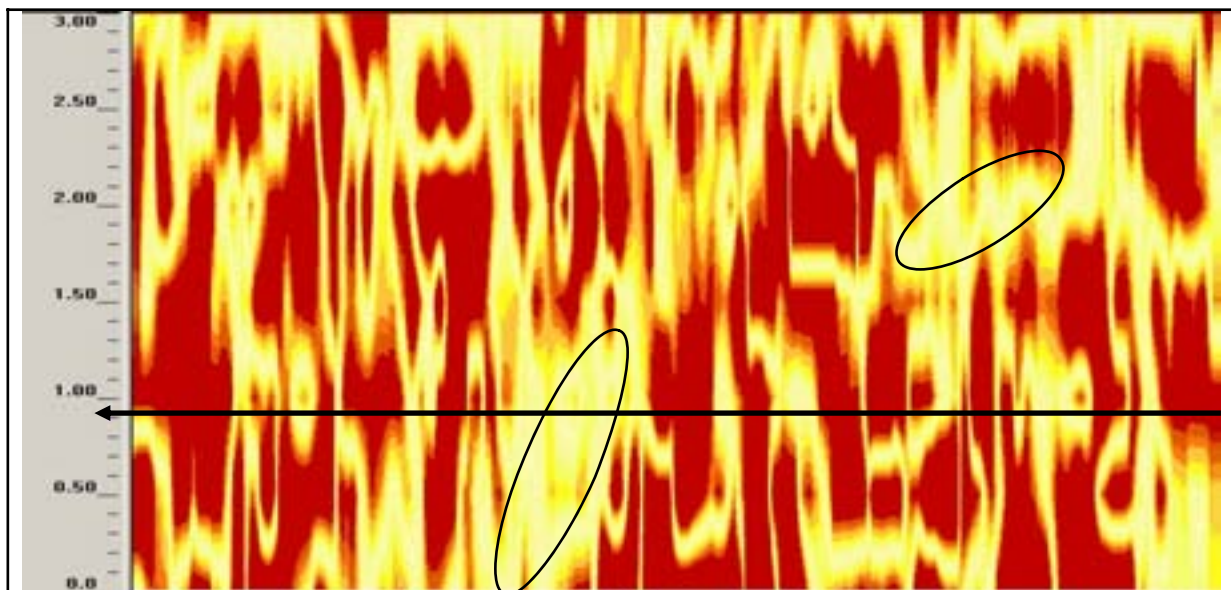


figure 69: time slide of radar measurement (GSSI, f = 270 MHz depth 0,8 m) in depth of echo of stone plates, at the marked areas no stone plates were found (look at picture at the beginning of the report), the top of the hill is on the right side, the arrow shows the position and direction of the radargram above

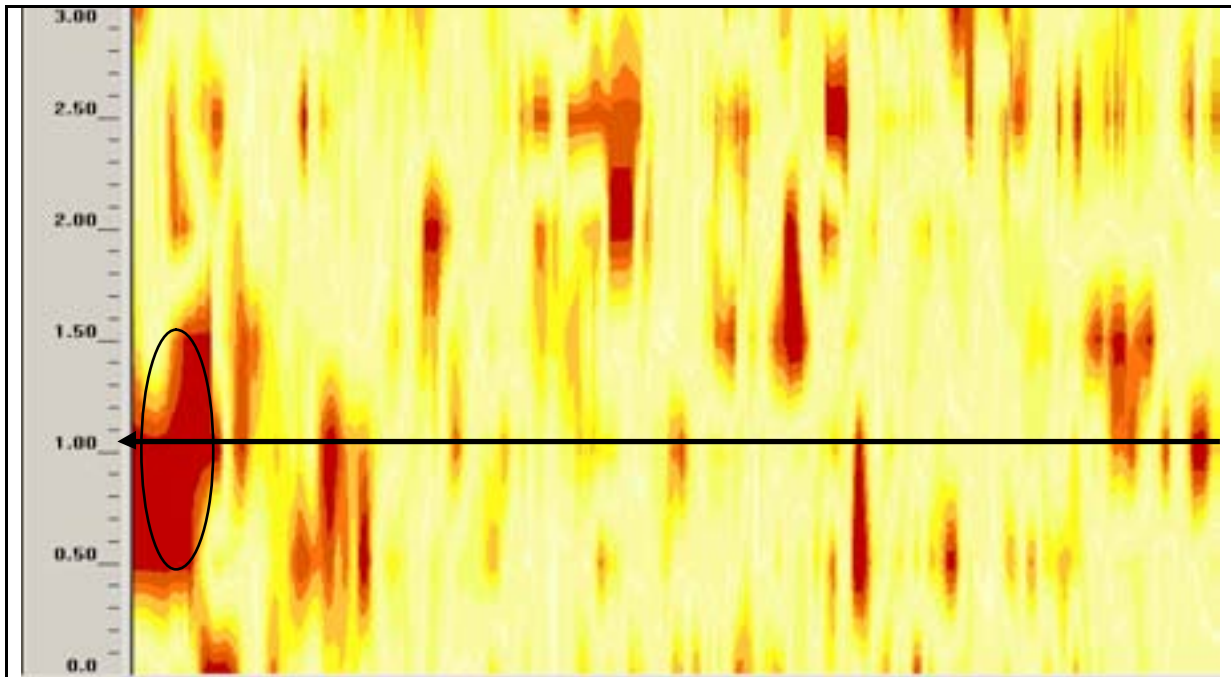


figure 70: time side of radar measurement (GSSI, f = 270 MHz depth 1,45 m) in depth of area between the two layers of stone plates, on the left side in this area echo from stone are received, the arrow shows the position and direction of the radargram above

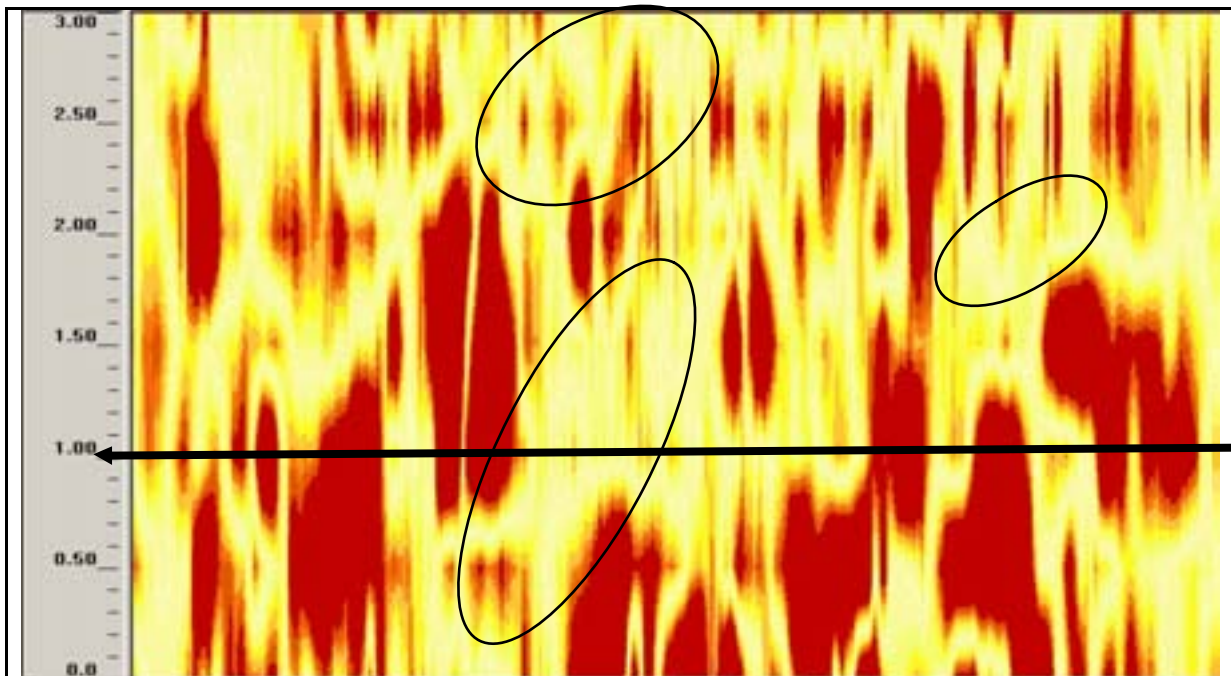


figure 71: time side of radar measurement (GSSI, f = 270 MHz depth 2,1 m) in depth 2,1 m of echo of second layer of stone plates with areas where no stone plates, the top of the hill is on the right side, the arrow shows the position and direction of the radargram above

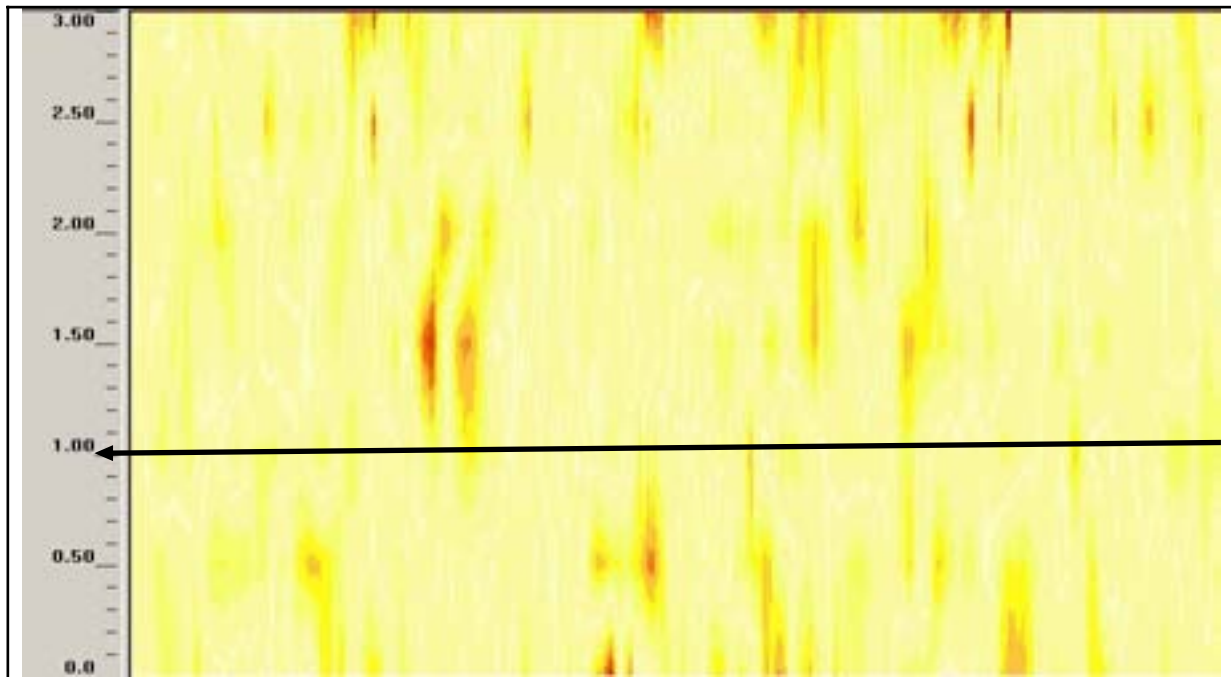


figure 72: time slice of radar measurement (GSSI, $f = 270$ MHz) in depth 2,7 m, no stone plates found

The wavelength of the 270 MHz antenna is three times smaller than of the 100MHz Antenna, that means the results are much sharper with the 270 MHz antenna. The results with the 100 MHz antenna are not as detailed. Deeper measurements were not possible because of the signal damping of wet clay.

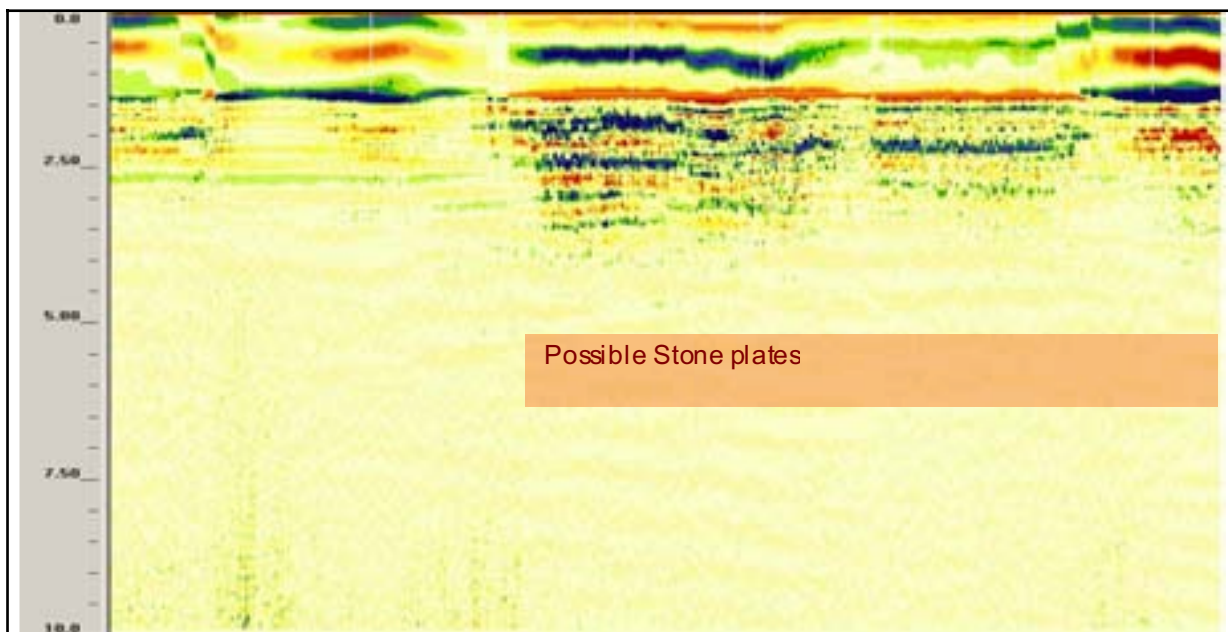
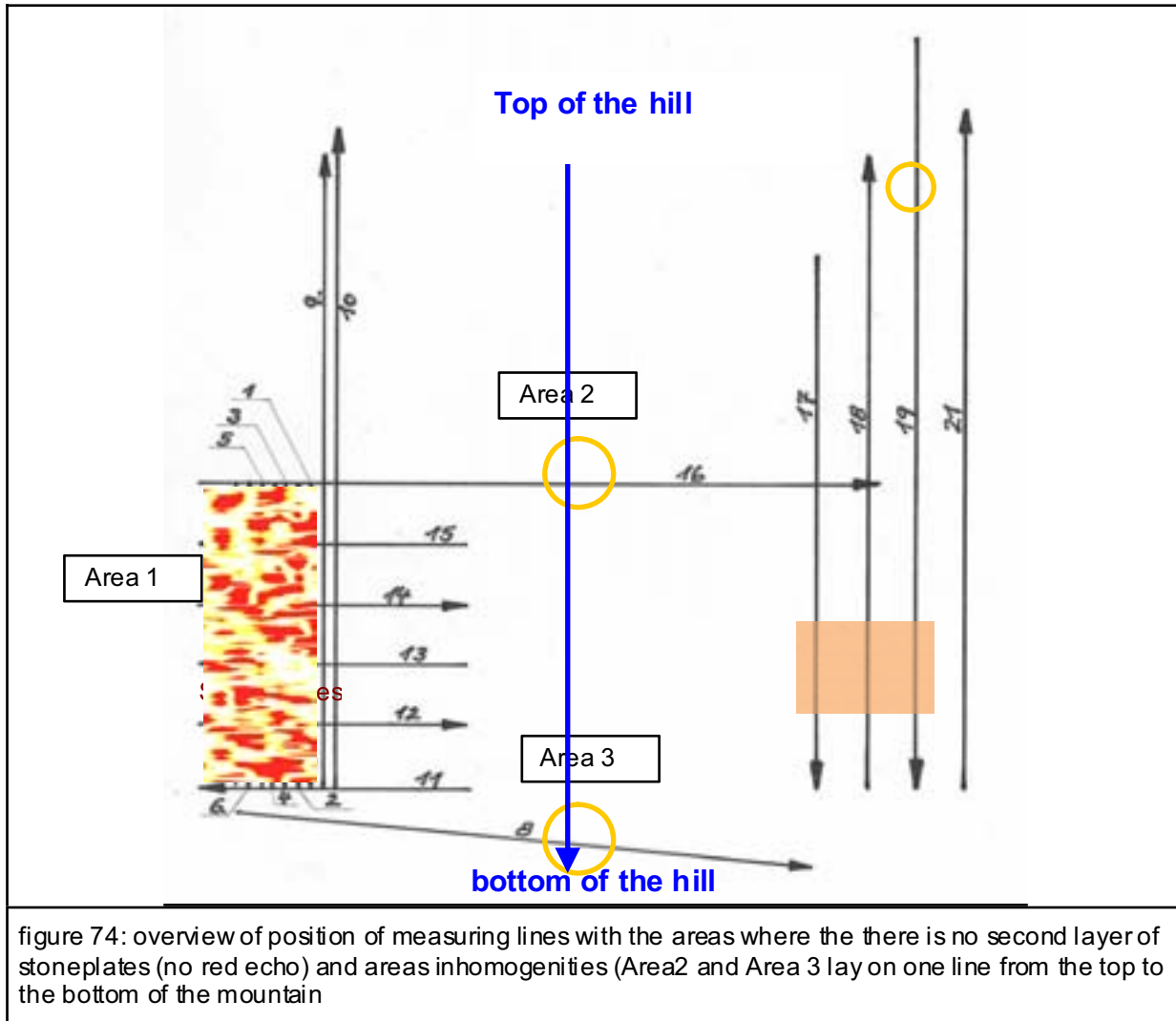


figure 73: radargram of a measuring along measuring line 23 (length: 8,5 m, GSSI, $f = 100$ MHz) stone plates on the left side, inhomogeneity on the right side

5.4 EVALUATION OF RESULTS



Area 1:	In some areas the stoneplates are just one layer
Area 2	Area hit by line 19 Depth of inhomogeneity: 1,2 m
Area 3	Area hit by line 19 Depth of inhomogeneity: 0,8 1,3 m

5.5 RADARGRAMS OF MEASUREMENTS

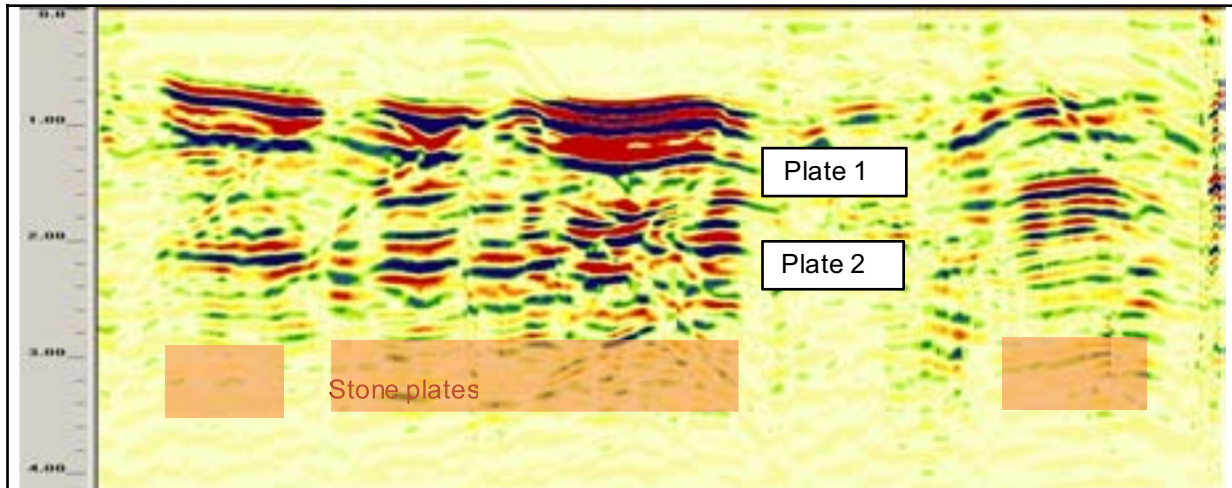


figure 75: radargram of a measuring along measuring line 1 (length: 13 m, GSSI, $f = 270$ MHz) with two layers of stone plates

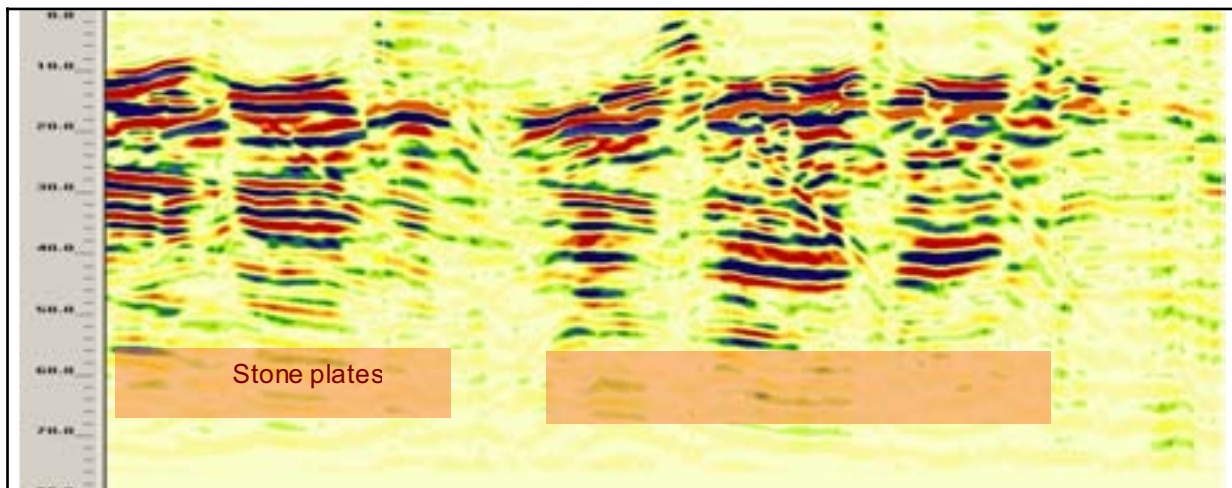


figure 76: radargram of a measuring along measuring line 2 (length: 13 m, GSSI, $f = 270$ MHz, depth in ns) with two layers of stone plates

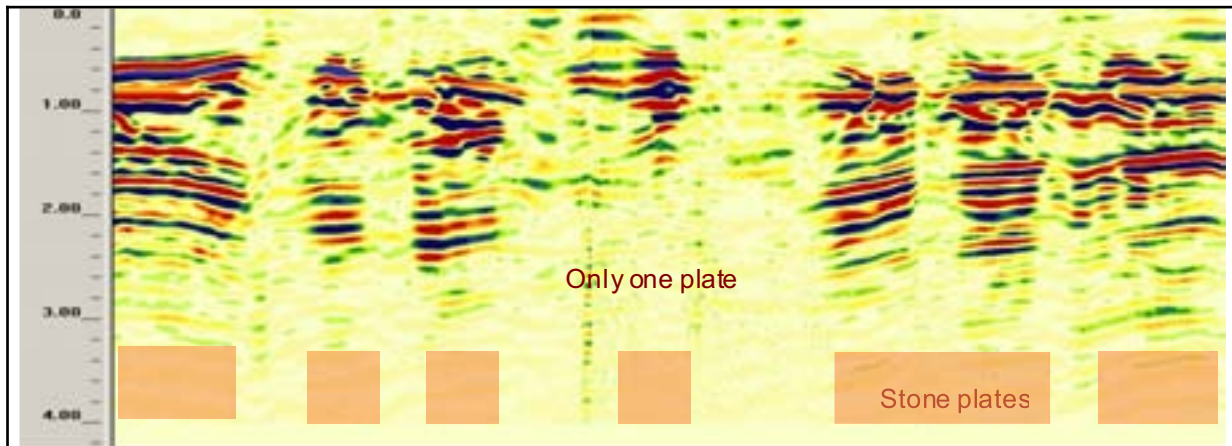


figure 77: radargram of a measuring along measuring line 3 (length: 12,4 m, GSSI, f = 270 MHz) with two layers of stone plates, in the middle of the measurement the second plate is missing

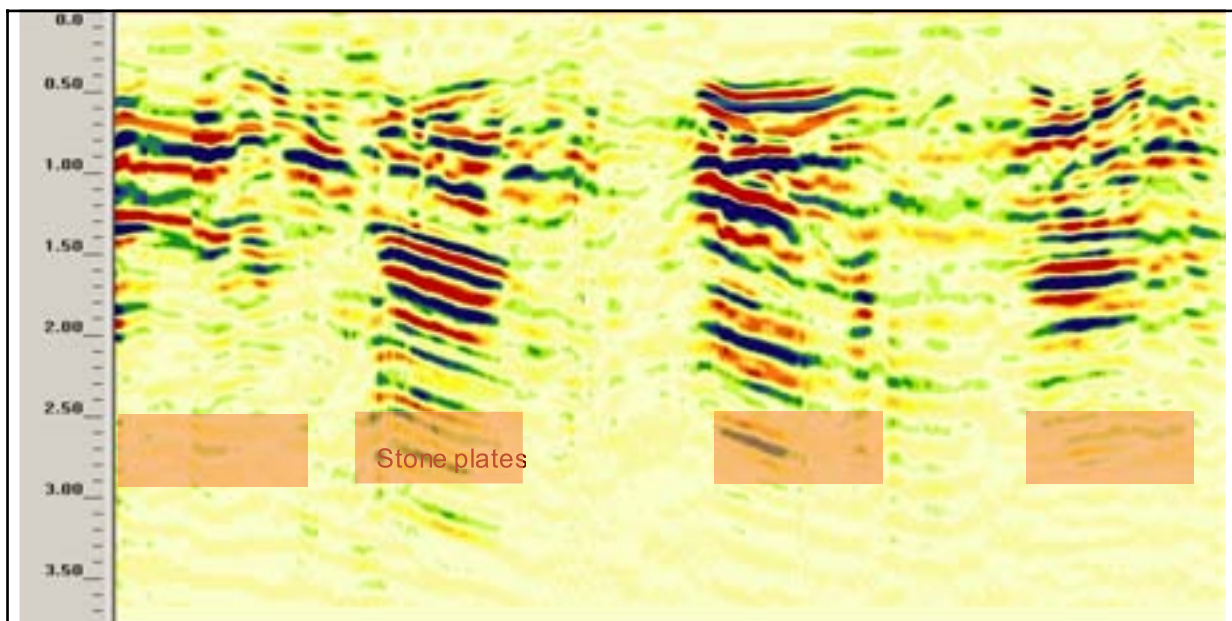


figure 78: radargram of a measuring along measuring line 4 (length: 12,5 m, GSSI, f = 270 MHz) echo of stone plates

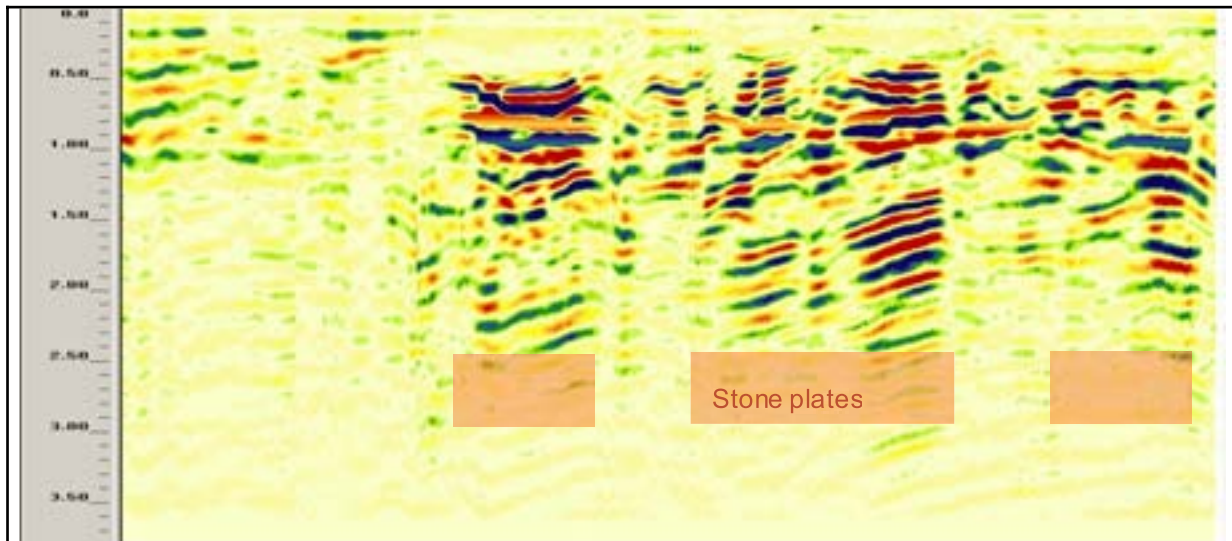


figure 79: radargram of a measuring along measuring line 5 (length: 12 m, GSSI, f = 270 MHz) with stone plates, the second layer of the plates is not parallel to the first layer

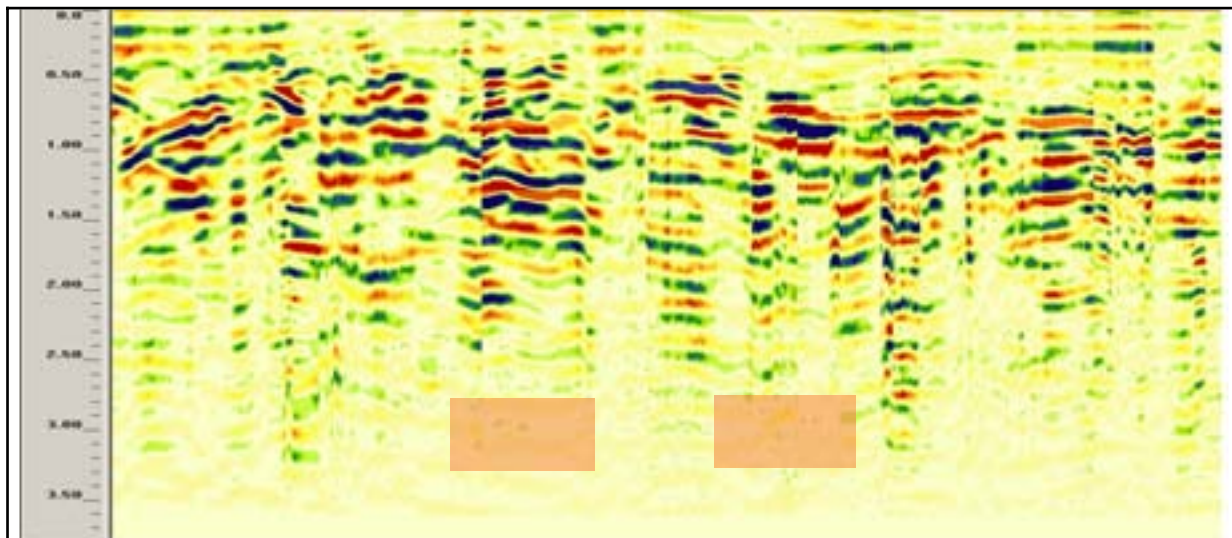


figure 80: radargram of a measuring along measuring line 6 (length: 13,5 m, GSSI, f = 270 MHz) with stone, at the edge of the stone plates just in the middle of the measuring line some stone plates are visible

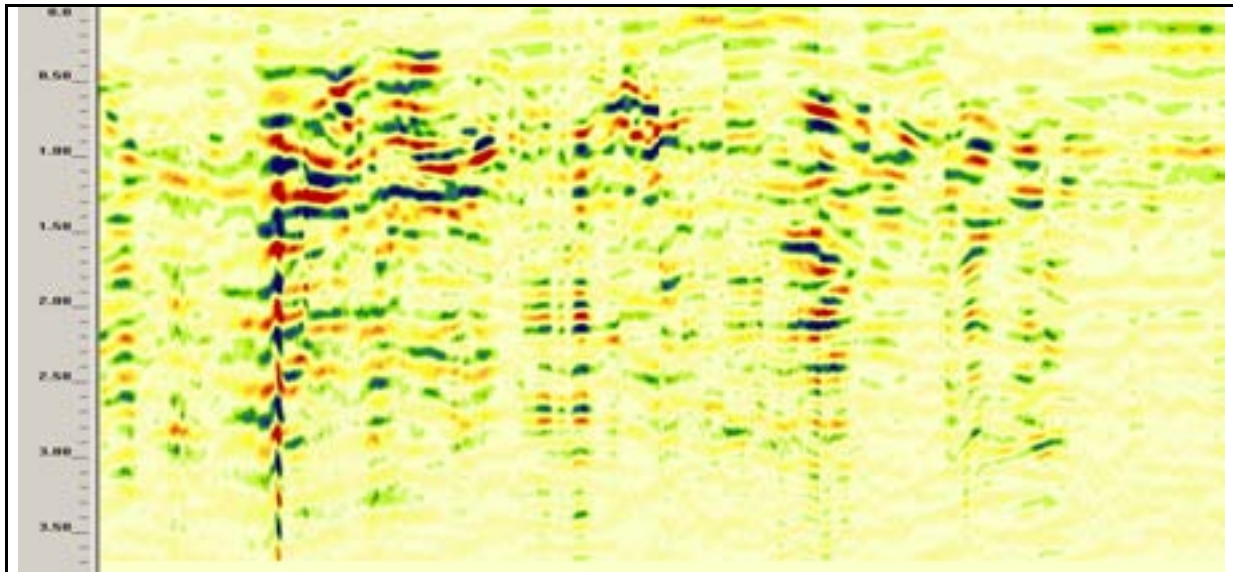


figure 81: radargram of a measuring along measuring line 7 (length: 15 m, GSSI, $f = 270$ MHz) closed to the edge of the stone plates

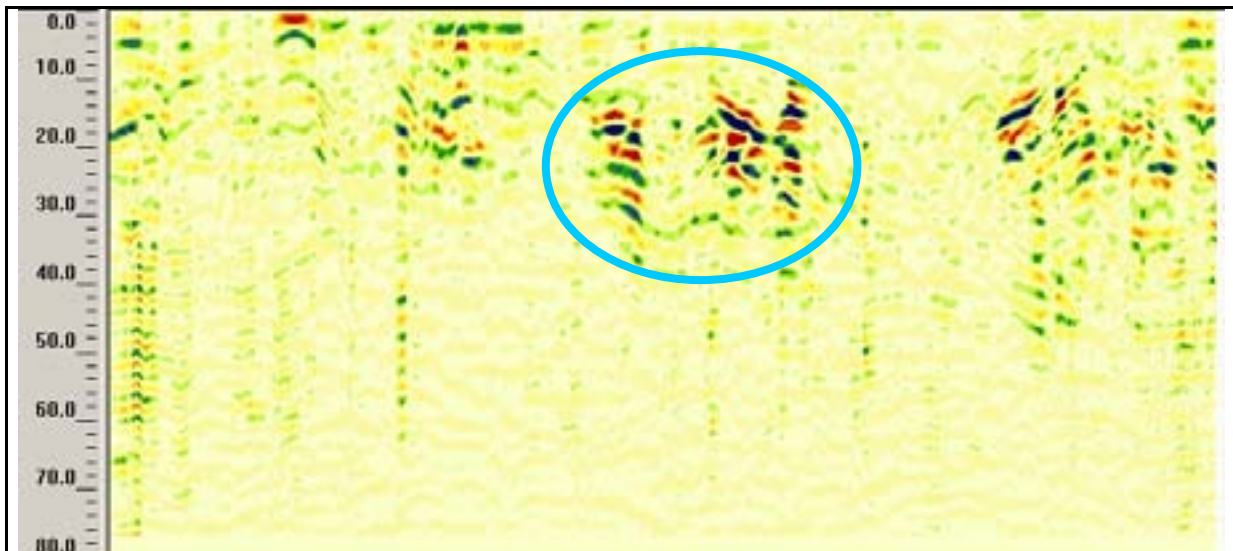


figure 82: radargram of a measuring along measuring line 8 (length: 24 m, GSSI, $f = 270$ MHz, depth in ns), one inhomogeneity

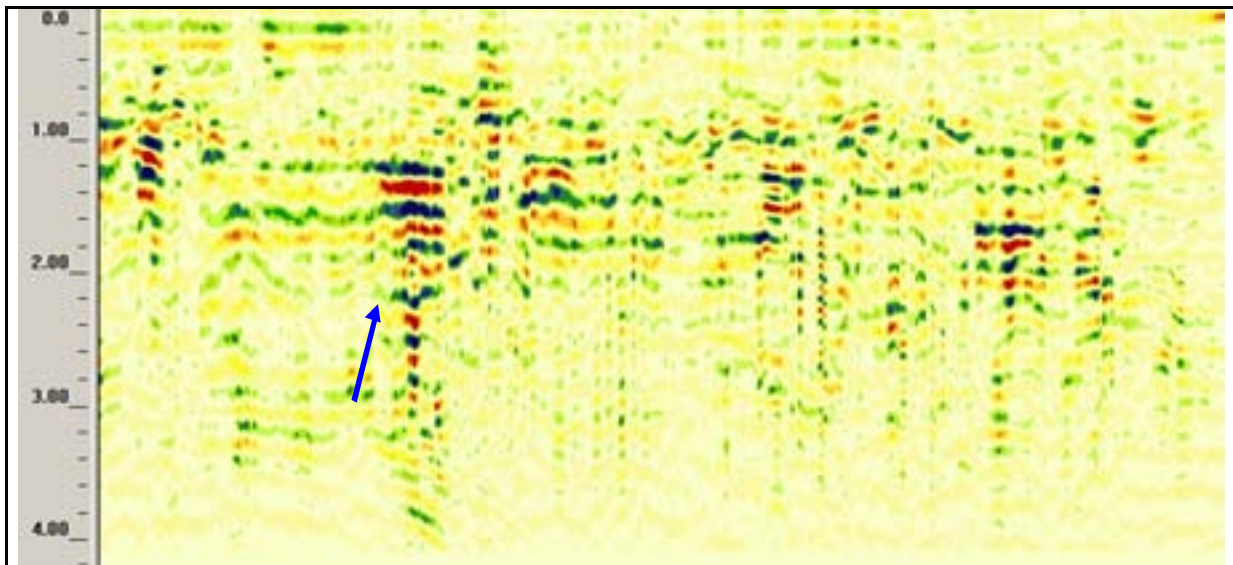


figure 83: radargram of a measuring along measuring line 9 (length: 26 m, GSSI, f = 270 MHz) a small part with a stone plates on the left side

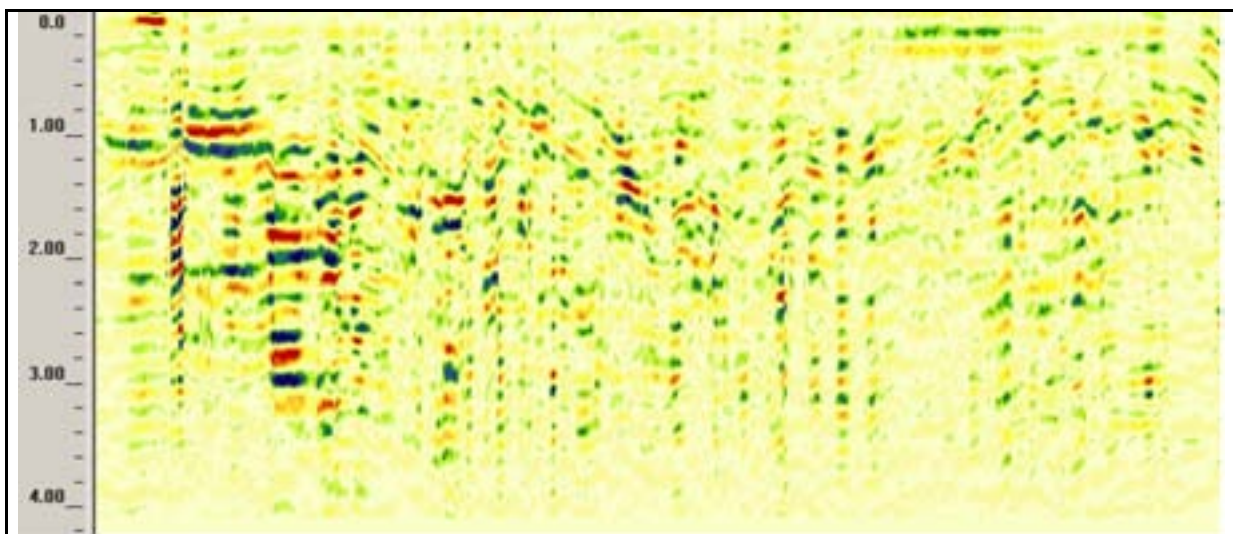


figure 84: radargram of a measuring along measuring line 10 (length: 27 m, GSSI, f = 270 MHz), no stone plates are visible

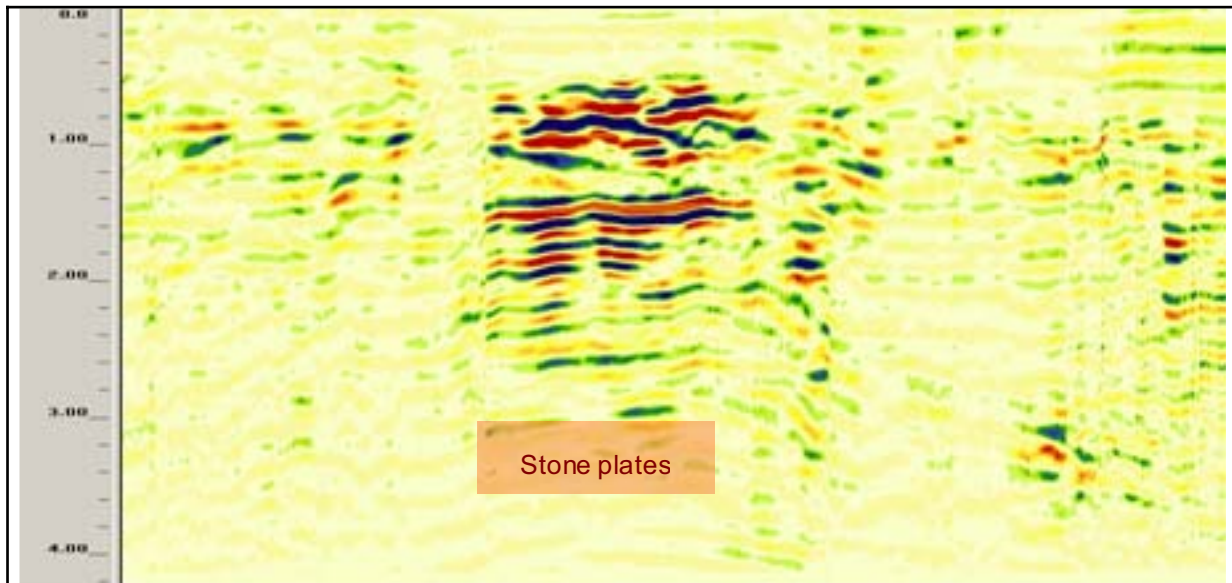


figure 85: radargram of a measuring along measuring line 11 (length: 9 m, GSSI, $f = 270$ MHz) stone plates in the middle of the line

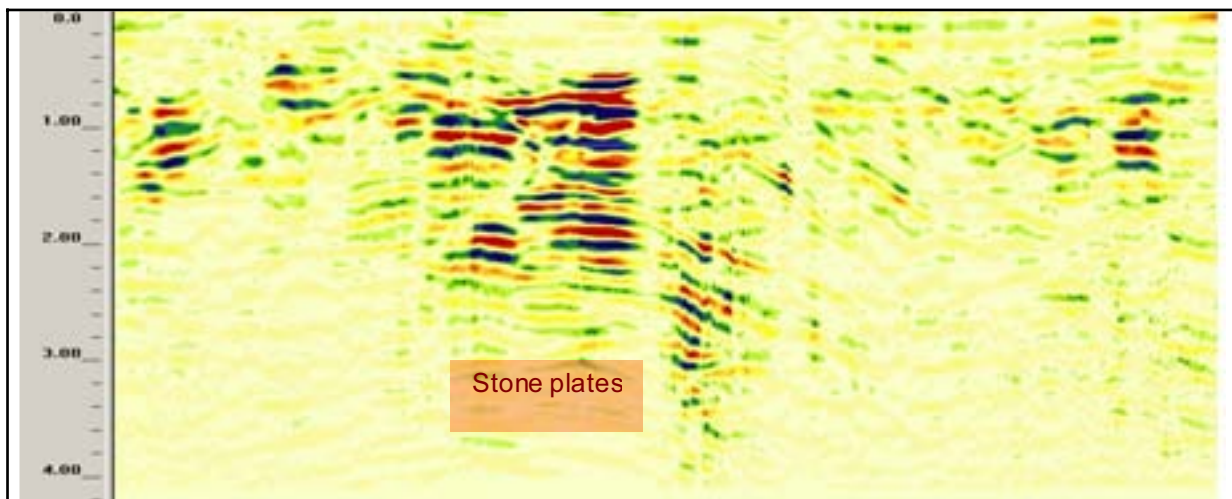


figure 86: radargram of a measuring along measuring line 12 (length: 12 m, GSSI, $f = 270$ MHz) stone plates in the middle of the line

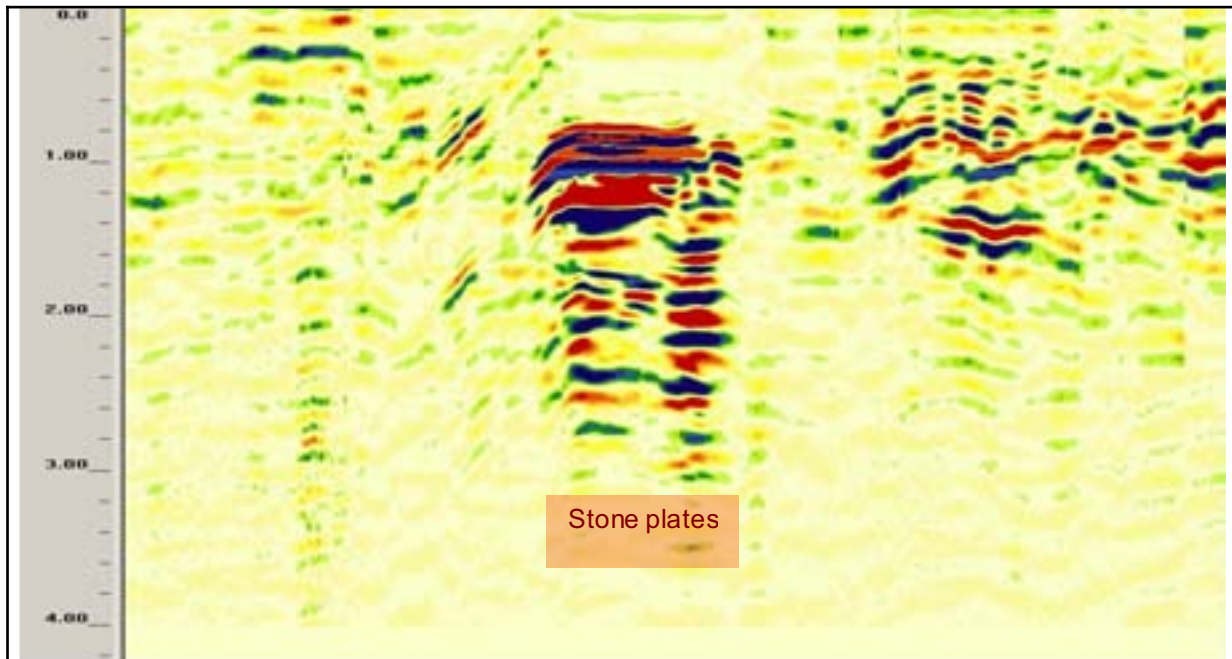


figure 87: radargram of a measuring along measuring line 13 (length: 11 m, GSSI, f = 270 MHz) stone plates in the middle of the line and some inhomogeneities

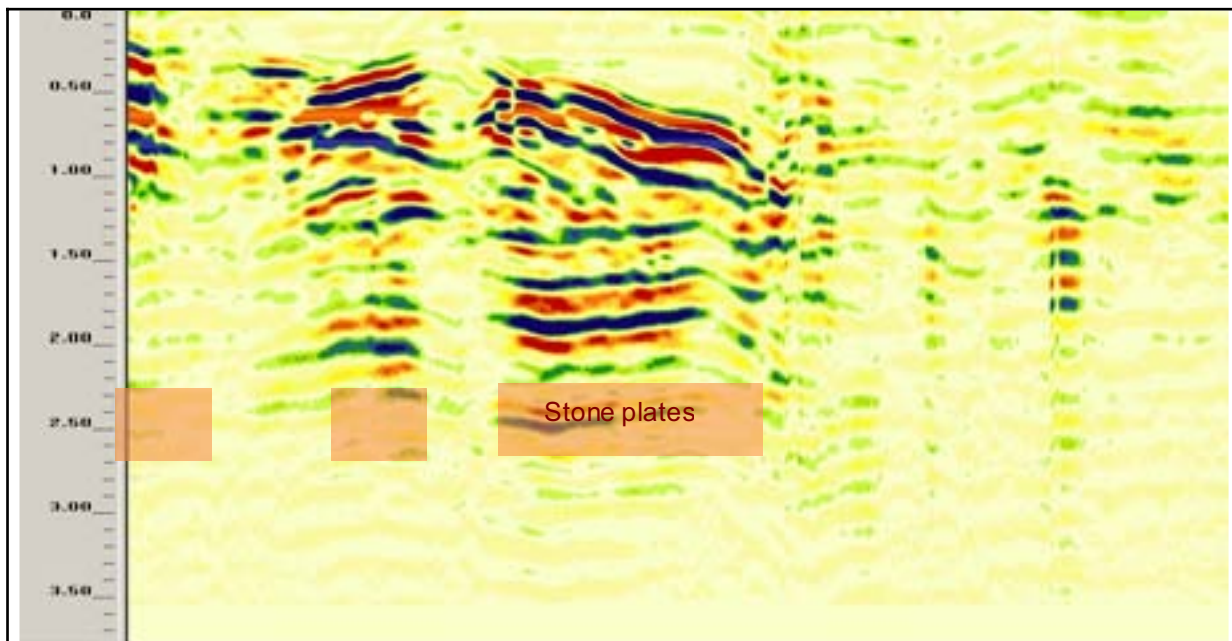


figure 88: radargram of a measuring along measuring line 14 (length: 11 m, GSSI, f = 270 MHz) with echo of stone plates

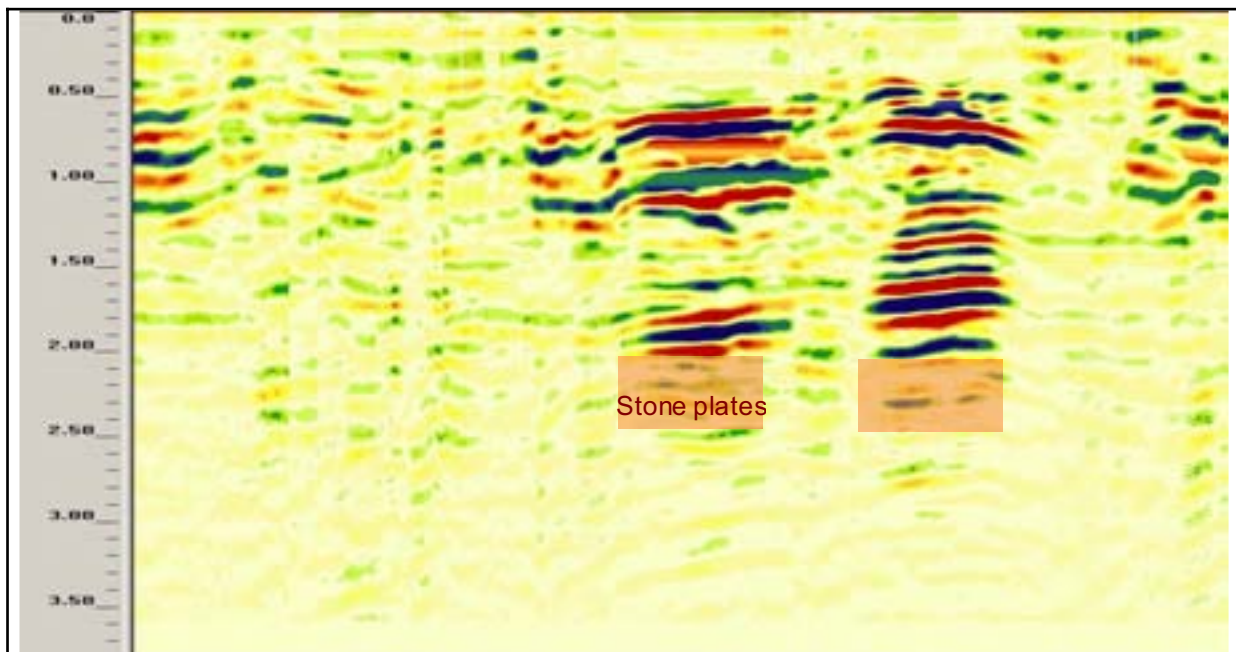


figure 89: radargram of a measuring along measuring line 15 (length: 10 m, GSSI, f = 270 MHz) with echo of stone plates

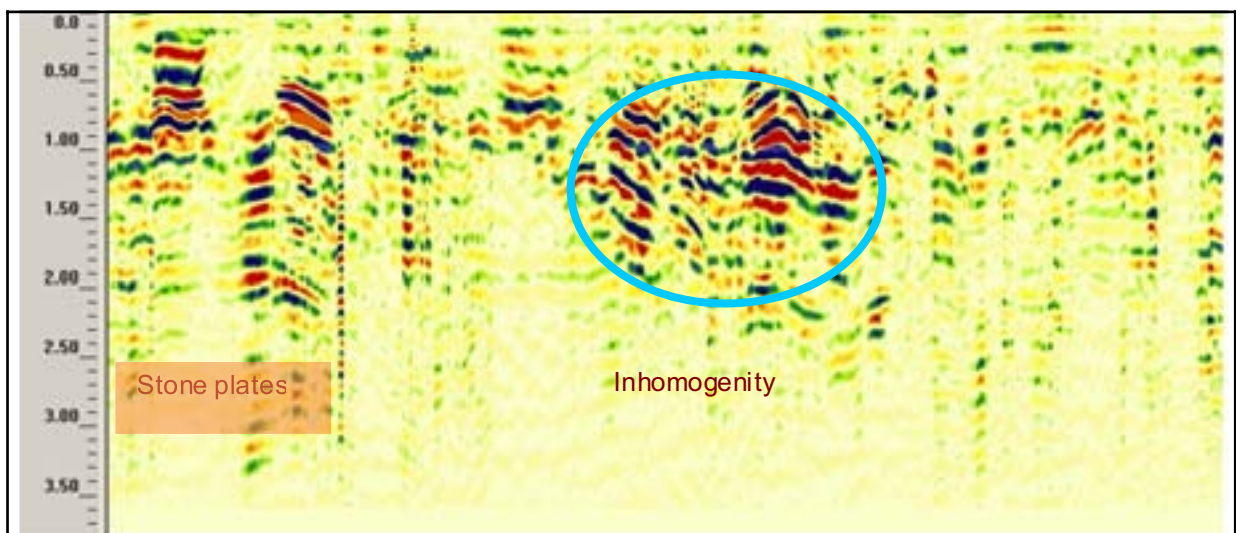


figure 90: radargram of a measuring along measuring line 16 (length: 28 m, GSSI, f = 270 MHz) stone plates on the left side, inhomogeneity on the right side(strong reflector)

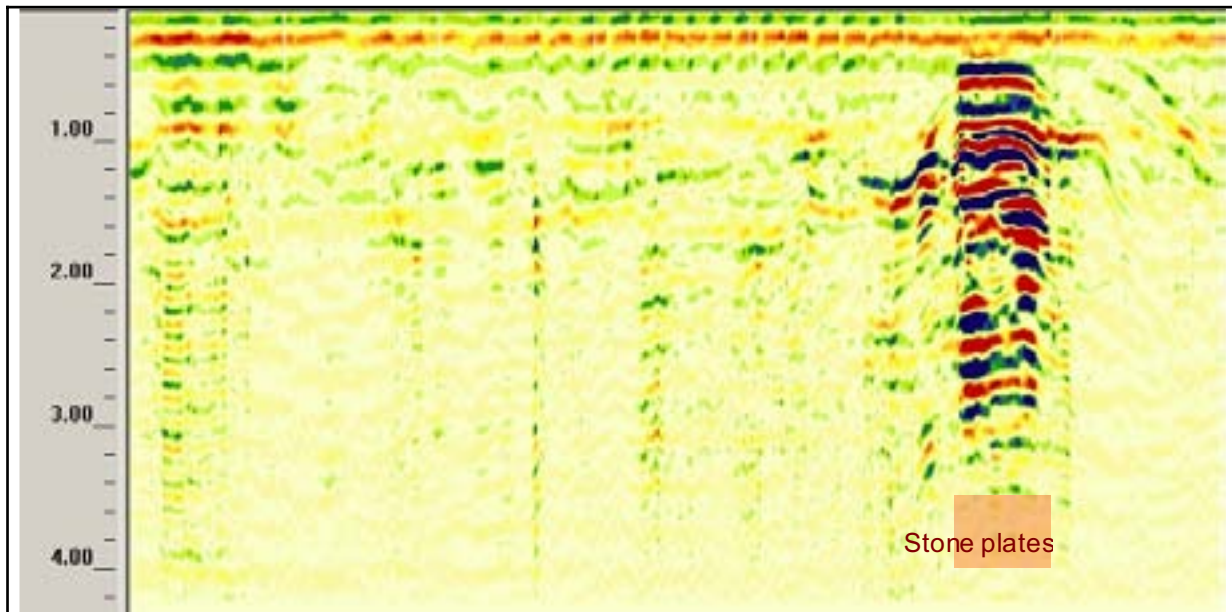


figure 91: radargram of a measuring along measuring line 17 (length: 22 m, GSSI, f = 270 MHz)

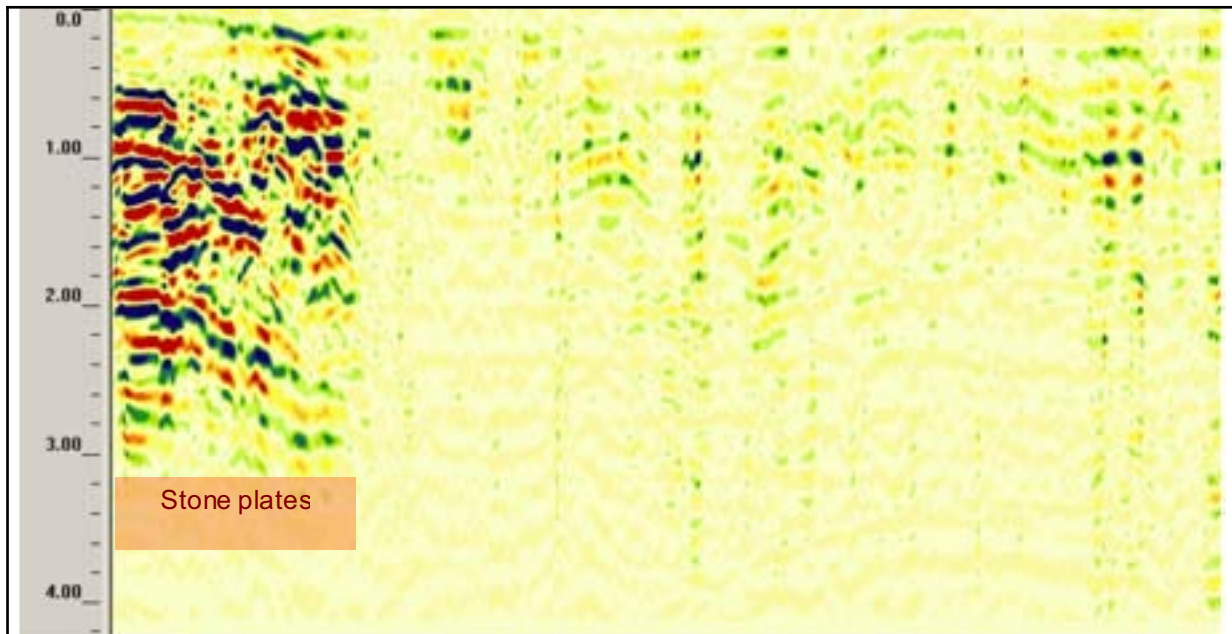


figure 92: radargram of a measuring along measuring line 18 (length: 26 m, GSSI, f = 270 MHz) stone plates on the left side

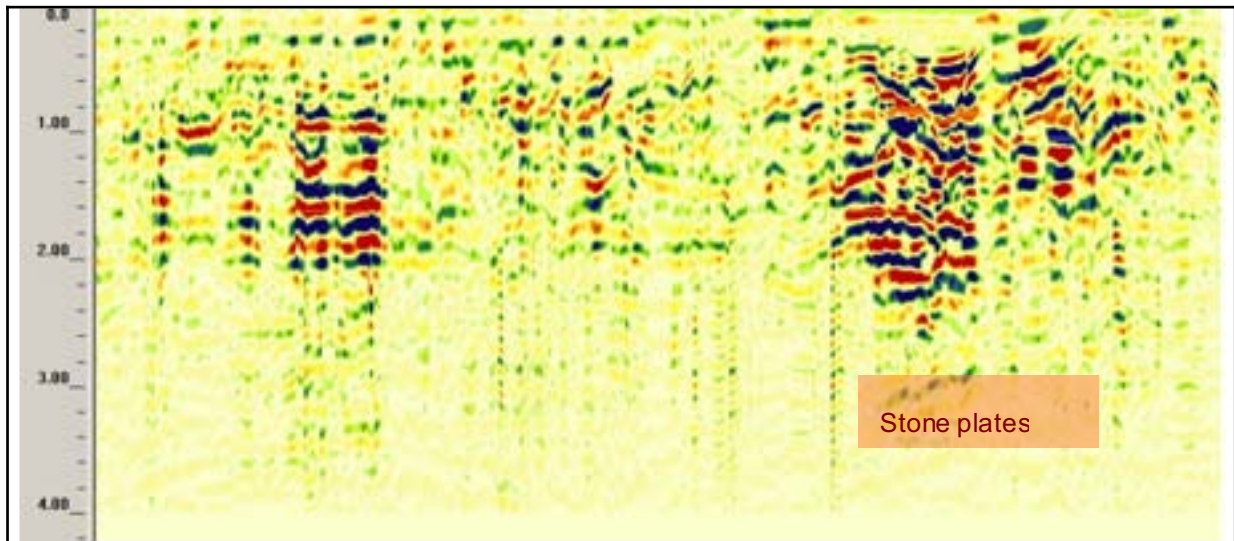


figure 93: radargram of a measuring along measuring line 19 (length: 31 m, GSSI, f = 270 MHz) stone plates on the right side, inhomogeneity on the left side

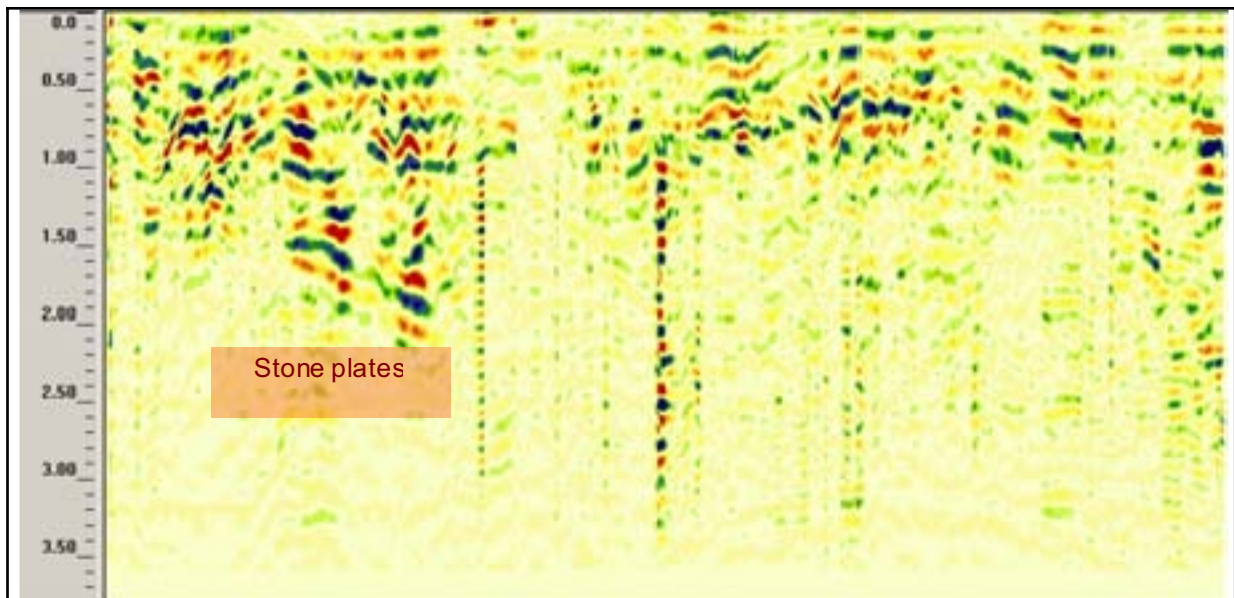


figure 94: radargram of a measuring along measuring line 21 (length: 28 m, GSSI, f = 270 MHz) stone plates on the left side

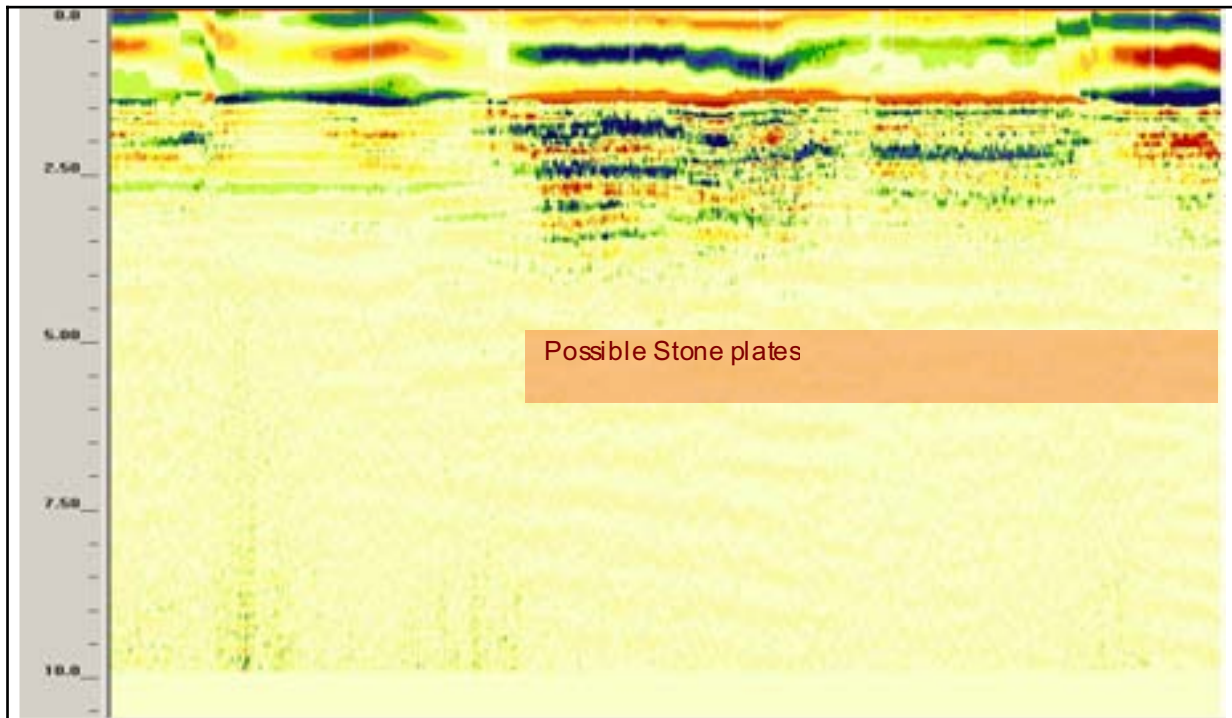


figure 95: radargram of a measuring along measuring line 23 parallel to line 3 (length: 8,5 m, GSSI, f = 100 MHz) stone plates on the right side

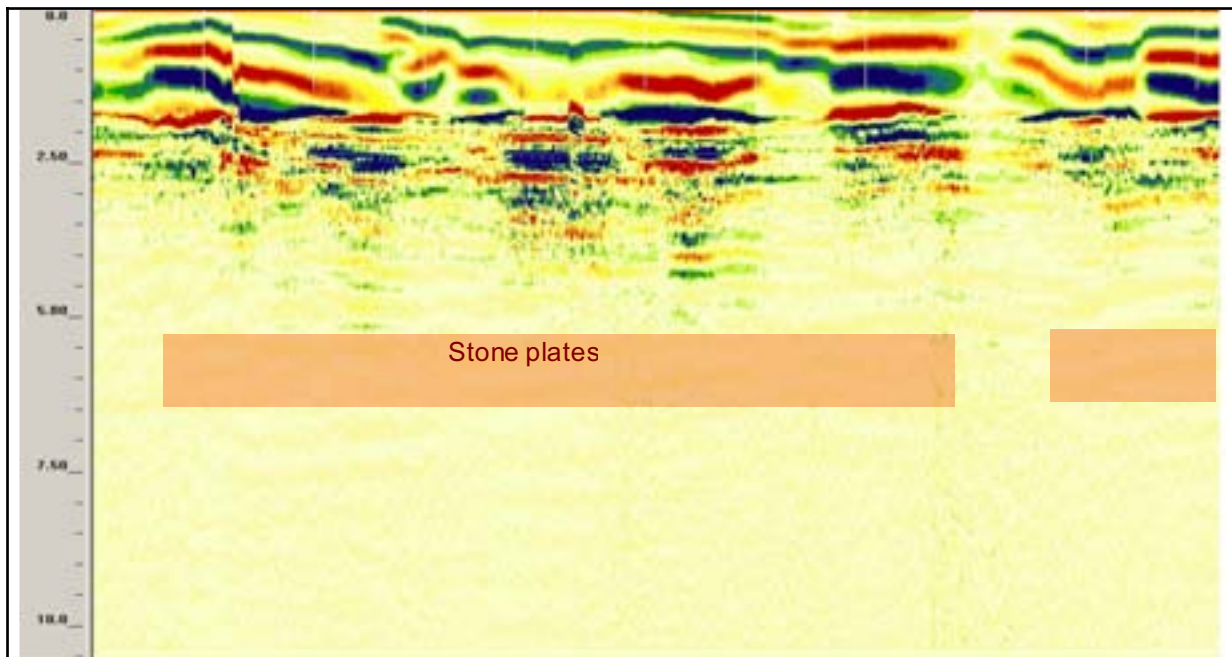


figure 96: radargram of a measuring along measuring line 24, parallel to line 4 (length: 10 m, GSSI, f = 100 MHz) with stone plates

6 MEASUREMENTS AT SONDE 12

6.1 Local conditions

The measurements were carried out at the Sonde 12 with tent.



figure 97: view of measurements at Sonde 12

6.2 RESULTS OF THE MEASUREMENTS

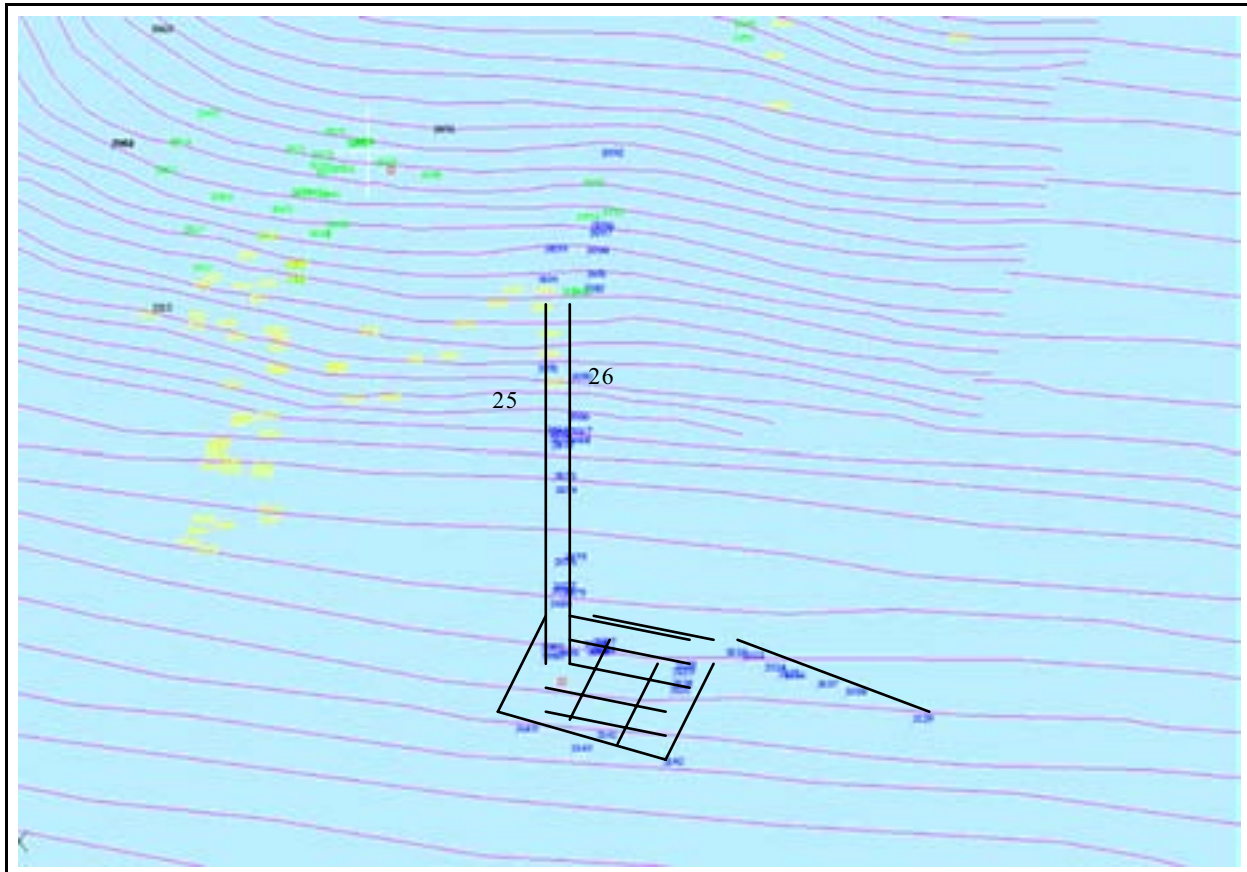


figure 98: overview of position of measuring lines

The measurements were done with a 270 MHz radar antenna. At Sonde 12 and in the forest the measuring area was so small, that it was not possible to use the larger 100 MHz antenna. In the forest the ground has been wet what results in a high damping of signals. Anywhere the results of the measurements were in the first 4 m very good.

Following the results of measurements at the area of Sonde 12 are shown.

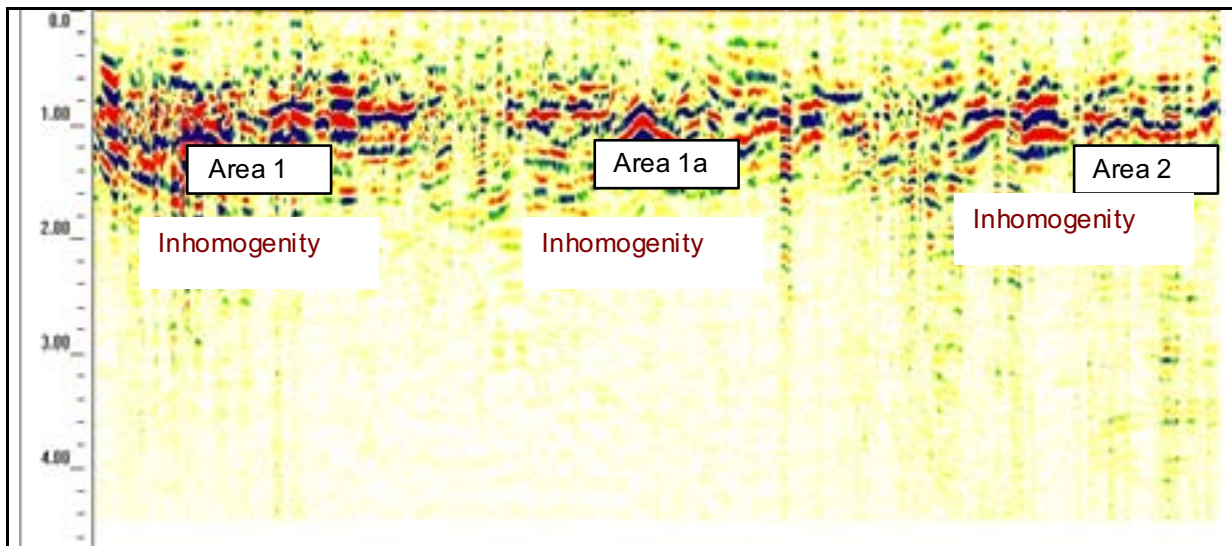


figure 99: radargram of a measuring along measuring line 25 (GSSI, f = 270 MHz) with inhomogeneities

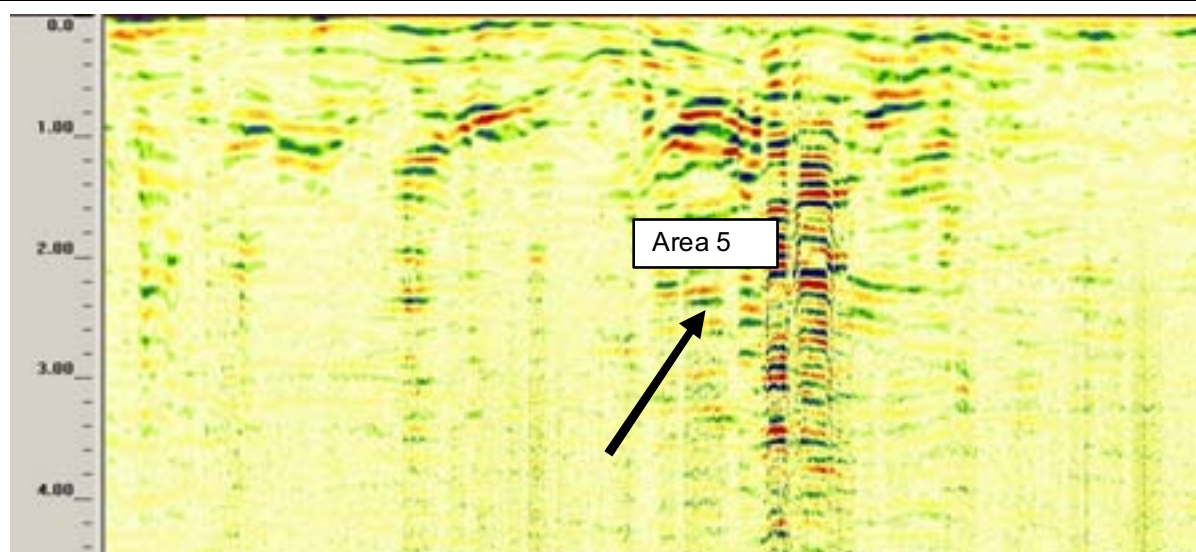


figure 100: radargram of a measuring along measuring line 27 (GSSI, f = 270 MHz) with position of cavity in ground

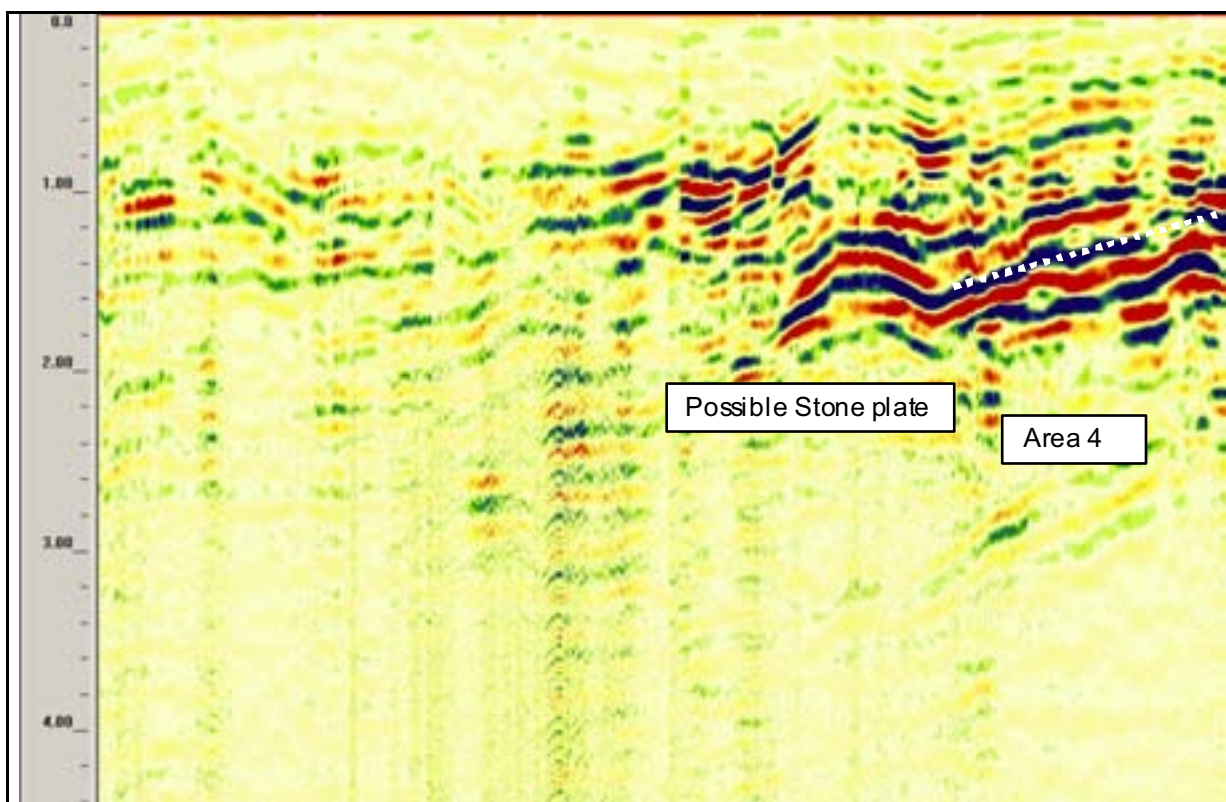


figure 101: radargram of a measuring along measuring line 30 (GSSI, f = 270 MHz) with inhomogenities

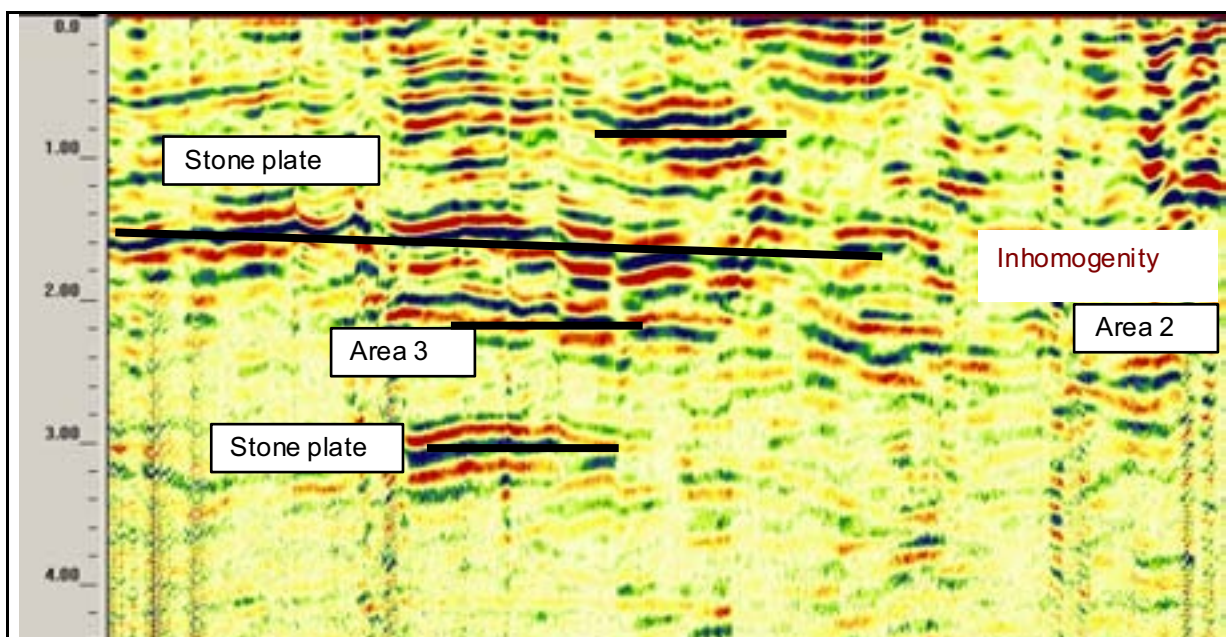


figure 102: radargram of a measuring along measuring line 31 (GSSI, f = 270 MHz) with inhomogenities

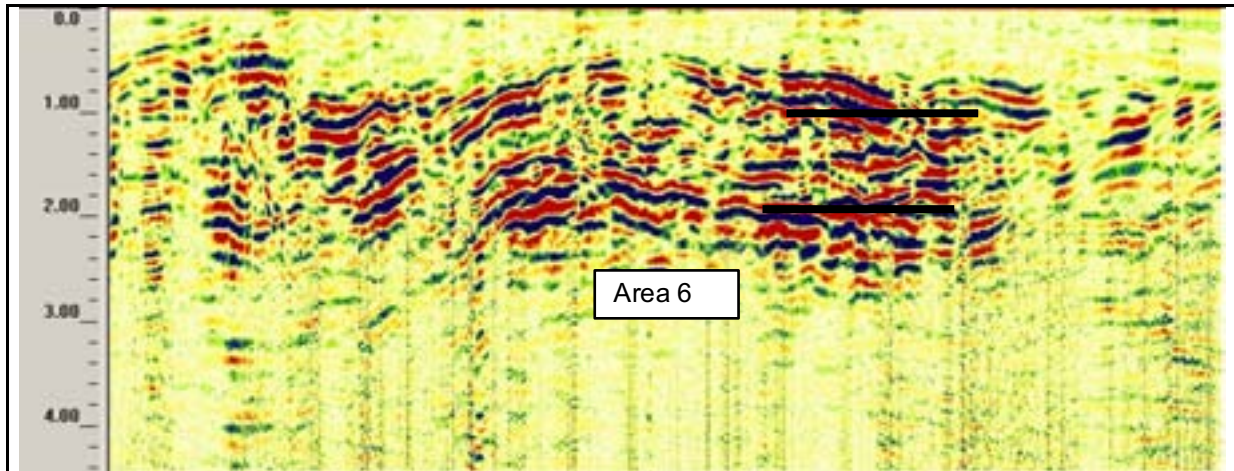


figure 103: radargram of a measuring along measuring line 32 (GSSI, $f = 270$ MHz) with inhomogenities

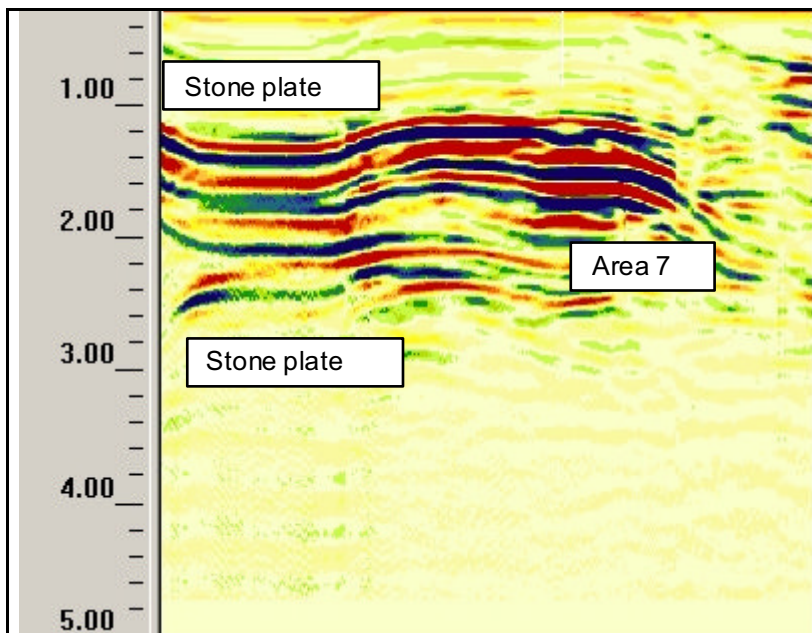


figure 104: radargram of a measuring along measuring line 33 (GSSI, $f = 270$ MHz) with very strong reflector (perhaps air under it)

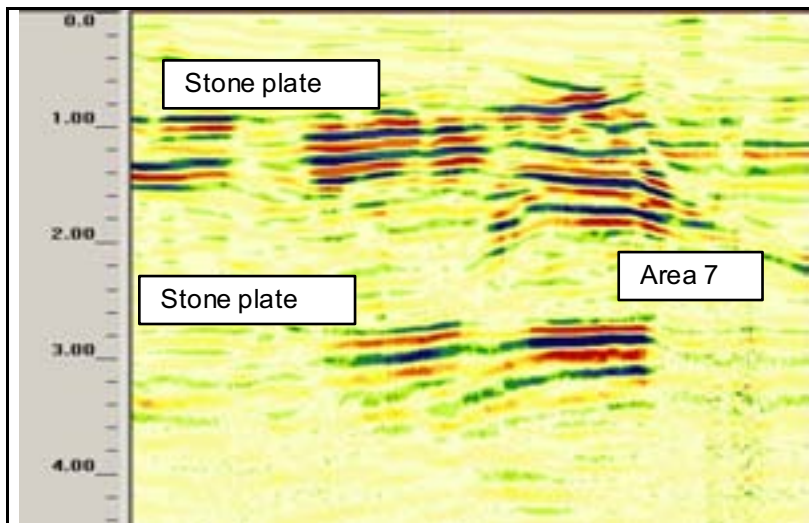


figure 105: radargram of a measuring along measuring line 36 (GSSI, f = 270 MHz) with inhomogenities

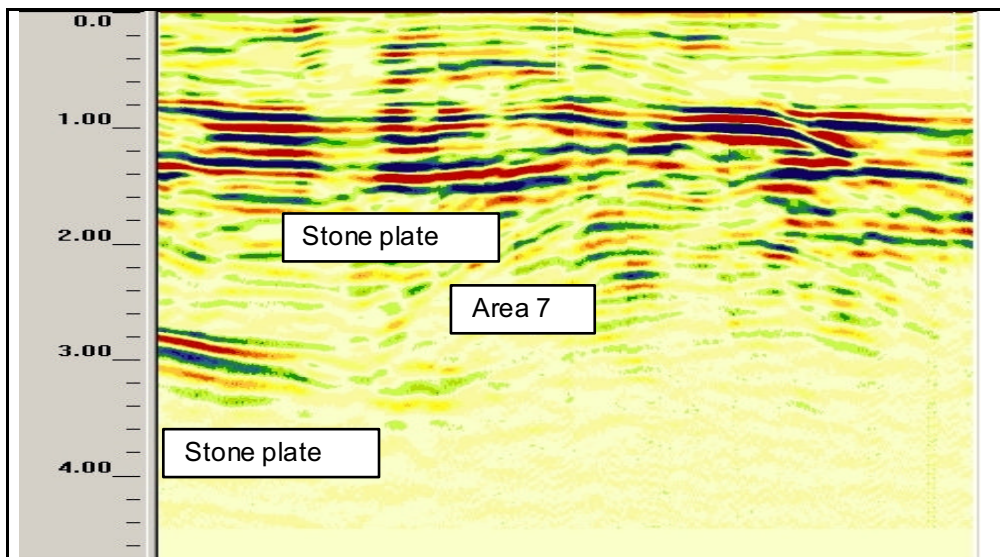
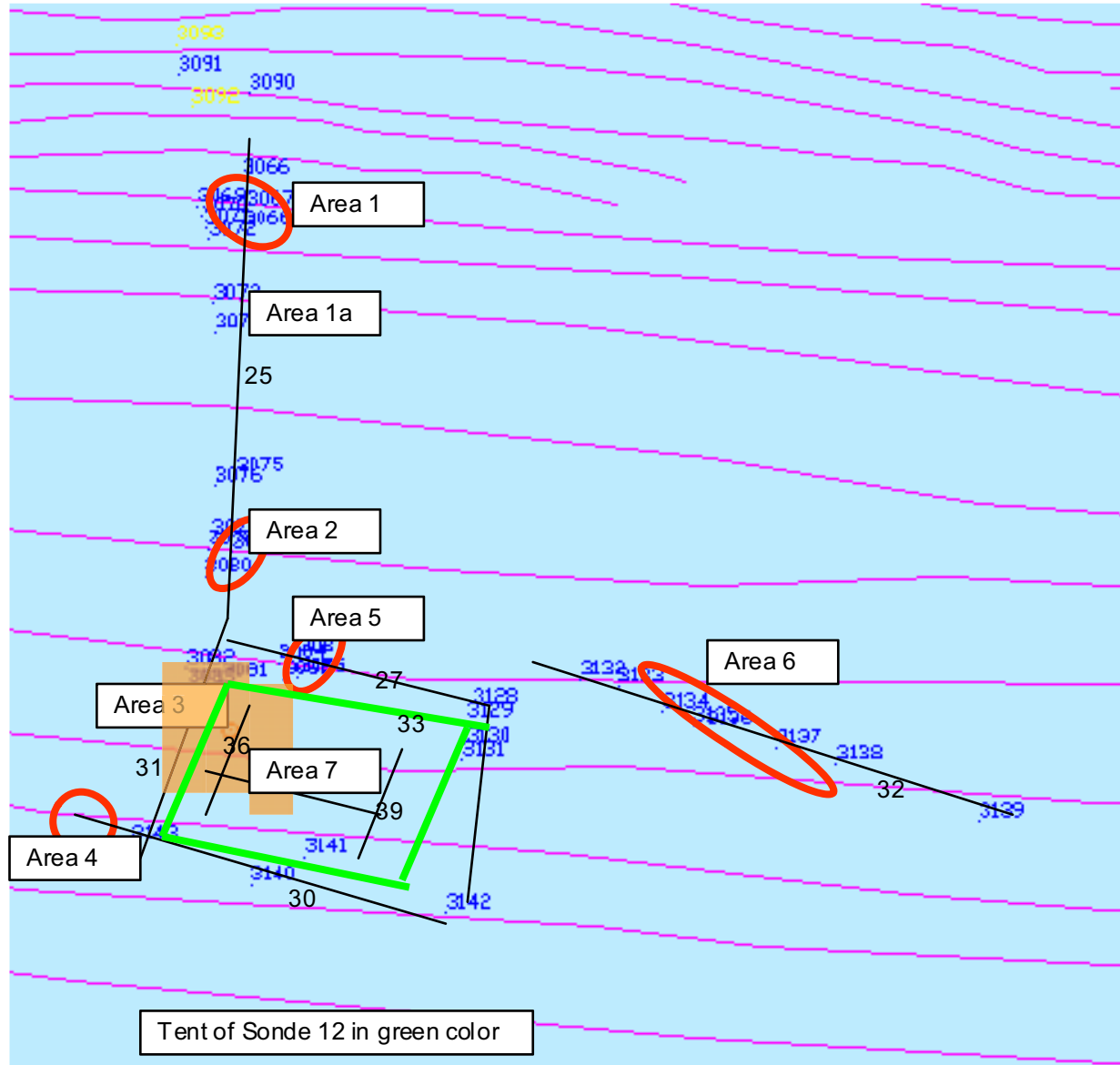


figure 106: radargram of a measuring along measuring line 39 (GSSI, f = 270 MHz) with inhomogenities

6.3 EVALUATION OF RESULTS

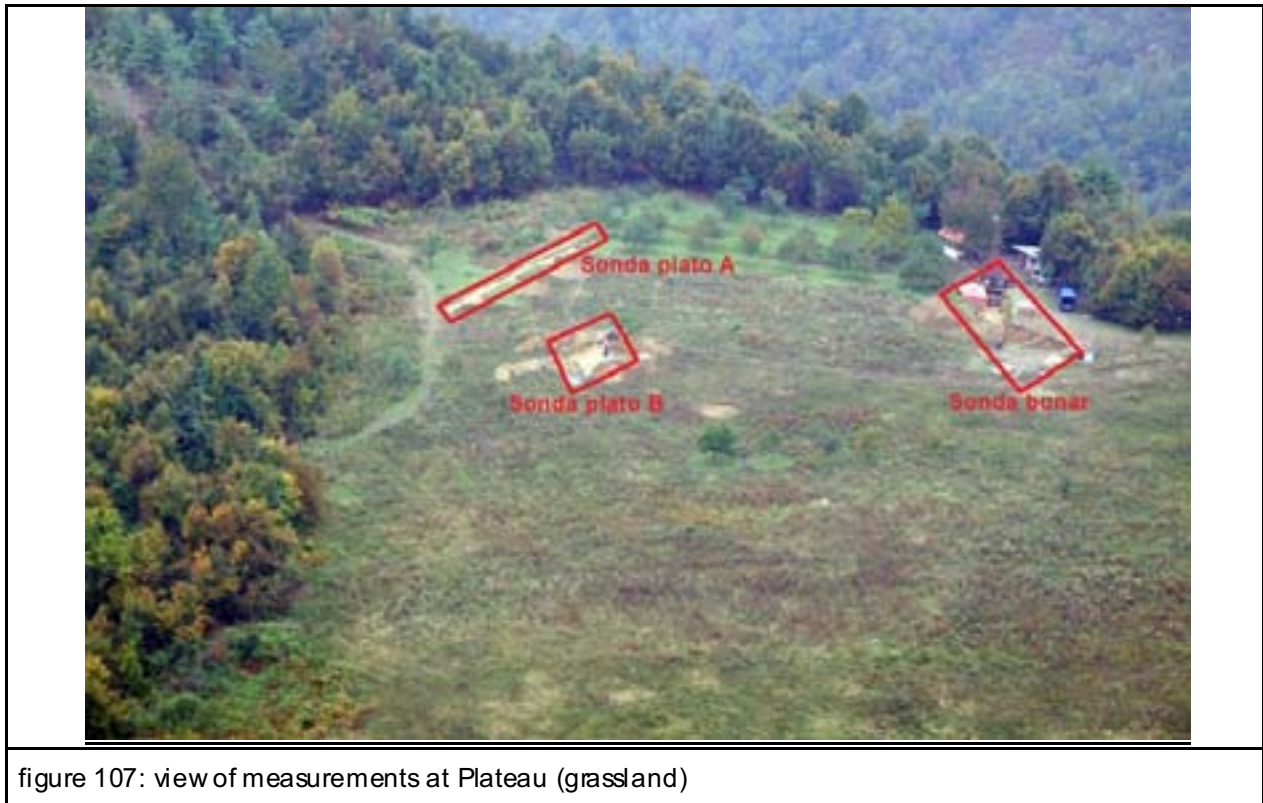


In the picture above the measuring lines and the areas with inhomogeneities are shown.

Area 1, Area 1a:	inhomogeneity along the measuring line in depth of: 1,0 – 1,2m
Area 2	Top of Area 1 Depth of inhomogeneity: 1,0 – 1,2m
Area 3:	Different layers of stone plates Depth of stone pates 0,8m; 1,3m; 3,0m
Area 4:	Stone plates in depth of 1,3 m – 1,6m
Area 5:	Crack going from Sonde 12 Depth: 0,9 - 1,0m
Area 6:	Two different Layers In depth of 0,9-1,1 m and 1,9 – 2,1m
Area 7:	In the tent of Sonde 12 One up to four layers of stone plates (ore cracked stone plates) Depth of: 0,9m; 1,4m; 1,8m; 3,0m

7 MEASUREMENTS AT PLATEAU A AND B

7.1 Local conditions



7.2 RESULTS OF THE MEASUREMENTS

The measurements were done with a 270 MHz and a 100 MHz radar antenna at the Plateau.

The ground has been wet what results in a high damping of signals.

Anywhere the results of the measurements were in the first 4 m very good. The results of measurements with the 100 MHz antenna brought no information.

Following the results of measurements at the plateau are shown.

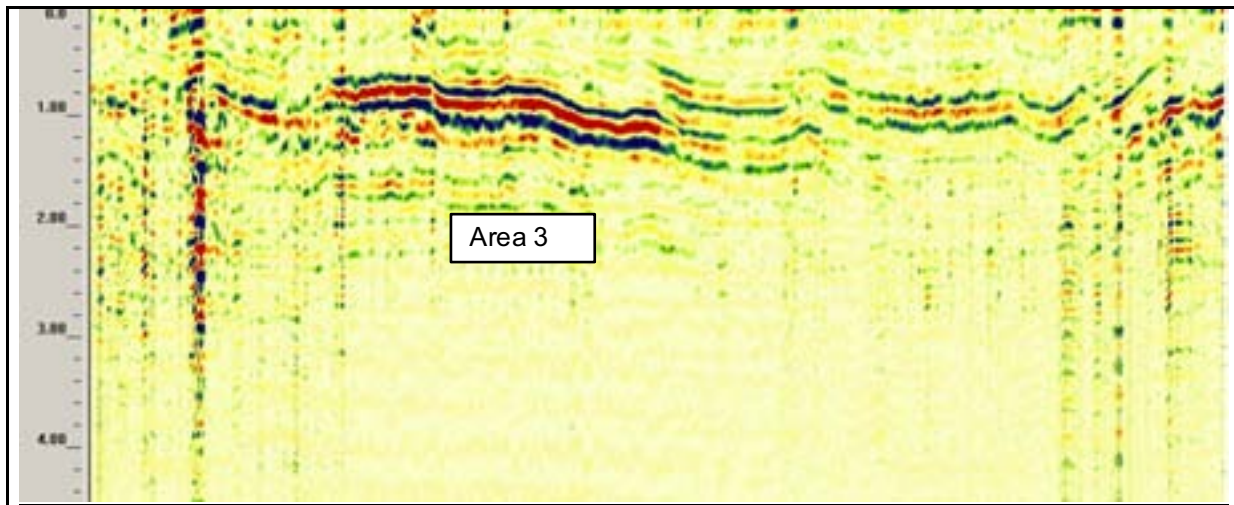


figure 108: radargram of a measuring along measuring line 42 (GSSI, f = 270 MHz) with inhomogenities

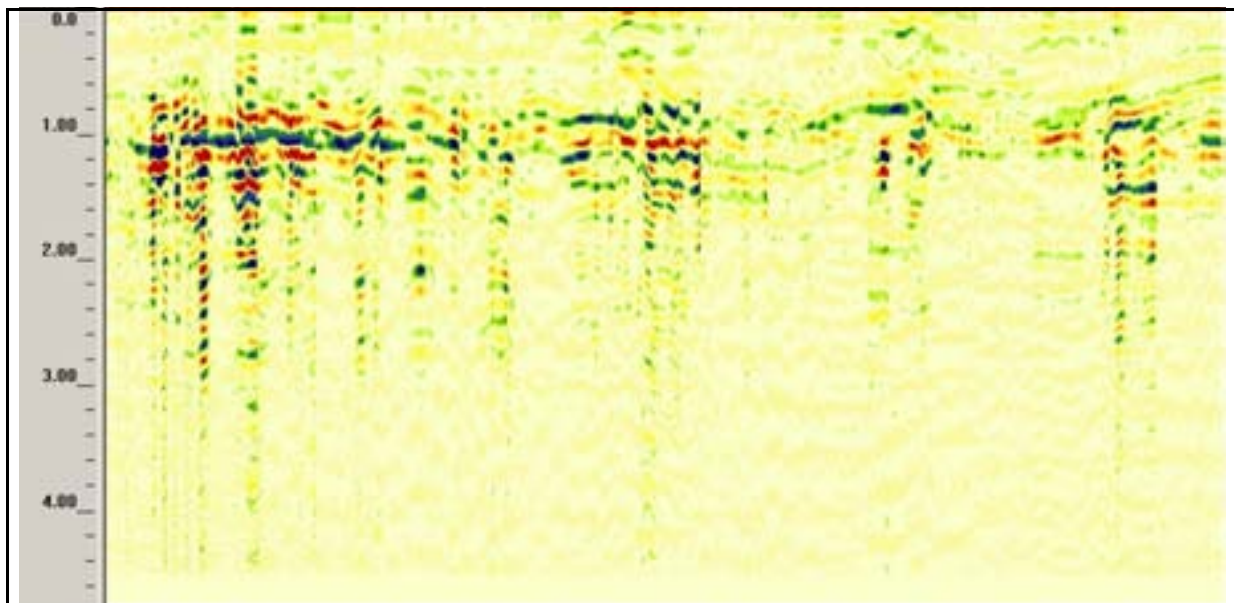


figure 109: radargram of a measuring along measuring line 44 along way (GSSI, f = 270 MHz) with inhomogenities

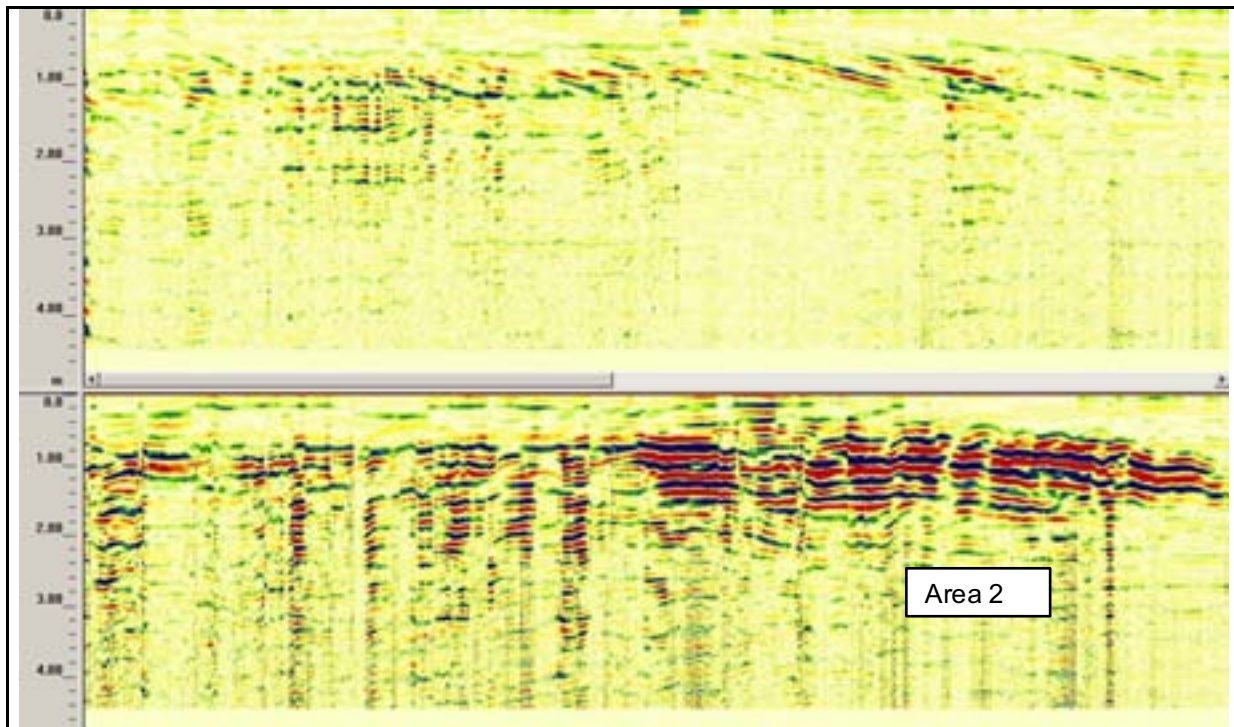


figure 110: radargram of a measuring along measuring line 49 (GSSI, $f = 270$ MHz) with inhomogenities

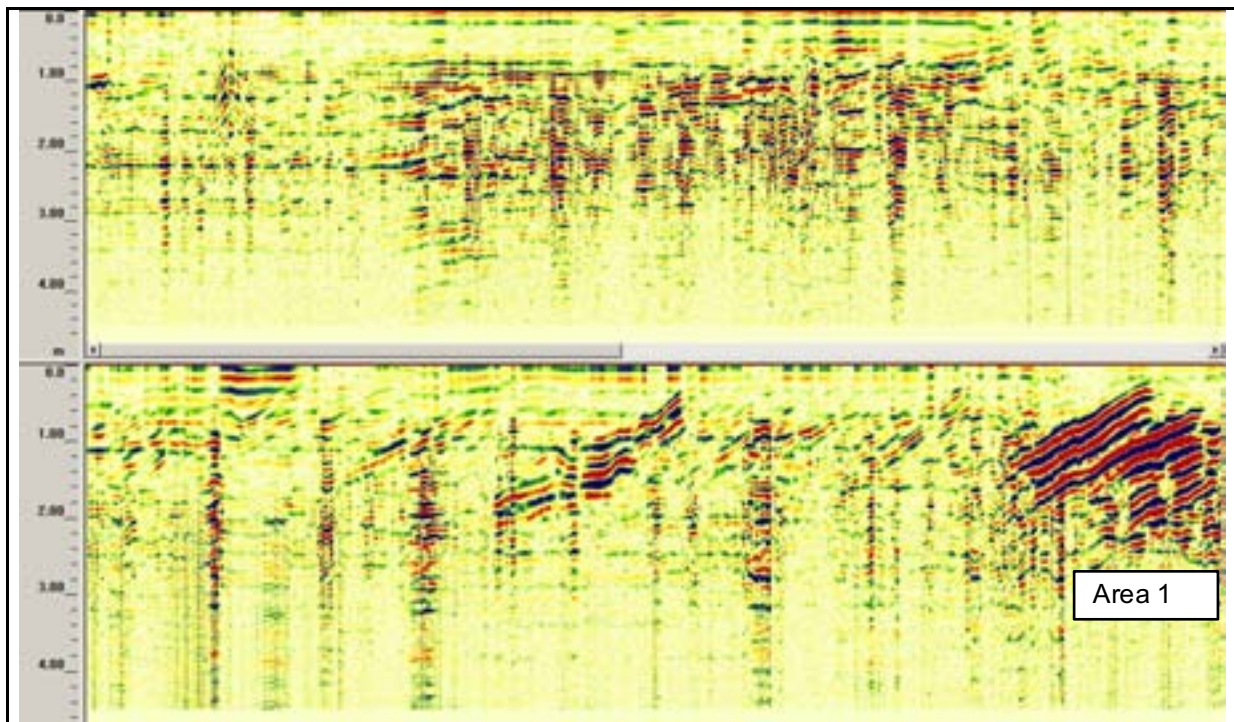


figure 111: radargram of a measuring along measuring line 54 (GSSI, $f = 270$ MHz) with inhomogenities

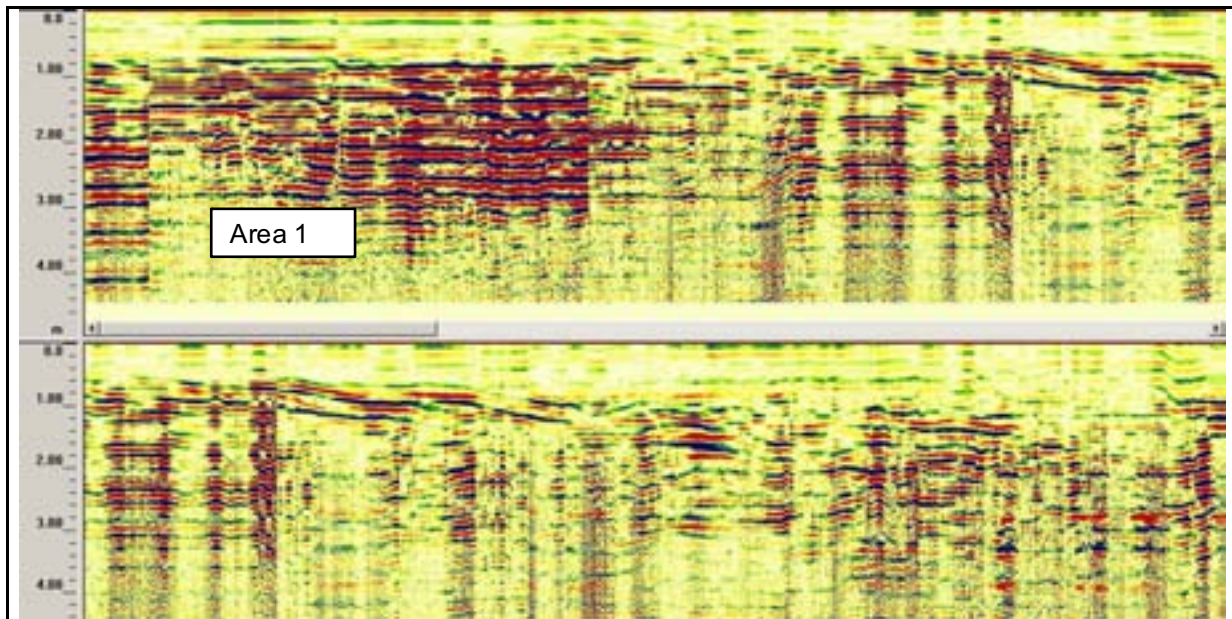
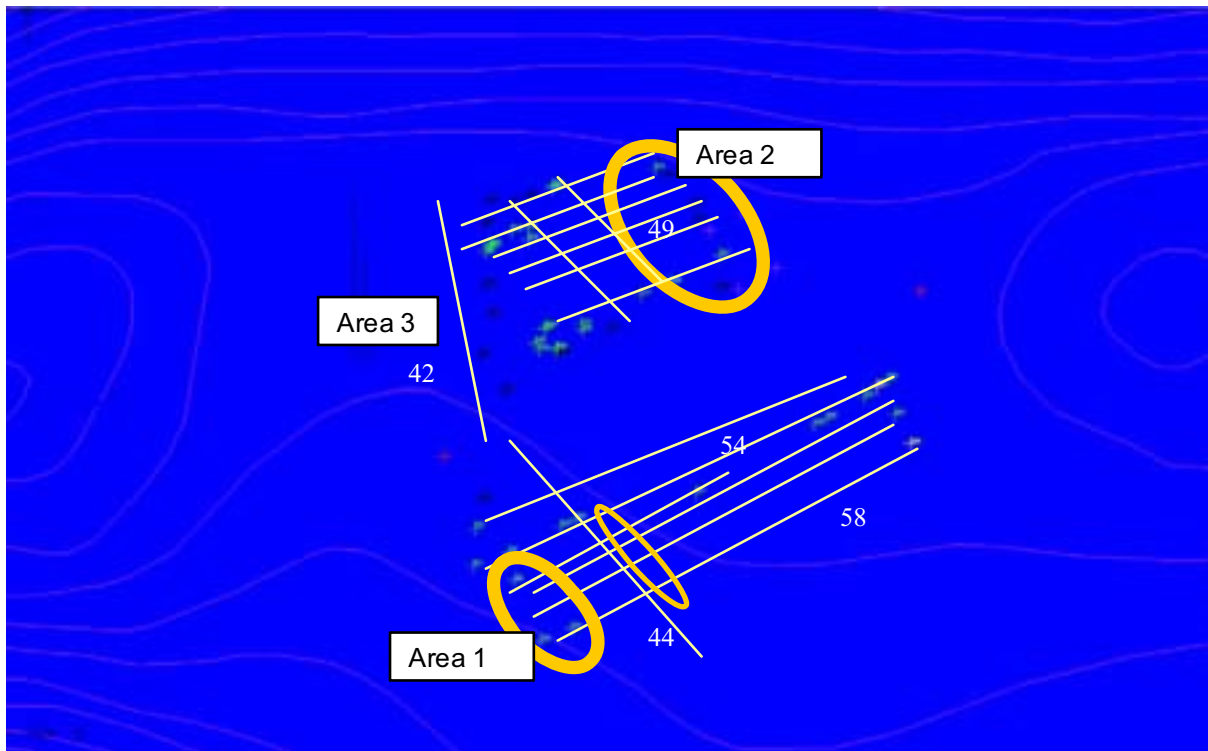
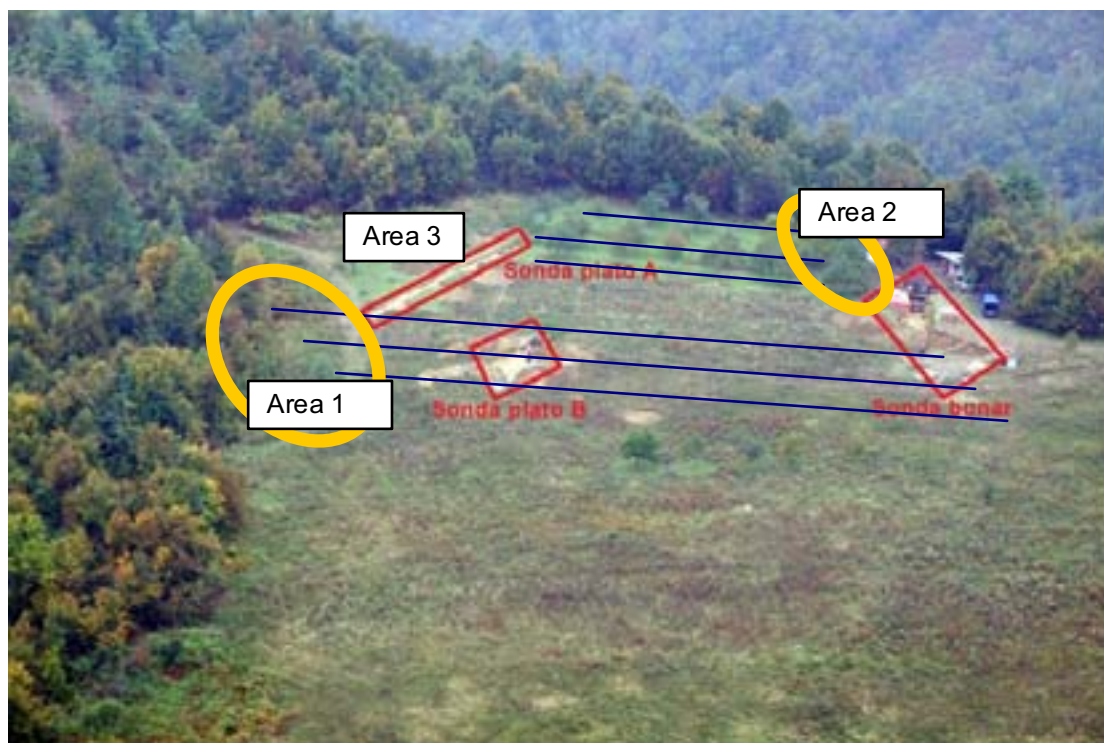


figure 112: radargram of a measuring along measuring line 58 (GSSI, f = 270 MHz) with inhomogenities

7.3 CONCLUSION OF RESULTS

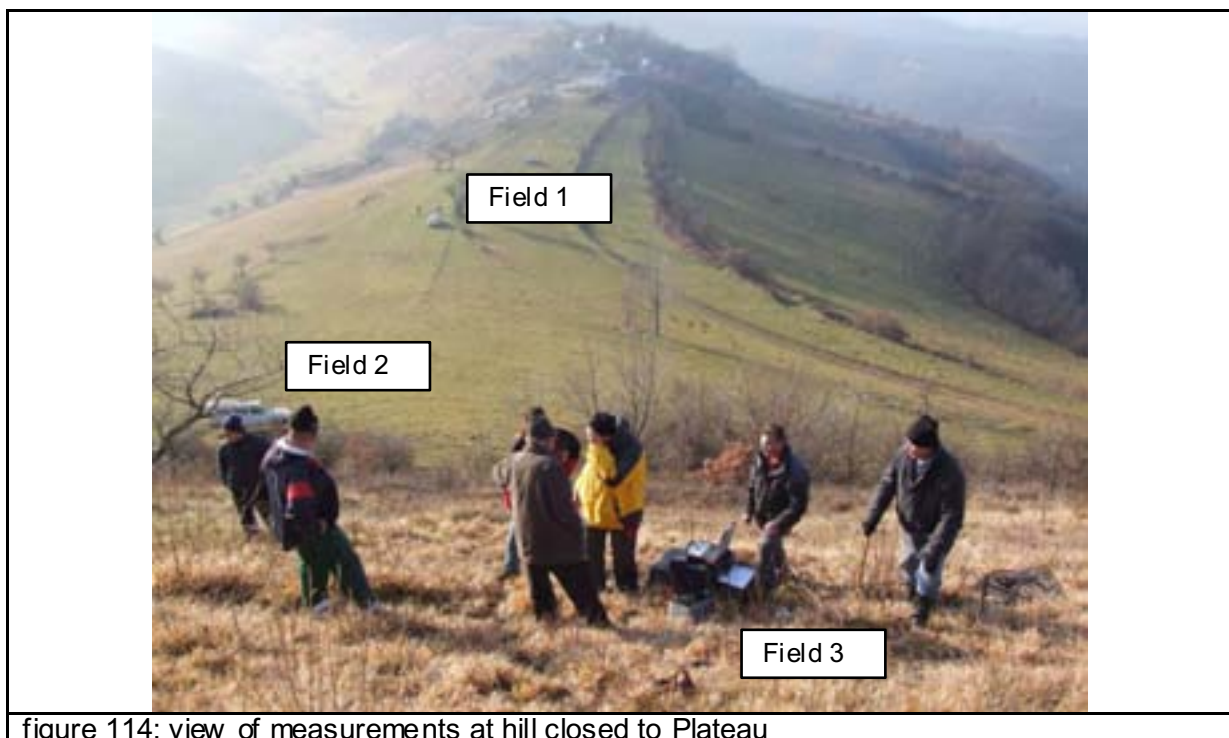
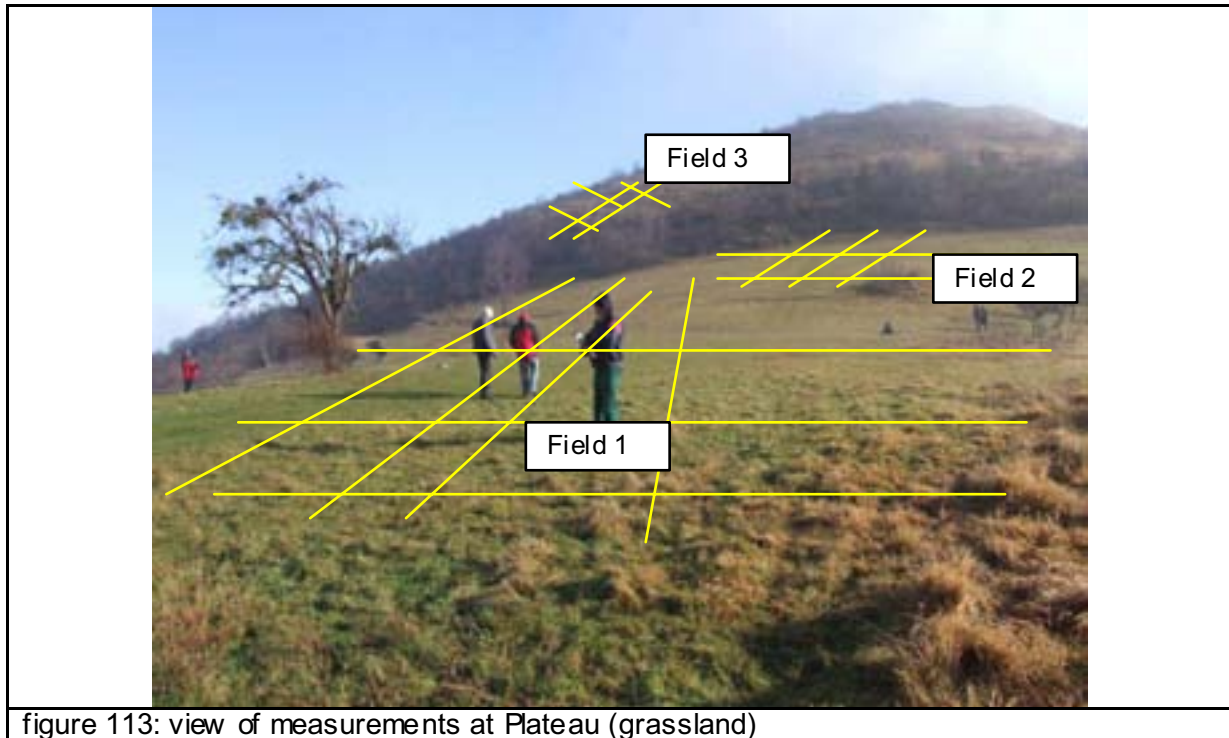




Area 1	At the end of grassland in depth of: 0,5 – 2,0m
Area 2	At the end of grassland with trees Depth of inhomogeneity: 0,7 – 1,3m
Area 3:	Parallel to stone plates Depth of inhomogeneity: 1,0 – 1,2m

8 MEASUREMENTS AT PLATEAU AND PYRAMIDE

8.1 Local conditions



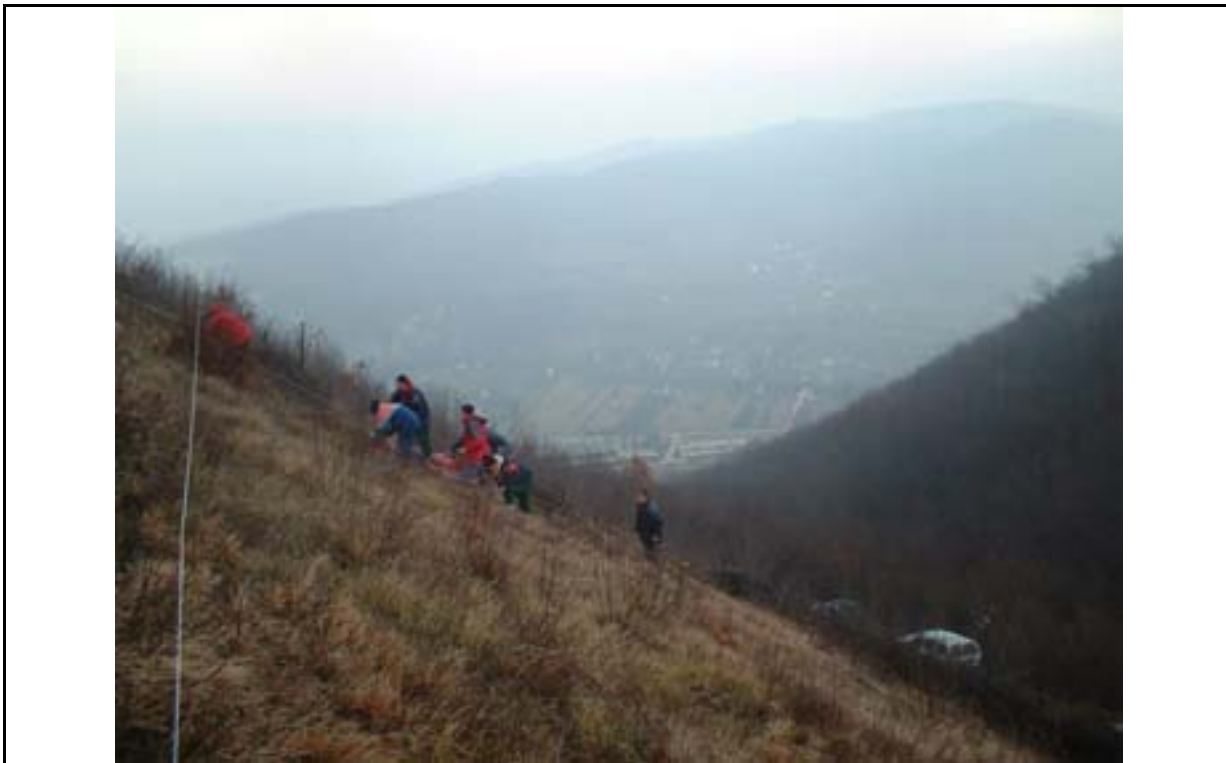


figure 115: view of measurements at field 4 (grassland)

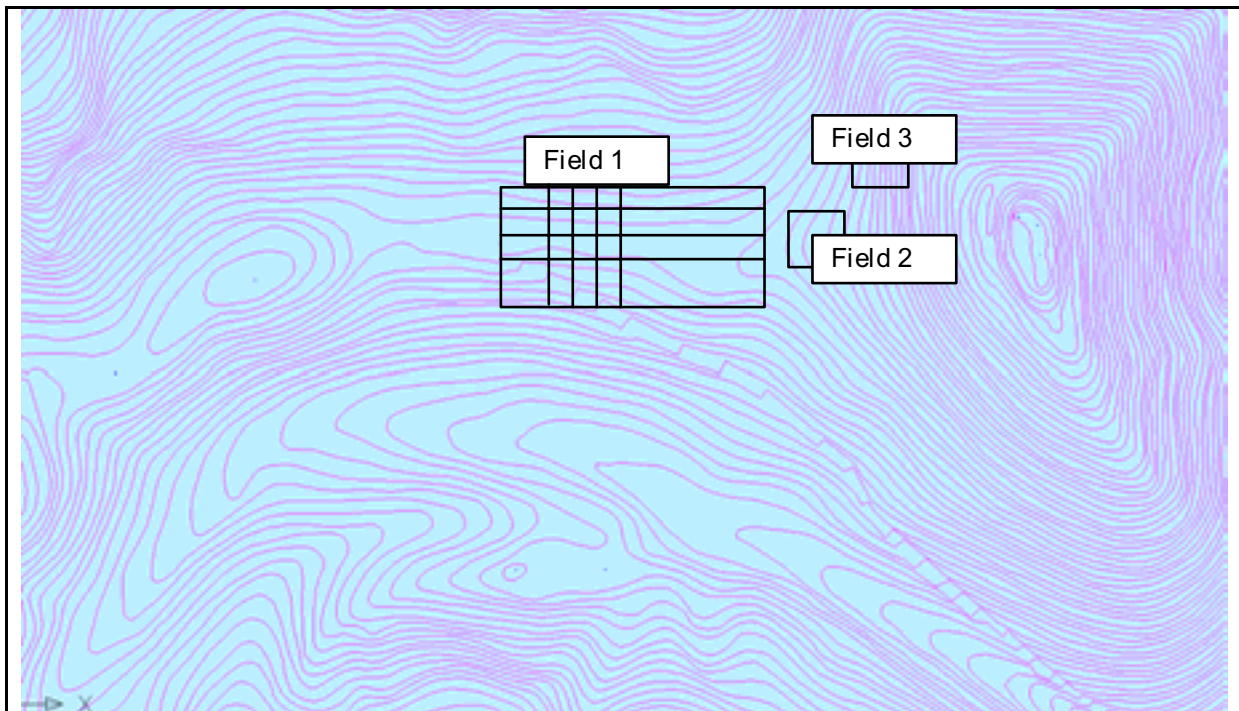


figure 116: view measuring fields, field 1: 4 long lines, 20 short lines

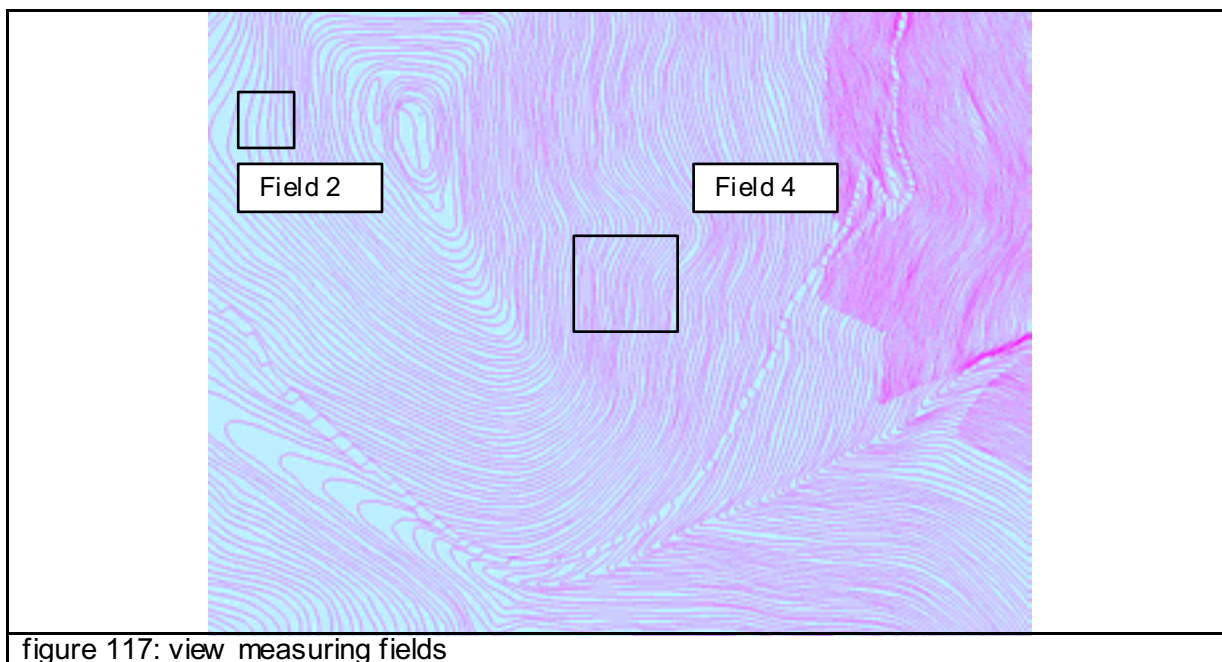


figure 117: view measuring fields

8.2 RESULTS OF THE MEASUREMENTS

The measurements were done with a 100 MHz radar antenna at the Plateau. The ground has been wet what results in a high damping of signals. Anywhere the results of the measurements were in the first 4 m very good.

Following the results of measurements at the plateau are shown.

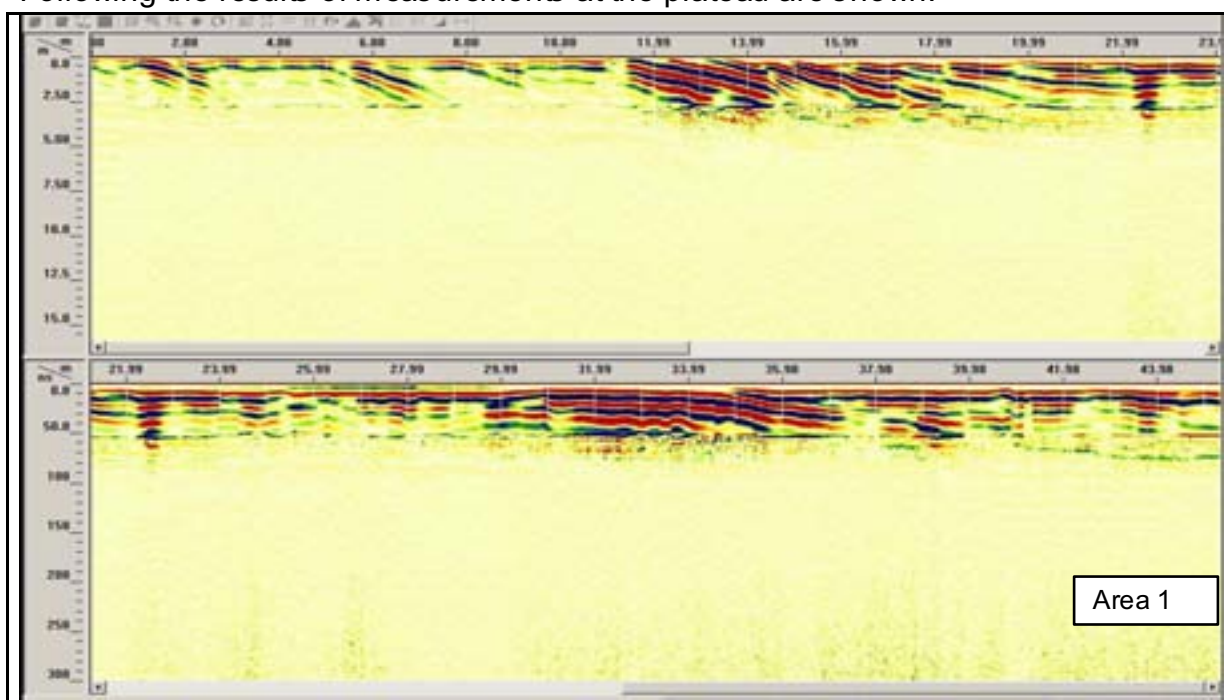


figure 118: radargram of a measuring along measuring line 1 (GSSI, $f = 100$ MHz) with inhomogeneities

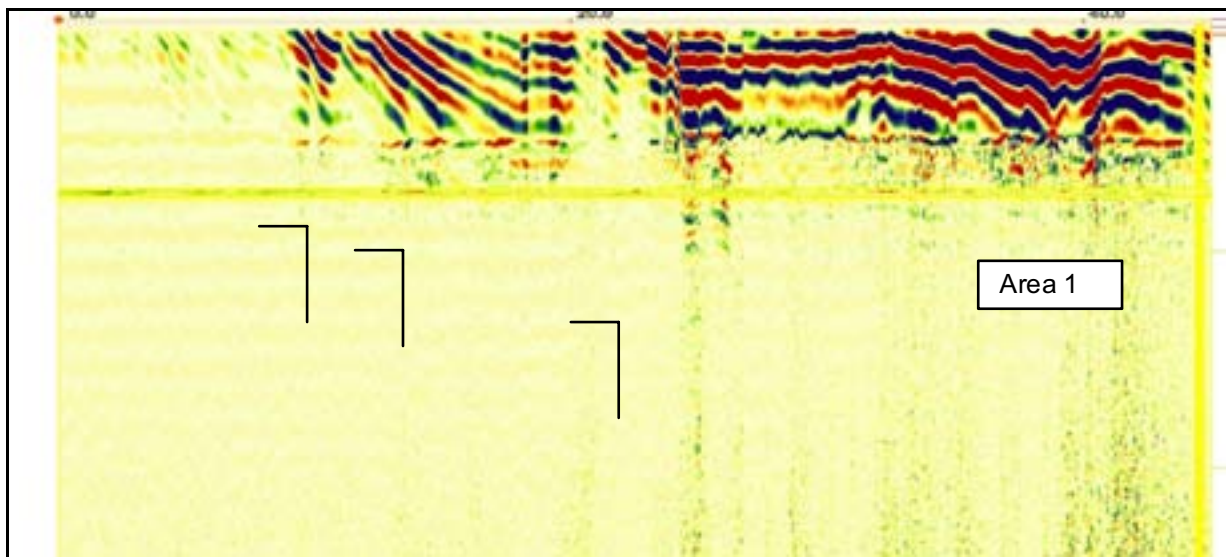


figure 119: radargram of a measuring along measuring line 3 (GSSI, $f = 100$ MHz) in field 1 with inhomogenities caused by stairs of stone

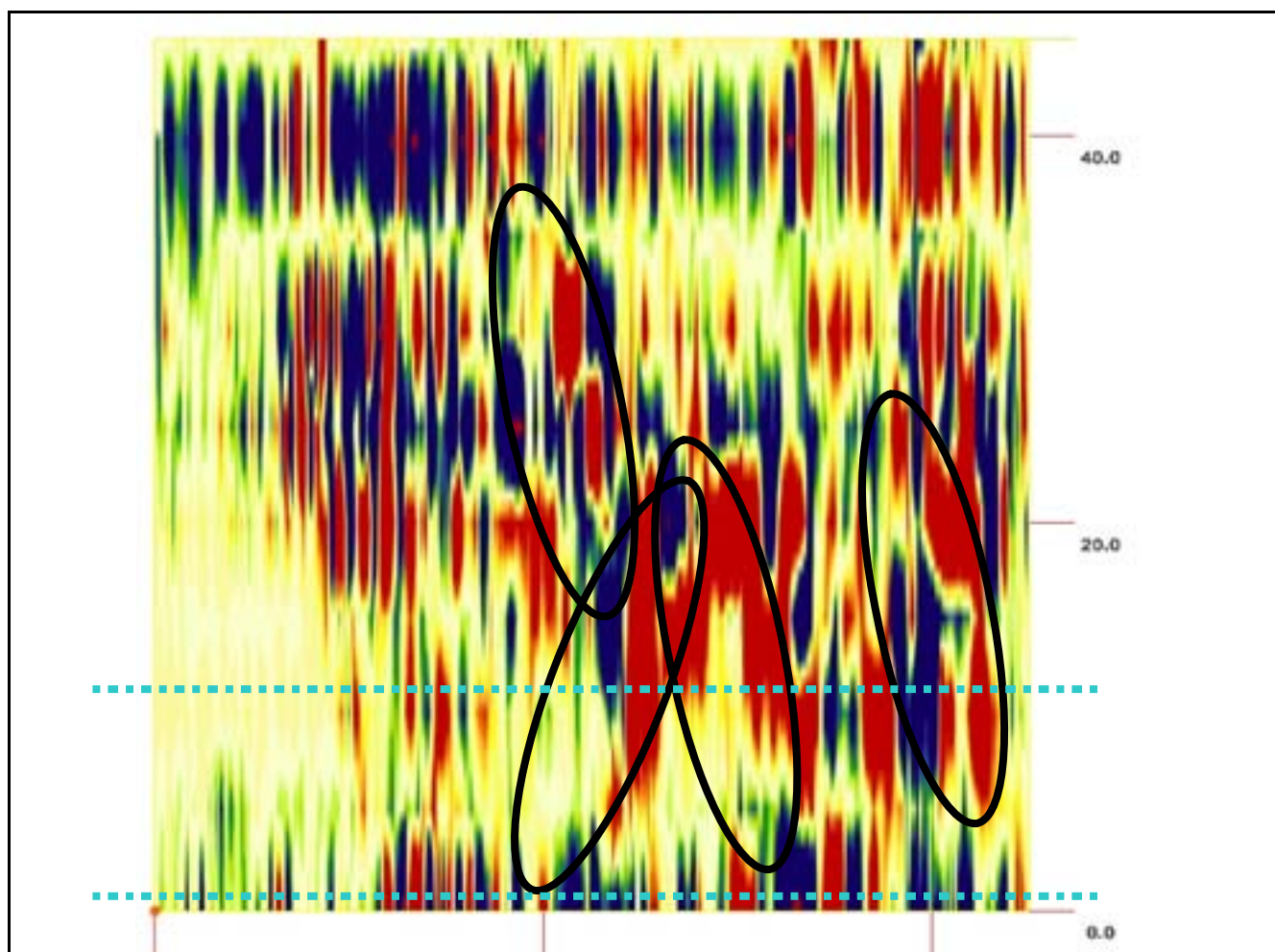


figure 120: timeslide of measurement of field 1 (first 45 m) depth 1,64 m with inhomogenities, pointed

lines: bottom line 1, upper – line 3

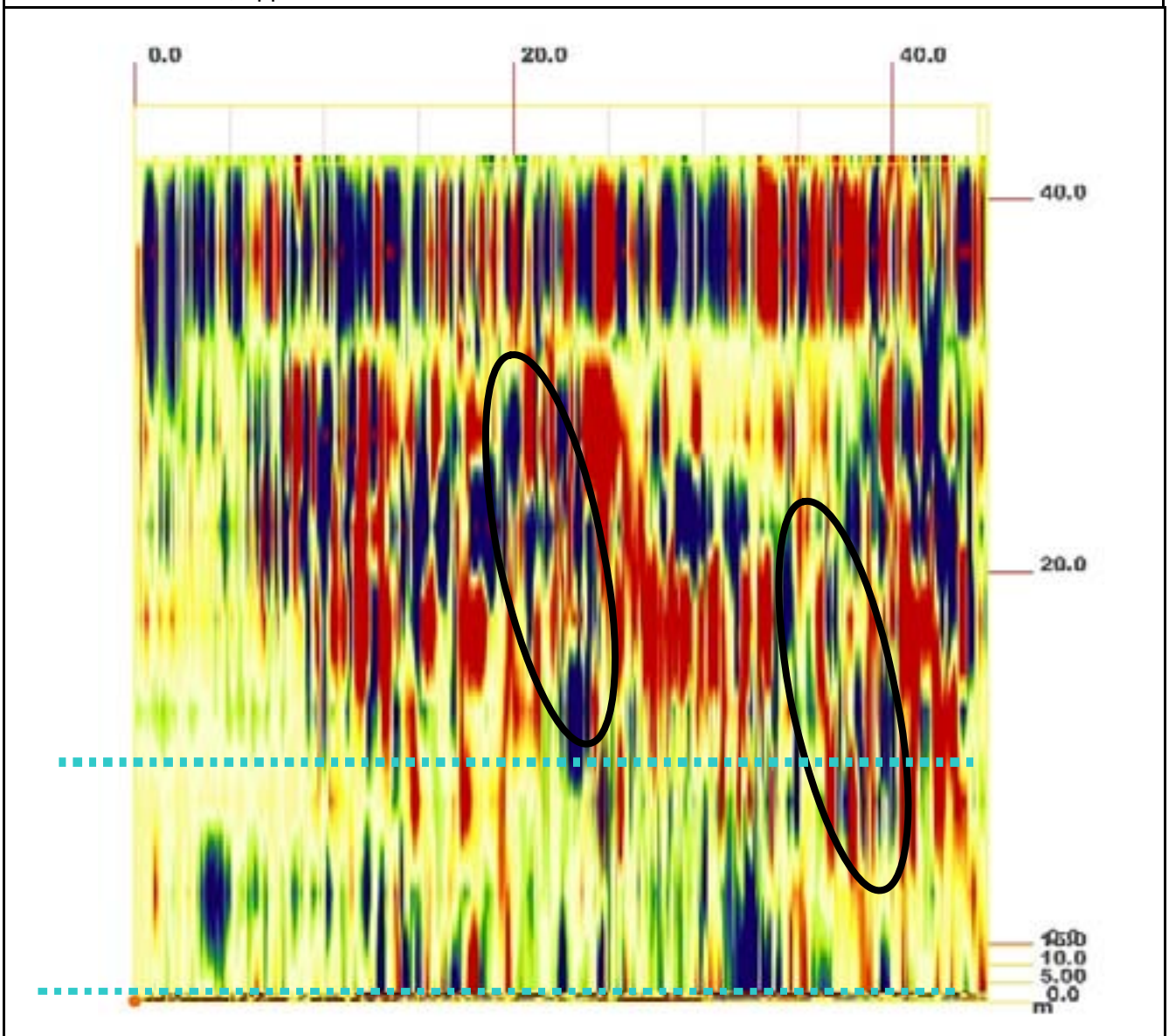


figure 121: timeslide of measurement of field 1 (first 45 m) depth 2,67 m with inhomogenities, pointed lines: bottom line 1, upper – line 3

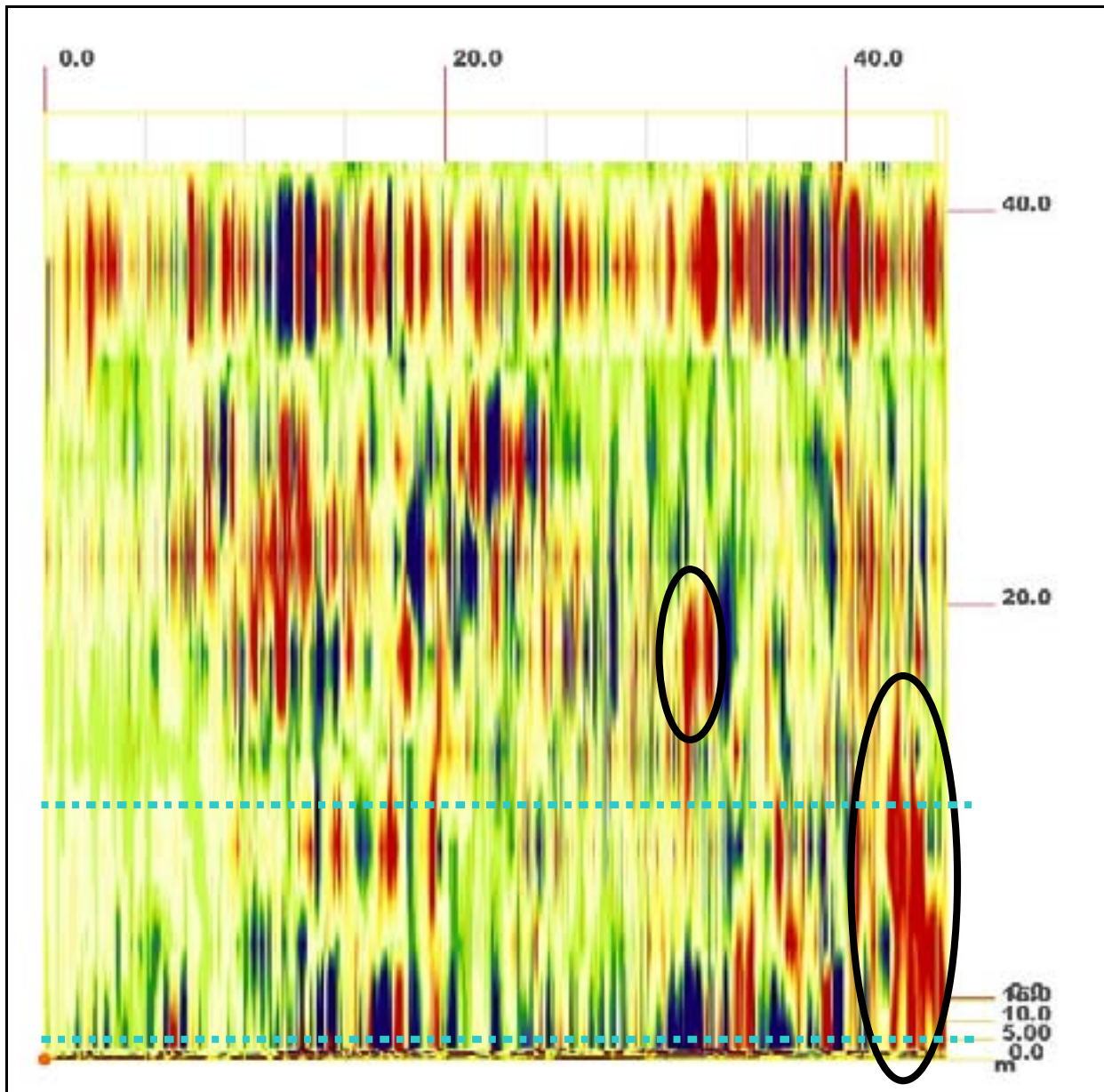


figure 122: timeslide of measurement of field 1 (first 45 m) depth 2,84 m with inhomogeneities, pointed lines: bottom line 1, upper – line 3

Inhomogeneity go from 2,8m as a diagonal to 1,6m with a length of 30 m

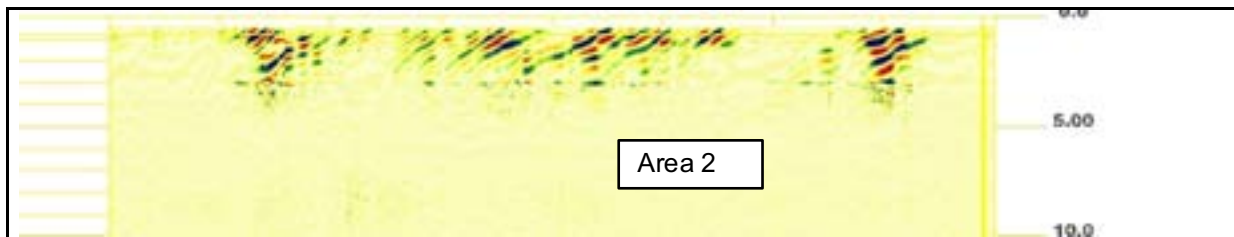


figure 123: radargram of a measuring along measuring line 16 at field 1 the right 45 m (GSSI, $f = 270$ MHz) with inhomogenities

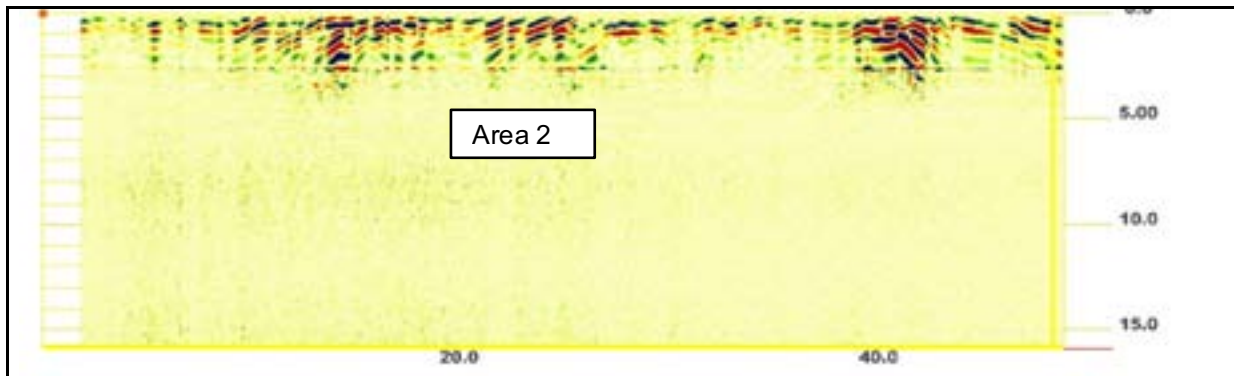


figure 124: radargram of a measuring along measuring line 15 at field 1 the right 45 m (GSSI, $f = 270$ MHz) with inhomogenities

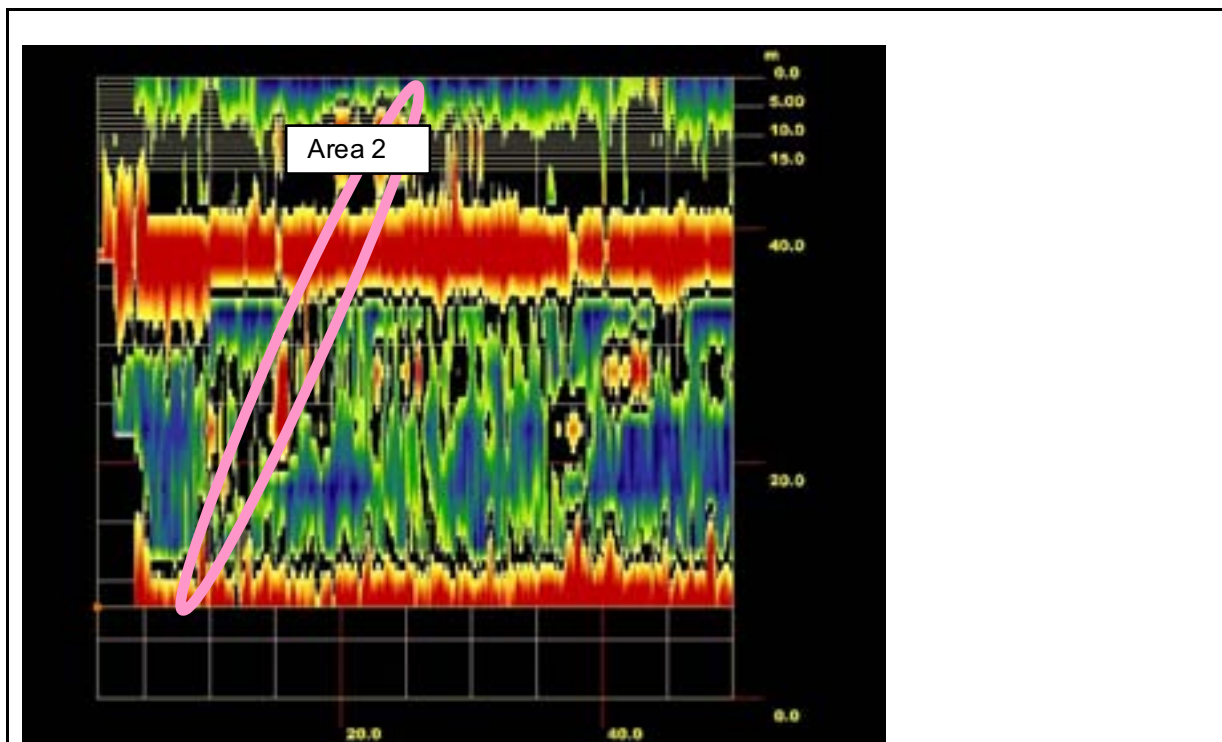


figure 125: timeslide of measurement of field 2 (second 45 m) depth 1,6m with inhomogenities

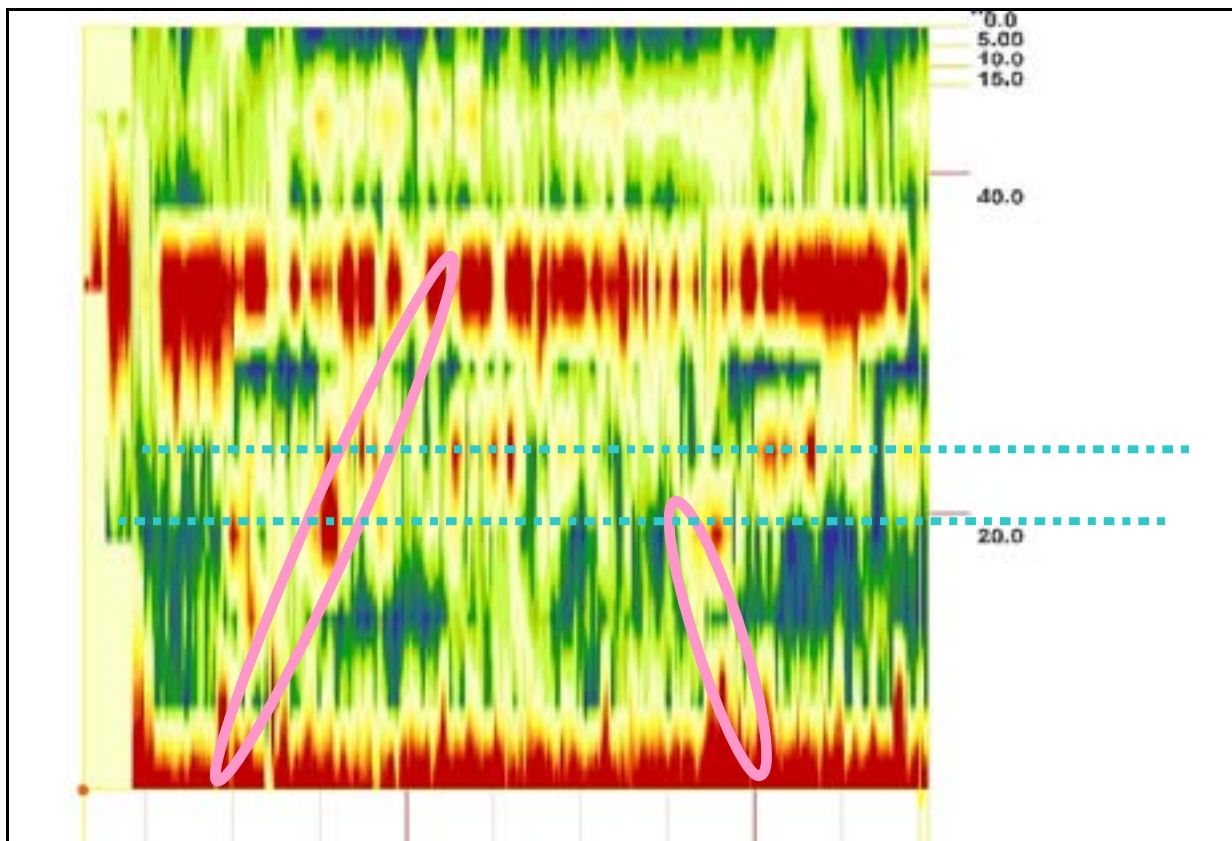


figure 126: timeslide of measurement of field 2 (second 45 m) depth 1,47m with inhomogenities, pointed lines: bottom line 15, upper – line 16

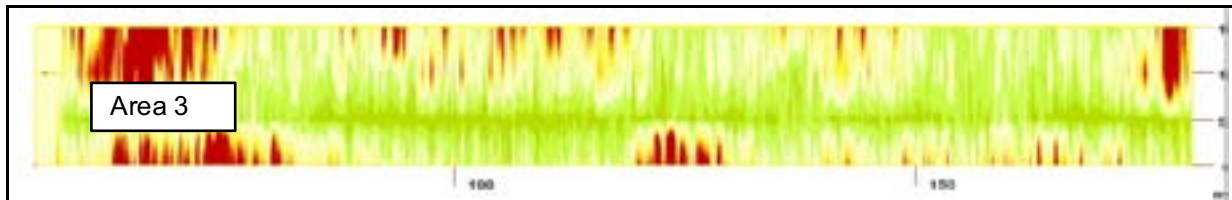


figure 127: timeslide of long lines in depth of 2,8m (GSSI, f = 100 MHz) with inhomogenitie (0,7 – 3,5m)

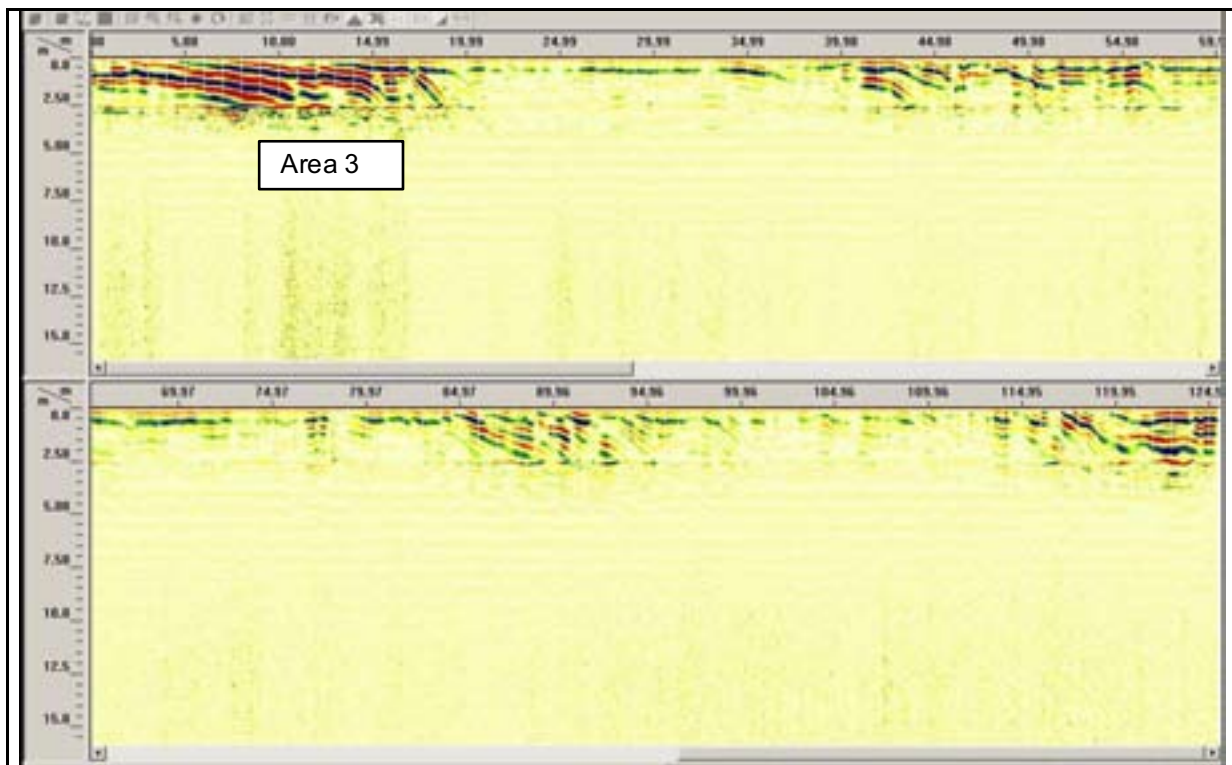


figure 128: radargram of a measuring along measuring line 23 (GSSI, f = 100 MHz) with inhomogenities

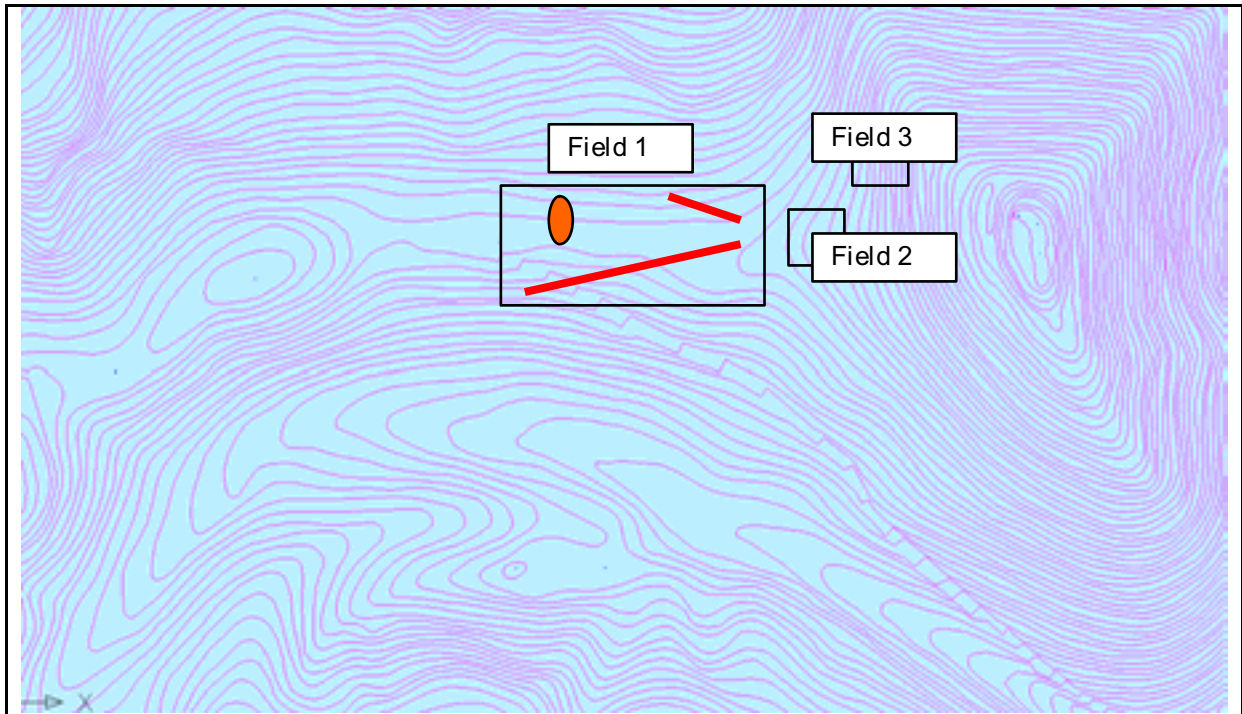


figure 129: view measuring fields

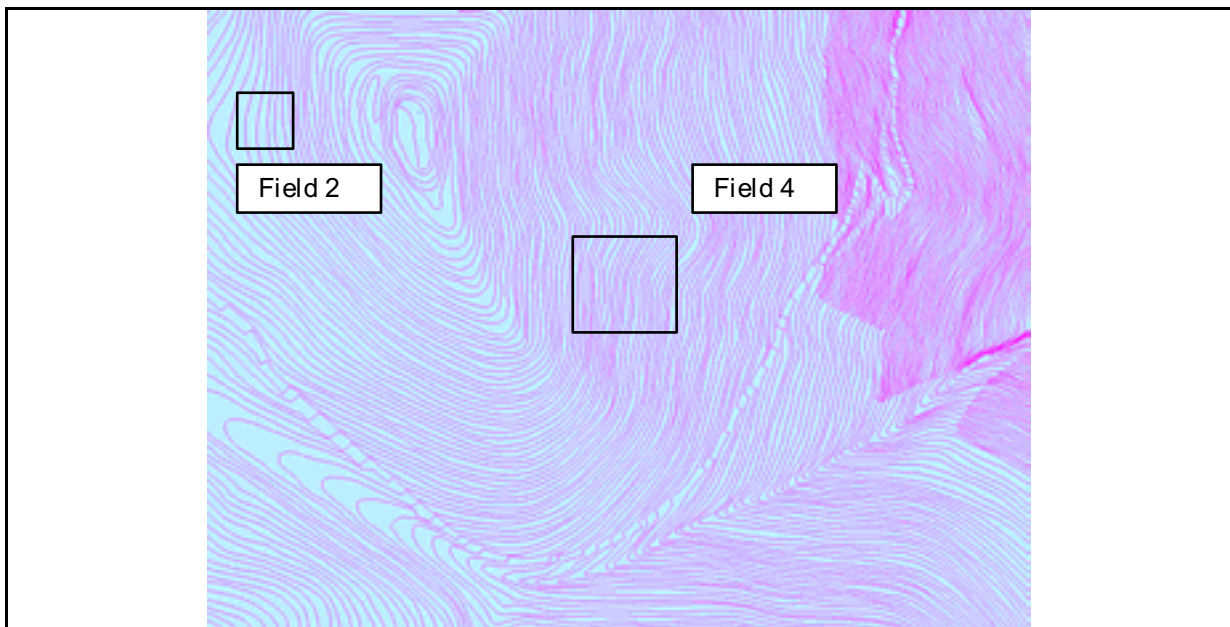


figure 130: view measuringfields

Field 1	
Area 1	On the right side inhomogenities in depth of: 1,6 – 2,8 m with length of 30 m
Area 2	Inhomogeneity in depth of: 0,8 – 2,0m
Area 3	Inhomogeneity in depth of: 0,7 – 3,5m
Field 2	
	Very strong damping of signals, few inhomogenities in the first 1-2m
Field 3	Very strong damping of signals, inhomogenities beginning 0,7 m from surface, no structure, no different pictures parallel and right angle to hill
Field 4	
	Grassland with small bushes, no reflections received, possible cause of no reflector or total damping of signal

9 MEASUREMENTS AT BOTTOM OF VALLEY

9.1 Local conditions

Inhomogene ground with civil structure in it.

9.2 CONCLUSION OF RESULTS

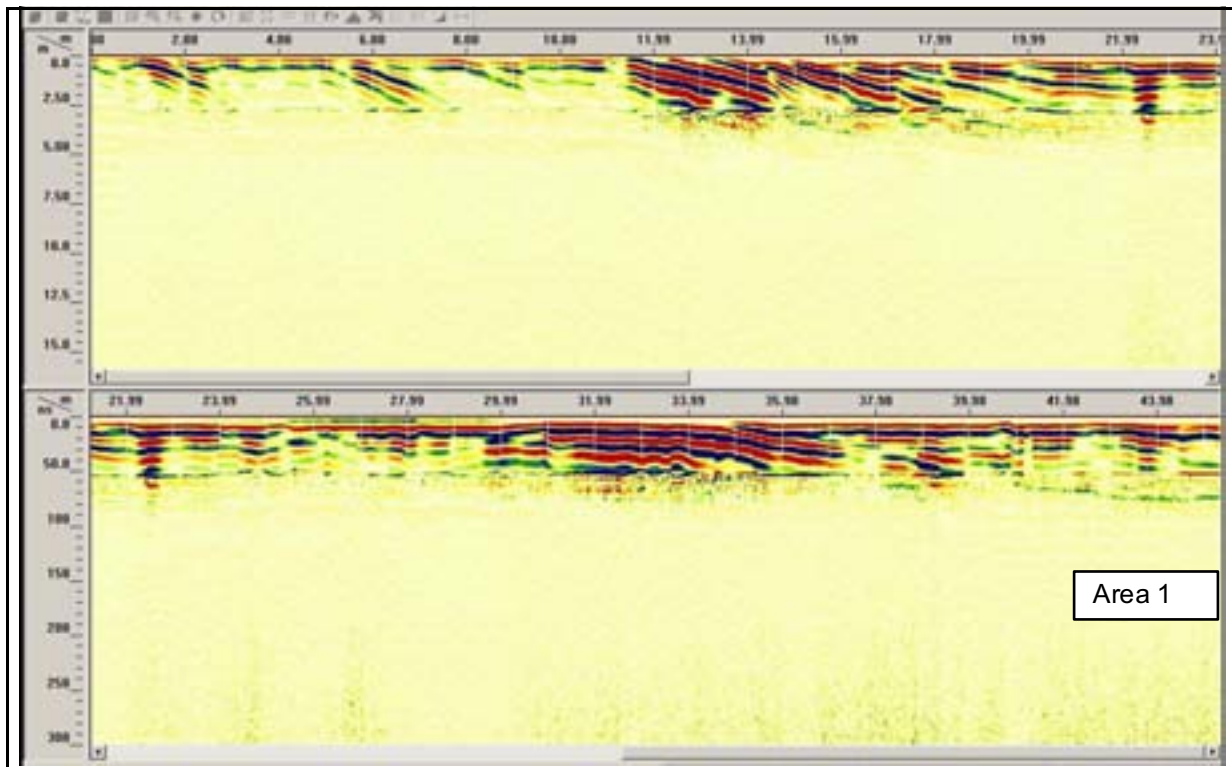


figure 131: radargram of a measuring along measuring line 1 (GSSI, $f = 100$ MHz) with inhomogeneities

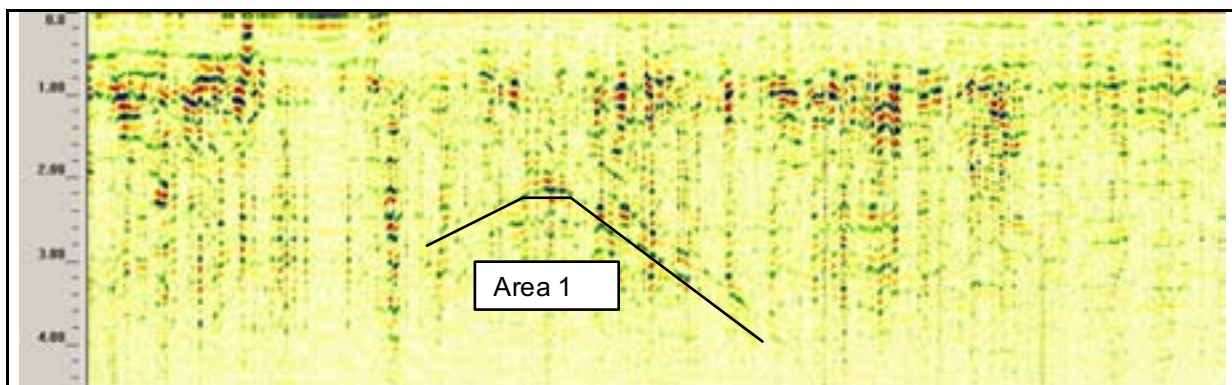


figure 132: radargram of a measuring along measuring line 37 (GSSI, $f = 270$ MHz) with inhomogeneities

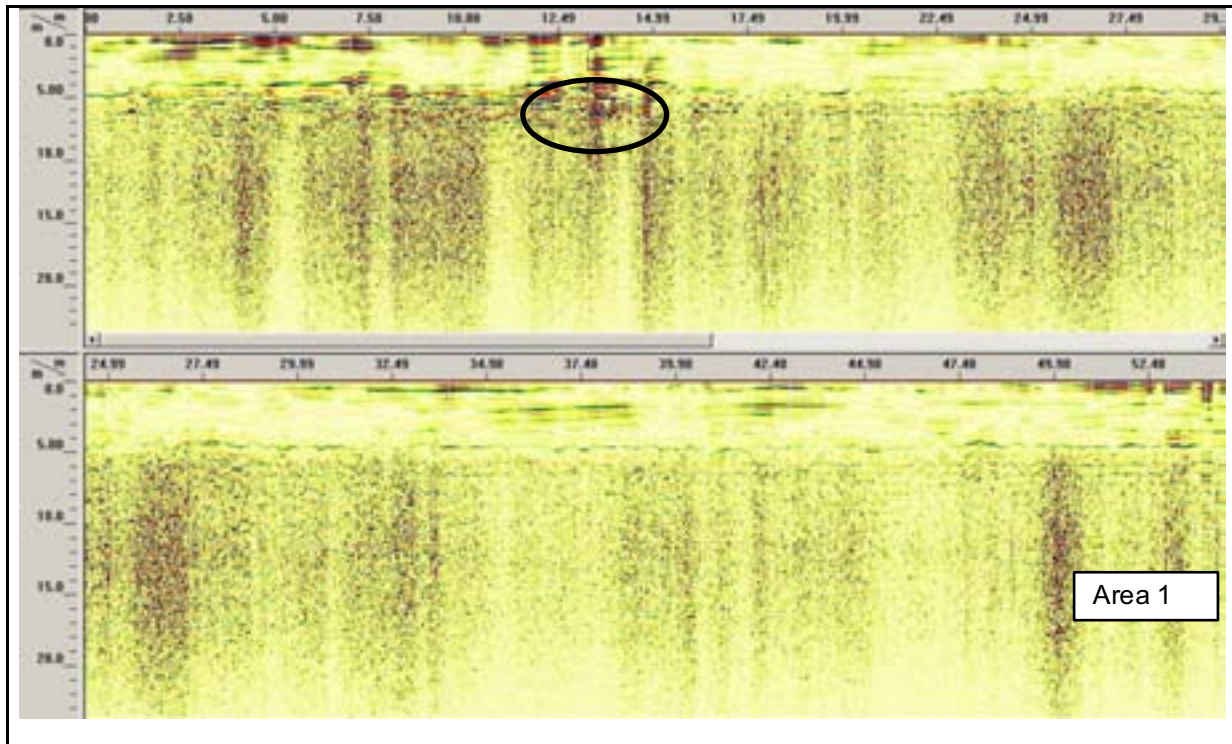


figure 133: radargram of a measuring along measuring line 38 (GSSI, $f = 100\text{MHz}$) with small inhomogeneity, but no clear echo

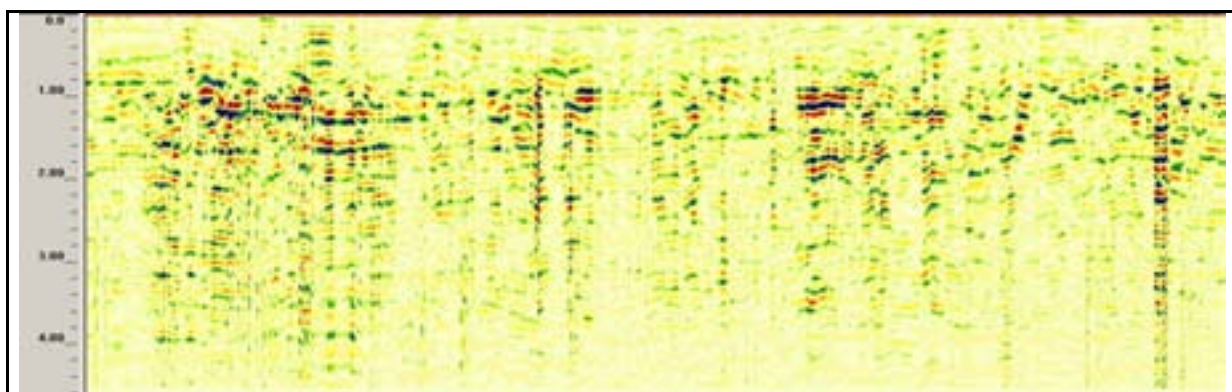


figure 134: radargram of a measuring along measuring line 40 (GSSI, $f = 270\text{MHz}$) with no echo, only inhomogeneities from closed structure

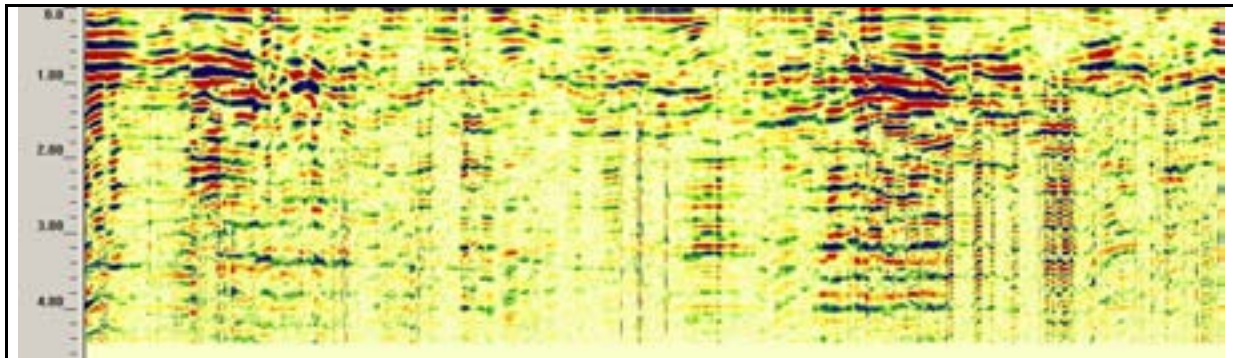
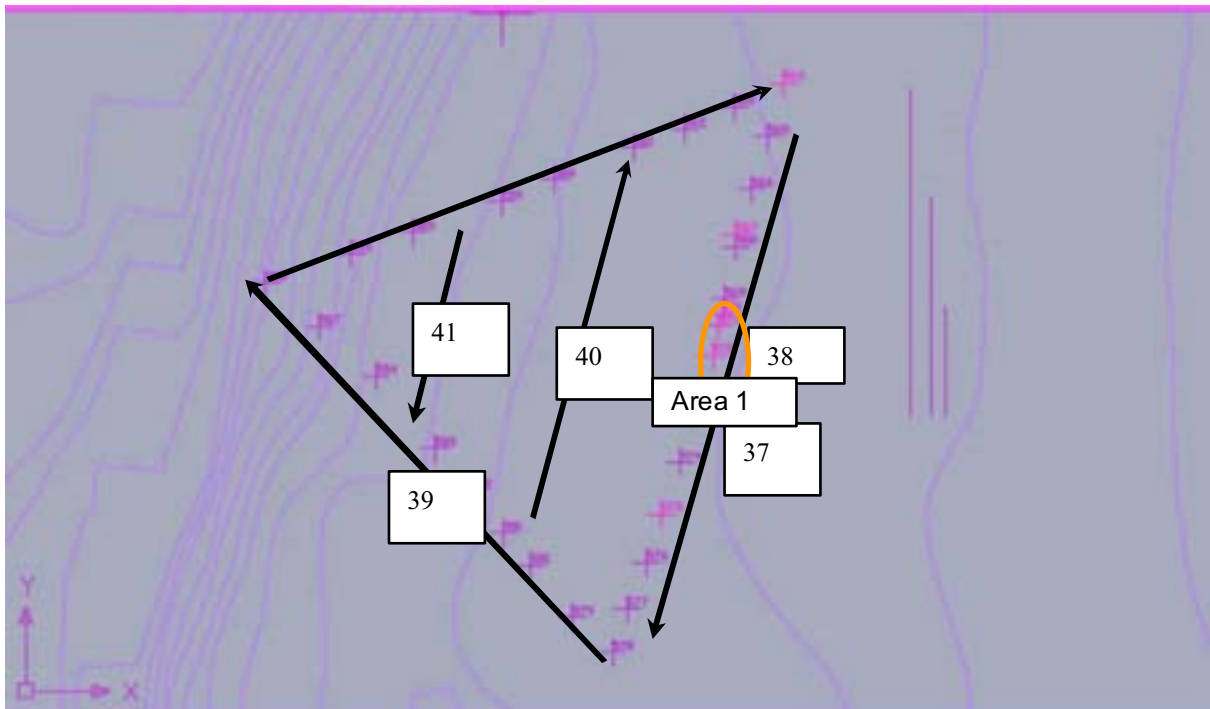


figure 135: radargram of a measuring along measuring line 39 (GSSI, $f = 270\text{MHz}$) with echo from closed structure



The measurements show, that it is very difficult to measure in an area with a lot of built structures – these inhomogenities disturb the radar measurements.

Only in one measuring line were some echo from deeper areas – in line 37. All other measuring lines had no results. The line 40 parallel to line 37 also had no results.

10 MEASUREMENTS AT VRATNICA KAMENI HRAM AND DOLOVI VALJAK

10.1 Local conditions

The measurements were carried out at two hills.

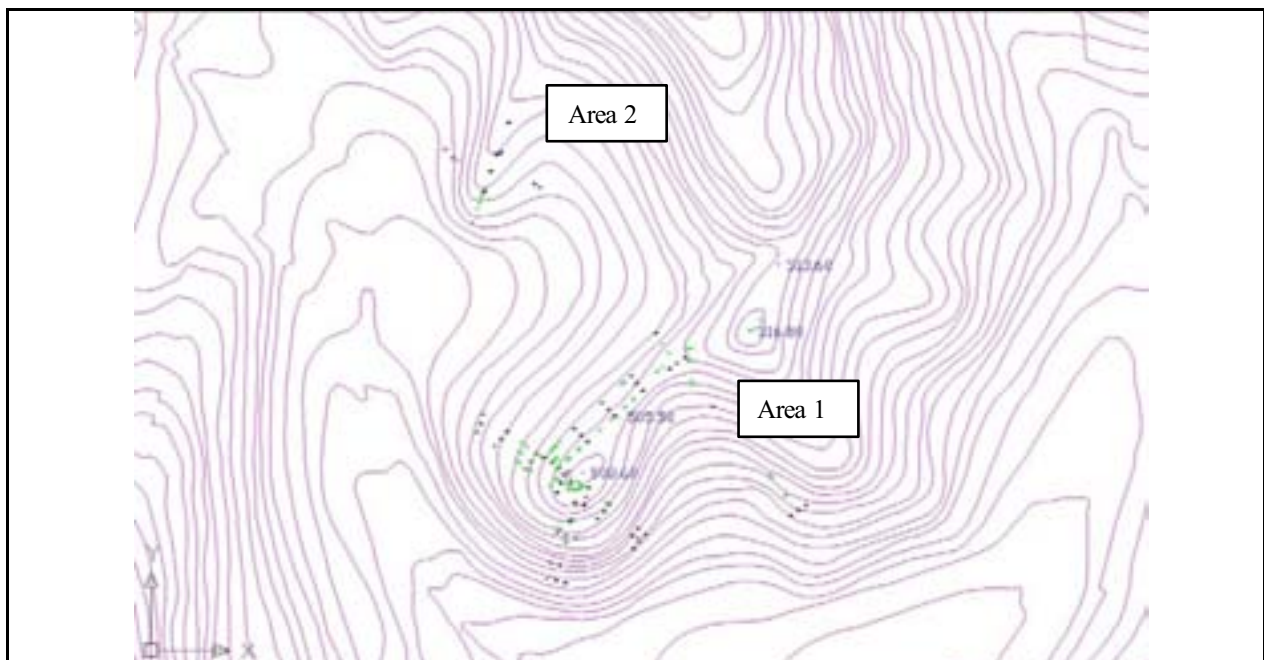


figure 136: view of measurements at Area VRATNICA KAMENI HRAM and DOLOVI VALJAK



figure 137: view of measurements at Area 1



figure 138: view of measurements at Area 1



figure 139: view of measurements at Area 1



figure 140: view of measurements at Area 1



figure 141: view of measurements at small hill (Area 2)

10.2 RESULTS OF THE MEASUREMENTS

The measurements were done with a 270 MHz radar antenna. Because of the weather the ground has been wet what results in a high damping of signals. Anywhere the results of the measurements were in the first 4 m very good.

Following the results of measurements at the area of VRATNICA KAMENI HRAM and DOLOVIVALJAK are shown.

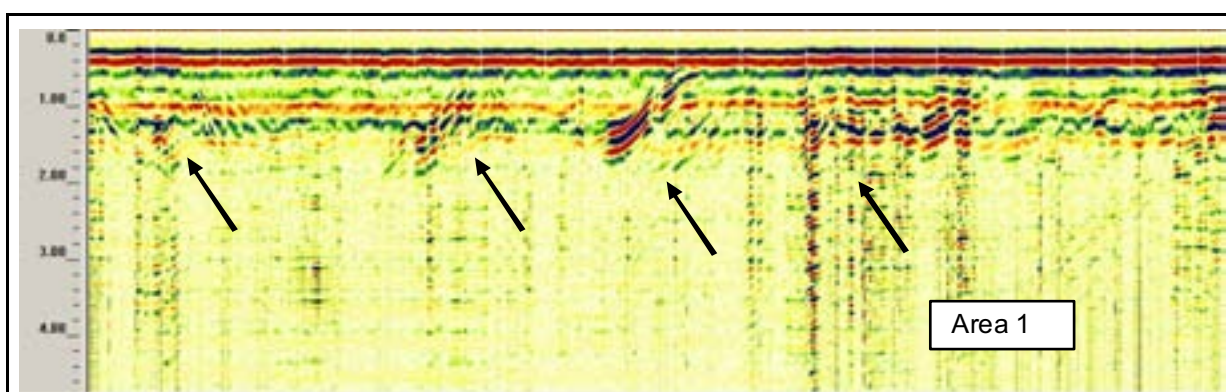


figure 142: radargram of a measuring along measuring line 6 (GSSI, f = 270 MHz) with position of "steps"

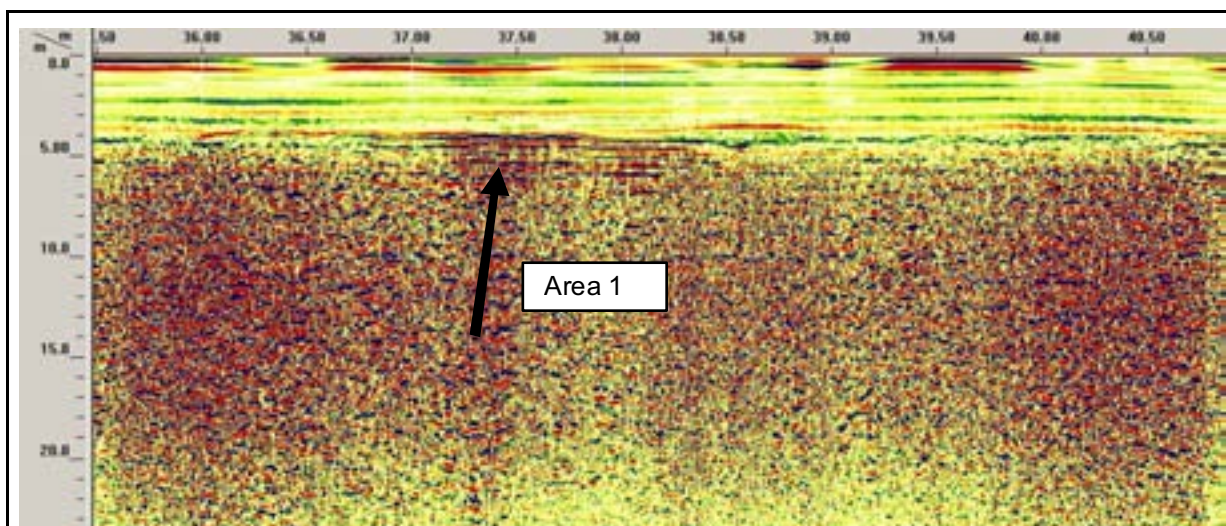


figure 143: radargram of a measuring along measuring line 7 (GSSI, f = 100 MHz) with position of inhomogeneity

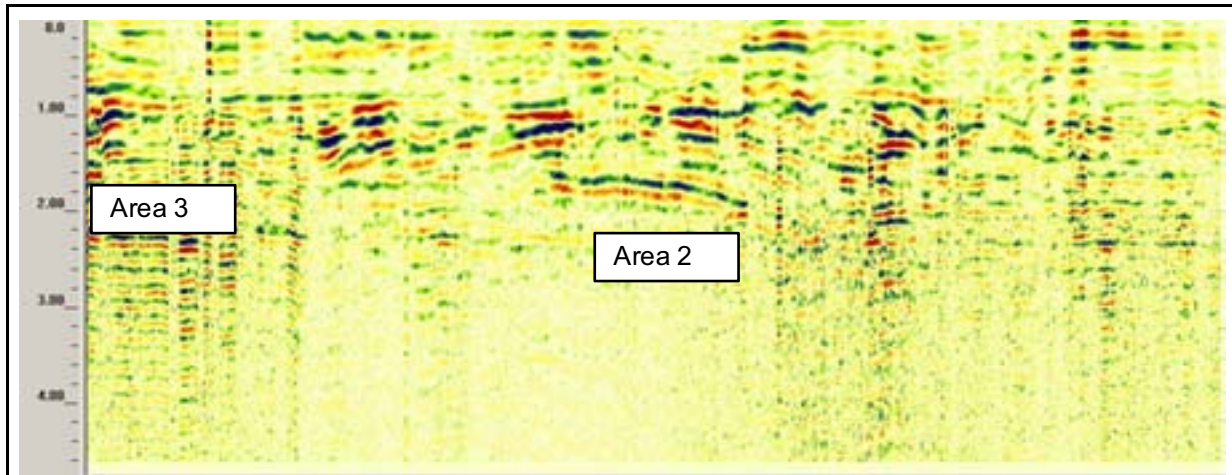


figure 144: radargram of a measuring along measuring line 8 (GSSI, $f = 270$ MHz) with position of inhomogeneity

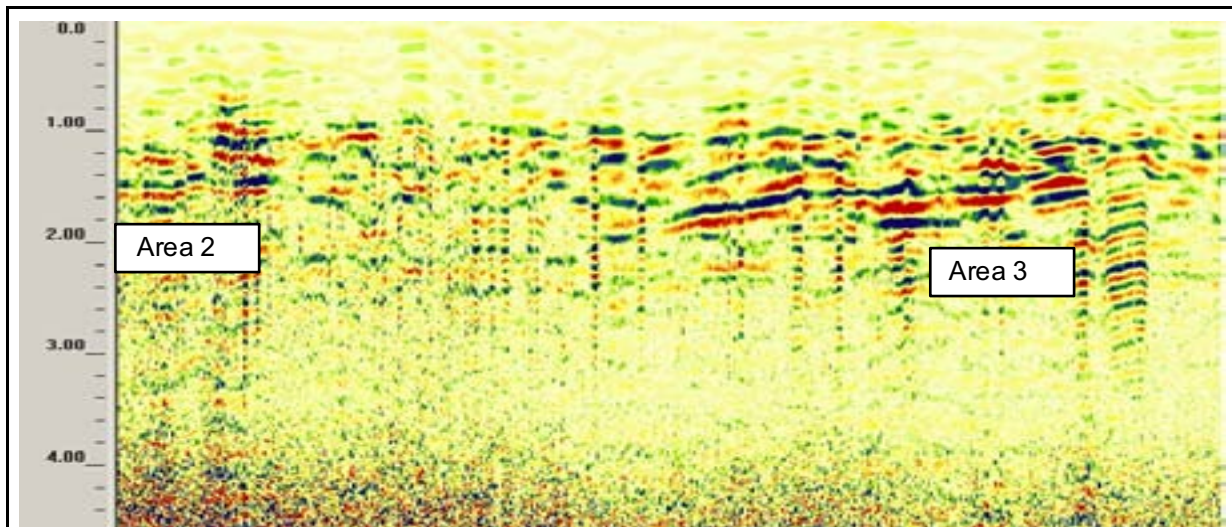


figure 145: radargram of a measuring along measuring line 9 (GSSI, $f = 270$ MHz) with position of inhomogeneity

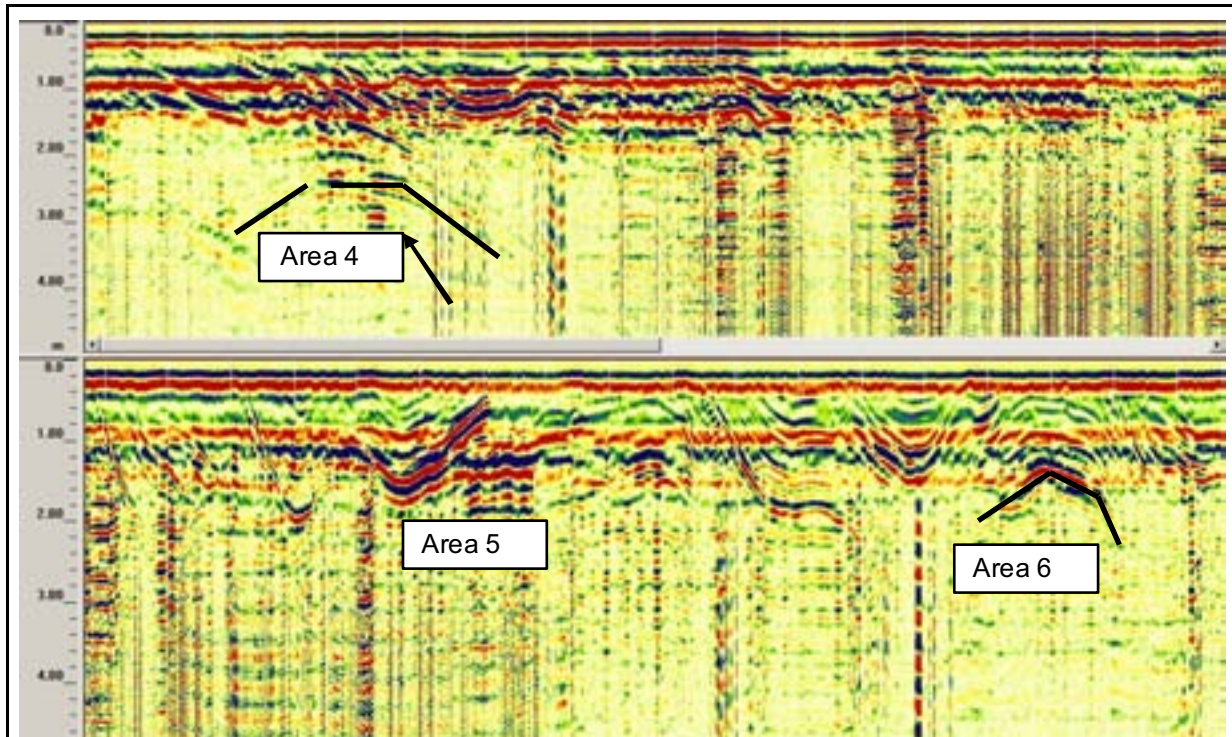


figure 146: radargram of a measuring along measuring line 13 (GSSI, $f = 270$ MHz) with position of inhomogeneity

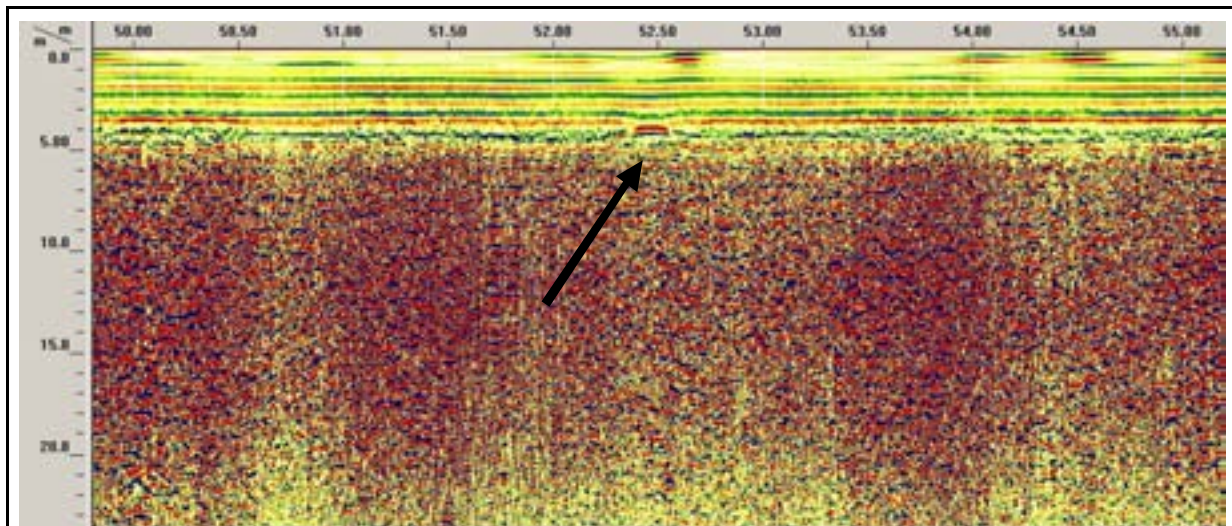


figure 147: radargram of a measuring along measuring line 16 (GSSI, $f = 100$ MHz) with position of inhomogeneity

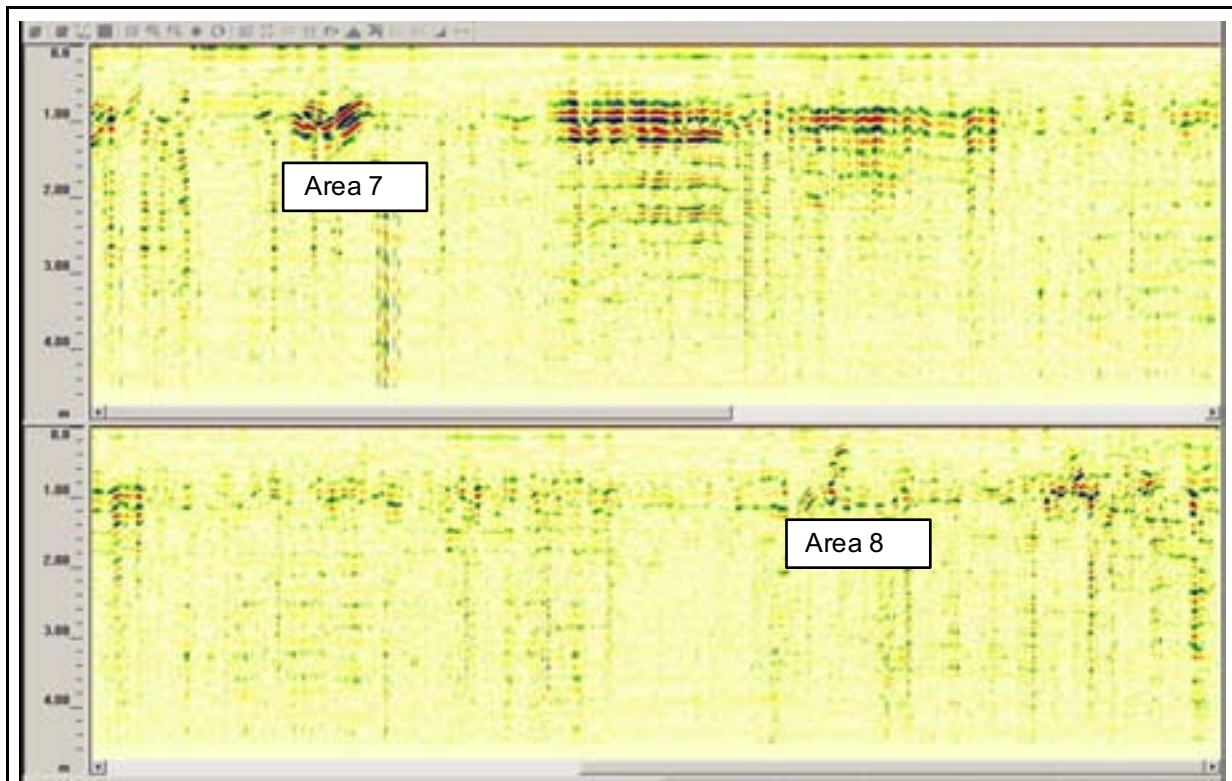


figure 148: radargram of a measuring along measuring line 20 (GSSI, $f = 270$ MHz) with position of inhomogeneity

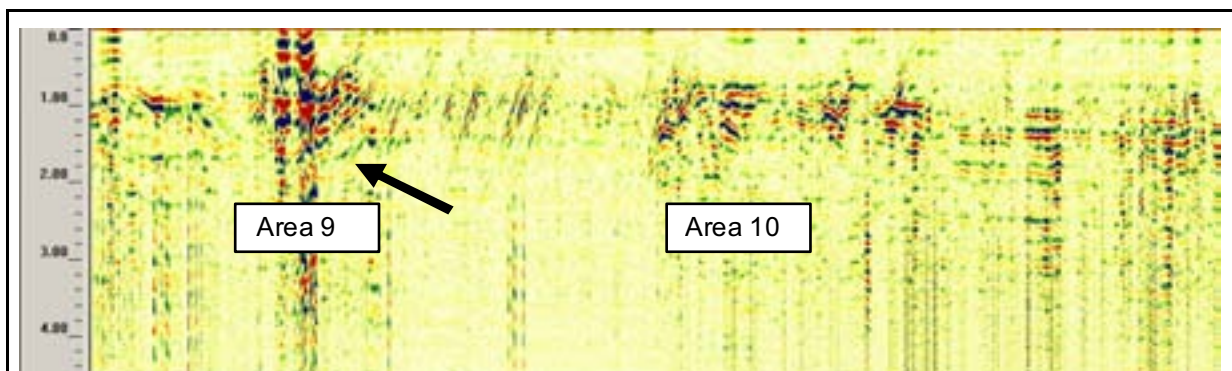


figure 149: radargram of a measuring along measuring line 28 (GSSI, $f = 270$ MHz) with position of inhomogeneity

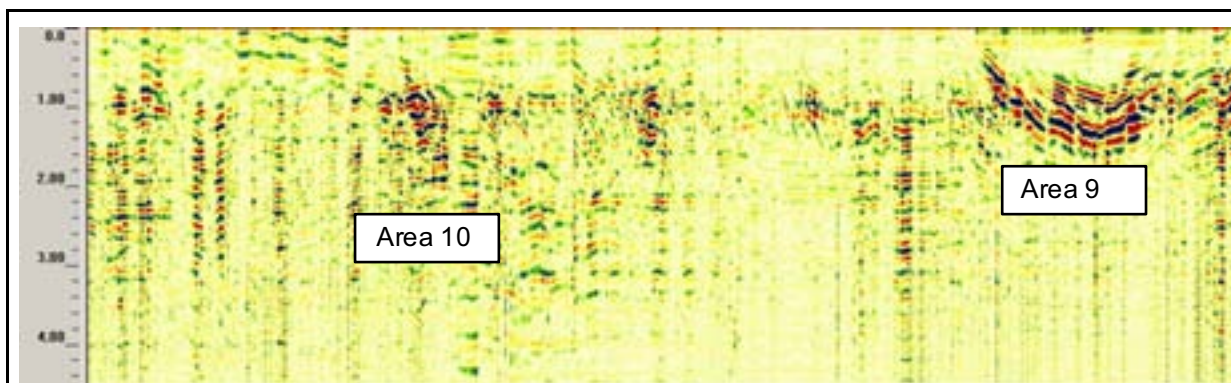


figure 150: radargram of a measuring along measuring line 29 (GSSI, $f = 270$ MHz) with position of inhomogeneity

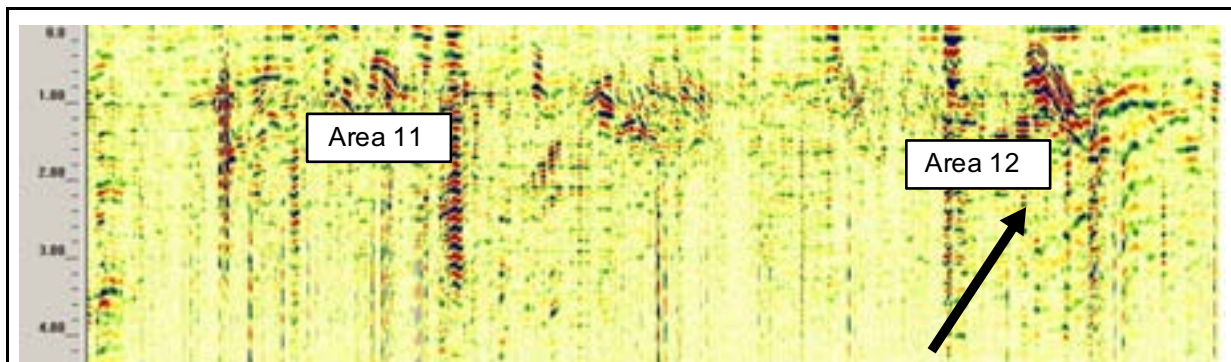


figure 151: radargram of a measuring along measuring line 31 (GSSI, $f = 270$ MHz) with position of inhomogeneity

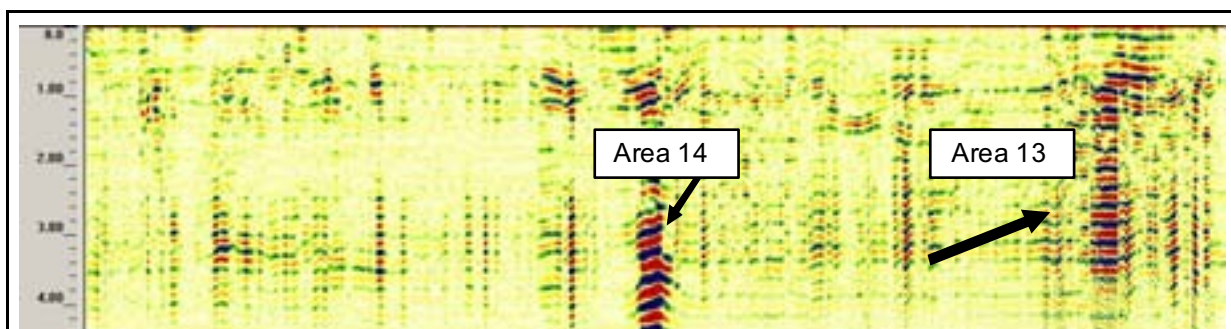


figure 152: radargram of a measuring along measuring line 32 (Field 2) (GSSI, $f = 270$ MHz) with position of inhomogeneity

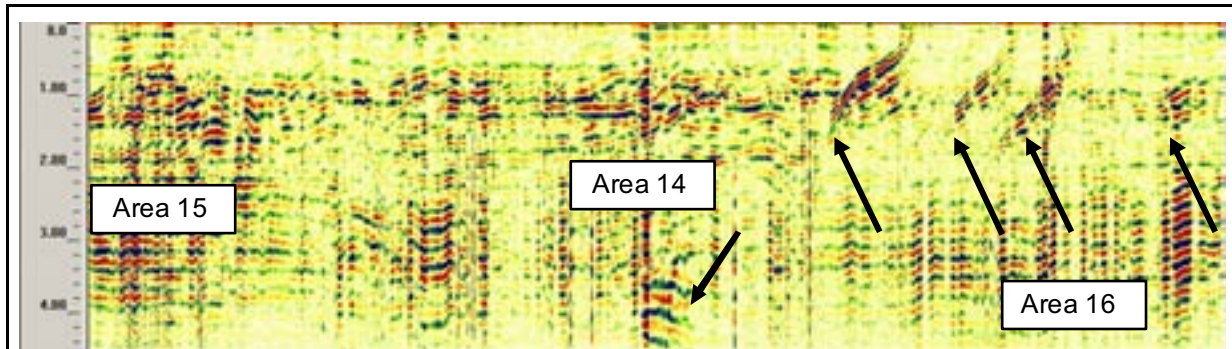
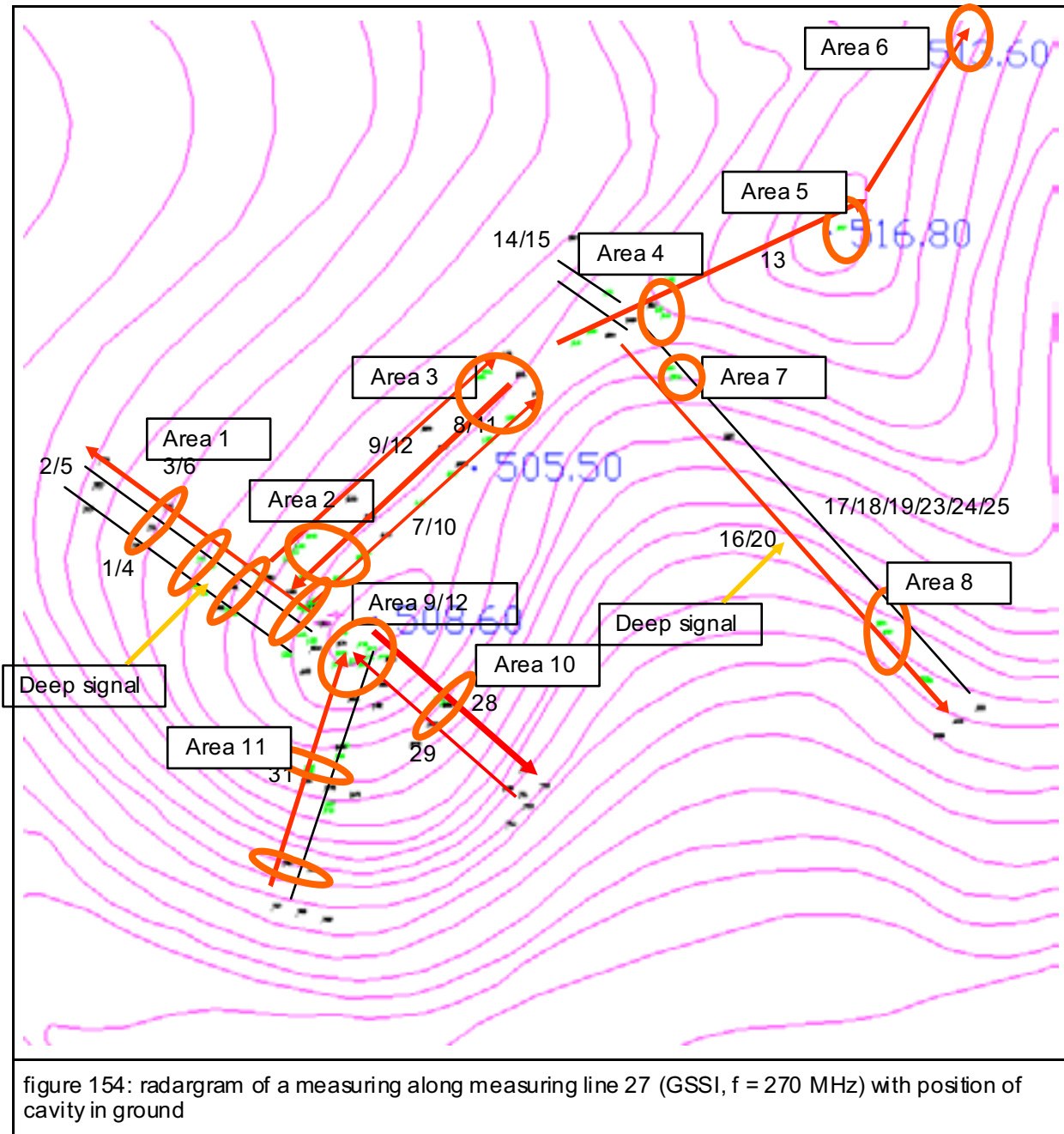


figure 153: radargram of a measuring along measuring line 33 (GSSI, $f = 270$ MHz) with position of inhomogeneity

10.3 EVALUATION OF RESULTS



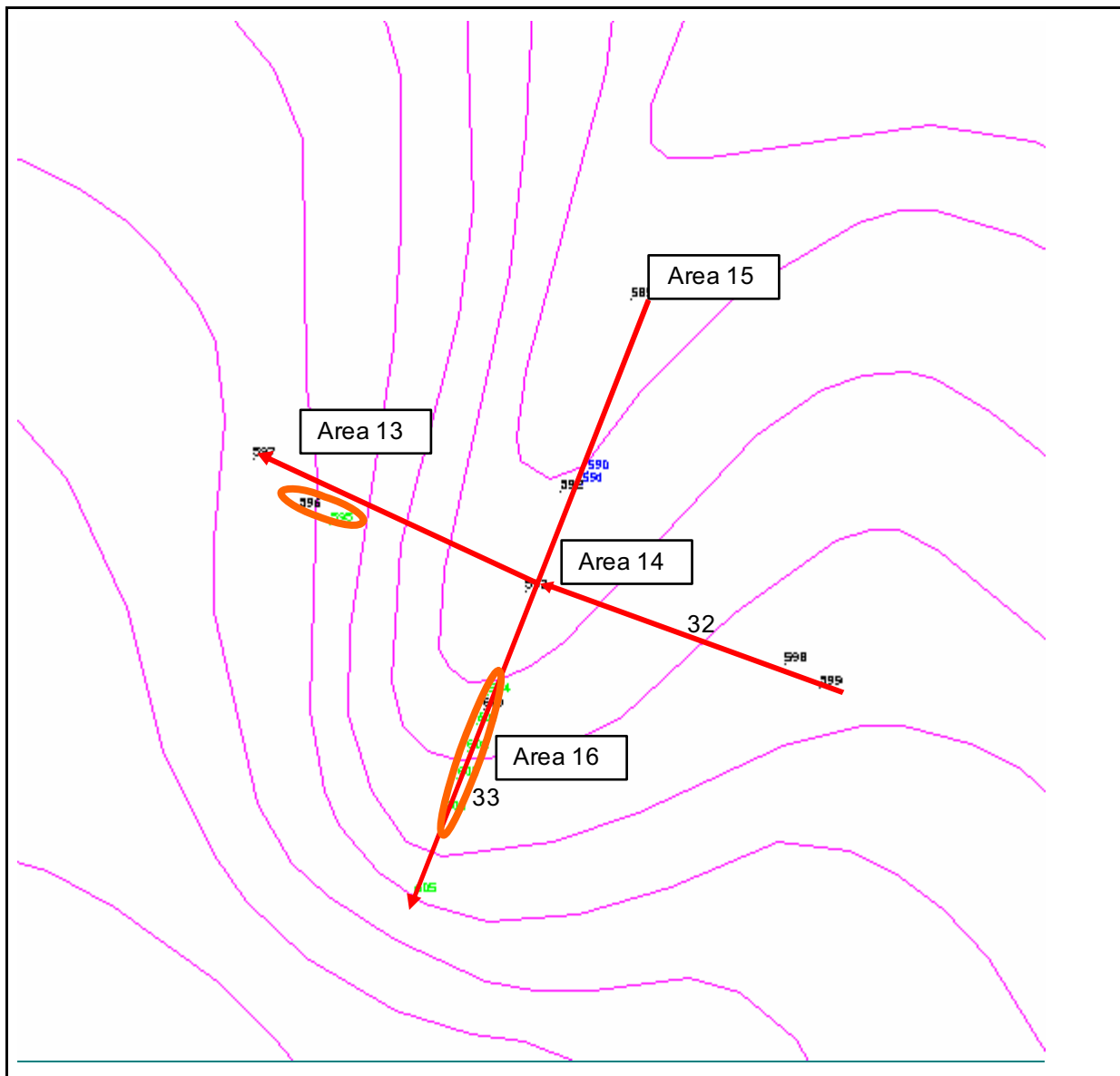


figure 155: radargram of a measuring along measuring line 27 (GSSI, f = 270 MHz) with position of cavity in ground

In the picture above the measuring lines and the areas with inhomogenities are shown.

Area 1	inhomogeneity along the measuring line (steps) in depth of: 0,8 – 1,2m deep reflection from 4,5 – 7m
Area 2	Top of Area 1 Depth of inhomogeneity: 1,0 – 1,2m, 1,8-2,0m
Area 3:	Depth of inhomogeneity: 1,6-2,0m
Area 4:	Depth of inhomogeneity: 2,4 – 3,2m
Area 5:	Depth of inhomogeneity: 1,2-1,6m
Area 6:	Depth of inhomogeneity: 1,6m
Area 7:	Depth of inhomogeneity: 0,8-1,2m
Area 8:	Depth of inhomogeneity: 0,8-1,2m
Area 9:	Depth of inhomogeneity: 0,6-1,8m
Area 10:	Depth of inhomogeneity: 0,8-1,6m
Area 11:	Depth of inhomogeneity: 0,6-1,2m
Area 12:	Depth of inhomogeneity: 0,4-1,2m
Area 13:	Depth of inhomogeneity: 1,0-2,5m
Area 14:	Depth of inhomogeneity: 2,8m
Area 15:	Depth of inhomogeneity: 0,8-1,4m
Area 16:	Four “steps” Depth of inhomogeneity: 1,2-0,6m

LGA Bautechnik GmbH
Bauwerksdiagnose

Bearbeiter:

M.Eng. Sven Homburg

Dr. –Ing. Andreas Hasenstab